ISSN 2959-1864 (Online)
ISSN 2958-0536 (Print)
Volume 4, Number 3
October 2025

Acta Botanica Caucasica

ISSN 2959-1864 (Online)
ISSN 2958-0536 (Print)

MINISTRY OF SCIENCE AND EDUCATION REPUBLIC OF AZERBAIJAN

BAKU STATE UNIVERSITY

Acta Botanica Caucasica

Volume 4, Number 3
October 2025

BAKU – BSU – 2025

AZƏRBAYCAN RESPUBLİKASININ
PREZİDENTİ YANINDA
ALİ ATTESTASİYA KOMİSSİYASI

The purpose of the journal is to stimulate the development of botanical science. The issues posed by the Journal are the publication of the results of research that are relevant for professional botanists.

The journal “Acta Botanica Caucasica” publishes the results of researches in various fields of fundamental Botany: Systematics, phylogeny, floristics, geobotany, morphology, structural Botany, Plant Physiology; articles on protection of the plant world, as well as the study of vegetation in the Caucasus; chronic materials on scientific events (symposiums, conferences); important botanical innovations; articles on the history of Botany. In the journal “Acta Botanica Caucasica” the Articles of Caucasian and foreign authors are published in English. Articles should include the latest, previously unpublished factual information and theoretical considerations.

POTENTIAL OF *JUNIPERUS COMMUNIS* L. IN DEGRADED AREAS OF FOREST ECOSYSTEMS OF AZERBAIJAN

Elshad Gurbanov[1]| https://orcid.org/0000-0003-4627-3760
Afaq Rzayeva[2]*| https://orcid.org/0000-0002-0395-2301

[1] Baku State University, Baku, Azerbaijan
[2]* Baku Engineering University, Baku, Azerbaijan

Correspondence: afrzayeva@beu.edu.az

Article Info:
DOI: https://doi.org/10.30546/abc.2025.001
Pages: 4-9
Received: July 12, 2025 | Revised: September 06, 2025 | Accepted: October 01, 2025

Abstract

The presented study evaluates the potential of Juniperus communis L. for ecological restoration of degraded forest ecosystems of Azerbaijan. These degraded areas are results of soil erosion, loss of biodiversity, and climate-related conditions. J. communis, a widespread coniferous species, can act as a significant species for forest regeneration due to its adaptability and key ecological functions. J. communis seeds were collected from five different regions of Azerbaijan, representing different climatic and altitudinal zones.

This experiment was performed to analyze the effect of low temperature (5°C) and scarification on germination percentage of Juniperus communis L. (Cupressaceae Bartl.) seeds collected from different regions. Seeds collected from Nakhchivan, Khizi, Turyanchay, Shamkir and Guba regions were subjected to cold stratification for 0, 4, 8, 12 and 16 weeks, and the effect of scarification was additionally evaluated. The highest germination at 5°C was observed during the 8-week stratification period and varied by region. Scarification significantly increased germination rates, with the highest results recorded in the 8-week period.

Overall, seed germination percentages were considerably higher under scarification treatment compared to conventional cold stratification. The results can easily demonstrate that both cold stratification and scarification serve as effective pre-germination techniques for overcoming deep physiological dormancy in Juniperus communis seeds. However, the enhanced response observed with scarification highlights its greater potential in promoting rapid and uniform germination. Among all treatment durations, the highest germination rate was recorded after 8 weeks of pre-treatment, suggesting that this period represents the optimal physiological period for dormancy release and metabolic activation of seeds.

These findings hold significant ecological and practical importance, particularly for restoration biology and forestry management. The evidence obtained in this study provides valuable guidance for designing successful artificial regeneration strategies and afforestation programs involving Juniperus communis, especially in arid and semi-arid ecosystems, where natural regeneration is often limited due to harsh environmental conditions and low seedling establishment rates. Therefore, incorporating scarification combined with an 8-week cold stratification period can be recommended as an effective approach to enhance germination success and support long-term conservation and reforestation initiatives for juniper populations.

Keywords: *Juniperus communis* L., seed germination, ecological restoration, Azerbaijan, scarification, stratification, biodiversity conservation, sustainable forestry, climate adaptation

INTRODUCTION

Juniperus communis L. (International protection status: LC - Least Concern) is a widely distributed species of juniper. Its natural habitat extends from the Altiagaj and Turianchai Natural Preserves to the Nakhchivan Autonomous Republic in Azerbaijan. This is a perennial shrub that grows to a height of 1-3 meters and can reach a diameter of 0.2 meters. The shrub has a dark green or gray crown and grows slowly, with an annual growth rate of 10 to 12 cm. Its branches are reddish-brown in color. Male plants typically have a conical-ovate crown, while female plants exhibit branched edges. The needles of the juniper are shaped like narrow leaves, measuring 16 to 20 mm in length and 0.7 to 1.5 mm in width, arranged in whorls of three. These leaves can remain on the plant for approximately four years. The cones are numerous, measuring 5 to 9 mm in diameter, and can be either oblong-ovate or spherical in shape, initially appearing light green. Ripe cones turn dark blue with a waxy covering and mature in the autumn of their second or third year. Each cone contains three triangular seeds, though in some cases, there may be one or two. Occasionally, immature cones take on an elliptical shape. The berry-like fruits contain up to 42% sugar, as well as dyes, organic acids (including formic, acetic, and malic acids), resin (2%), and 0.27% ascorbic acid (Gurbanov E., Rzayeva A., 2019).

Juniperus communis L. is an ornamental plant. The following variations are used in landscaping (Adams et all. 2014):

- *J.communis var.montana*
- *J.communis var.nana Syme J.communis var.Prostrata Beissn.*
- *J.communis var.Suecica Beisssn.*
- *J.communis var." Obergarthen " Bruns.*
- *J.communis var." Depressa aurea"*
- *J.communis var." Compressa "*
- *J.communis var.Cracovica*
- *J.communis var. Columnaris*

Historically, vegetative reproduction was the only method available for humans to select and preserve genetic variability and valuable traits developed over centuries. However, since coniferous plants display significant differences in their morphological and physiological characteristics, it is essential to consider this diversity when selecting reproduction methods. Seed reproduction is the only technique that allows for the creation of new hybrid forms (Bewley J.D., Black M., 1994). However, the structure of conifer seeds and their delayed growth characteristics can make this method challenging. Given the economic and ornamental importance of seeds, it is crucial to improve seed reproduction techniques. Since seed reproduction is vital for developing new hybrid ornamental and ecological features in plants, this research focuses on addressing this issue.

MATERIALS AND METHODS

Seeds were collected from five different regions in the Republic of Azerbaijan: The Nakhchivan Autonomous Republic (South-East Caucasus), Khizi (North-East), Turyanchay State Nature Reserve (south of the Greater Caucasus), Guba (North-East), and Shamkir (North-West). Table 1 presents the average annual temperature, altitude above sea level, and annual precipitation for these regions.

Table 1. The average annual temperature, altitude above sea level, annual precipitation of compared areas

Areas	Altitude above sea level (m)	Average annual temperature (℃)	Annual precipitation (mm)
Nakhchivan AR	1400	13	251
Khizi	859	11	530
Turyanchay	1025	14	500
Shamkir	331	12.5	520
Guba	600	7	700

Cones were collected from at least 10 medium generative (g 2) and healthy trees in each region. The seeds were separated from the cones manually and the seeds suspected of being damaged by insects were removed. For each region 4 trials and one control variant, 30× 5 = 150 seeds were selected for the stratification experiment and 150 seeds were selected for the implementation of complex stratification and scarification treatment.

Due to the thickness of the cover on juniper seeds, they are typically difficult to germinate naturally. In the wild, juniper seeds undergo natural scarification as they pass through the digestive tracts of animals that consume these cones. In the laboratory, scarification was carried out using a method proposed by Loutfy [3], which involves immersing the seeds in 98% sulfuric acid. A total of 150 Juniperus communis L. seeds, divided into five groups of 30 seeds each, were placed in the sulfuric acid solution for 10 minutes. After this scarification process the next stage of stratification begins.

For stratification, seeds were stored in Petri dishes (100 × 15 mm) at low temperatures (5°C) for 4, 8, 12, 16 weeks between germination papers (Munktell Filtrak ™ Grade 3 Qualitative High Purity Lab Filter Papers). Filter papers were soaked in 0.6 ml of water every 5 days.

The obtained seeds were placed in germination rooms after stratification. A stable temperature of 22 ± 1 ℃ is provided in the germination room. The seeds were examined daily and the seeds with radicle normally growing and reaching 3 mm was considered to have germinated seeds.

RESULTS AND DISCUSSION

A comparative analysis of germination rates for seeds collected from five distinct regions in the Republic of Azerbaijan, after undergoing stratification and scarification treatments at 5°C, suggests that the duration of stratification plays a crucial role in influencing these rates.

A comparison of the results by region reveals significant variations in seed germination rates, emphasizing the effects of environmental factors and stratification treatments on seed viability. Among the five regions studied, seeds collected from the Turyanchay State Nature Reserve demonstrated the lowest germination percentage. The most remarkable response to stratification measures was observed in these seeds. Under standard conditions, their germination rate was comparable to that of the other regions, but after undergoing an 8-week stratification period, germination increased by a substantial 39%. This significant improvement suggests that the seeds from Turianchai experience a strong dormancy mechanism that can be effectively overcome through cold stratification. The high response to stratification in this region may be attributed to climatic conditions, seed physiology, or genetic factors that necessitate a prolonged cold period for successful germination. This indicates that seeds from this area may possess a higher degree of dormancy, face environmental constraints that affect their viability, or have specific ecological adaptations that render them less responsive to standard germination conditions Tigabu M., et all 2007).

Seeds collected from the Khizi area showed a significantly higher germination rate under control conditions, with 21% seeds. This suggests that Khizi seeds may have inherently lower dormancy levels or experience more favorable conditions for natural germination. Furthermore, after undergoing an 8-week stratification process, the germination rate of the Khizi seeds improved by an additional approximately 10%. This indicates that while stratification positively affects the breaking of dormancy, its impact is relatively moderate compared to seeds from other regions.

The seeds collected from Shamkir showed the most notable response to stratification measures. Under standard conditions, their germination rate was similar to that of seeds from other regions. However, after an 8-week stratification period, their germination rate substantially increased by 35%. This significant improvement indicates that the seeds from Shamkir have a strong dormancy mechanism that can be effectively overcome through cold stratification.

A study on seed germination in the Guba region found that an 8-week stratification period at a constant temperature of 5°C resulted in a germination rate of 29%. However, when scarification was added as a pre-treatment, the germination percentage significantly increased to 41%. This suggests that physical or chemical scarification effectively breaks seed dormancy, allowing for improved water absorption and gas exchange, which ultimately enhances germination. As shown in Table 2, the application of scarification following stratification at 5°C significantly enhanced the germination rate. This indicates that breaking the seed coat and exposing the embryo to cold conditions helps to overcome seed dormancy.

The study revealed that after an 8-week stratification period, common juniper seeds collected from the Nakhchivan Autonomous Republic exhibited the highest germination rate. In this population, the combination of scarification and stratification resulted in a 51% germination success, suggesting that seeds from this region respond particularly well to these treatments. This response may be attributed to genetic adaptations in juniper populations growing in Nakhchivan, where climatic conditions can favor seeds that require prolonged stratification and mechanical weakening for successful germination.

In contrast, juniper seeds collected from the Khizi area showed a different response to the pre-treatment methods. While scarification alone led to a 29% germination rate, the addition of an 8-week stratification period only increased this percentage by 5%, reaching a total of 34% germination. This relatively modest improvement suggests that seeds from the Khizi population may have different dormancy mechanisms or environmental adaptations, making stratification less effective compared to those from Nakhchivan. The variation in germination responses highlights the importance of region-specific strategies when developing methods to enhance seedling establishment and forest regeneration (Rzayeva A.A.,2020).

These findings underscore the need for further research to refine stratification techniques for different populations of *Juniperus communis*. Factors such as the duration of stratification, temperature fluctuations, and moisture conditions may need to be tailored based on the specific requirements of seeds from various geographic locations. Additionally, the influence of seed coat thickness and internal physiological barriers on germination success should be further explored.

Understanding the optimal pre-treatment methods for *Juniperus communis* seeds has significant implications for conservation, reforestation, and afforestation projects. By applying targeted scarification and stratification techniques, it is possible to improve the natural regeneration of juniper forests, particularly in regions facing deforestation or climate-related habitat changes. Continued research and experimentation will help develop more effective strategies for enhancing germination rates, ensuring the sustainability of juniper populations across diverse ecological zones.

Table 2. Comparison of germination rate of *Juniperus communis* L. (*Cupressaceae* Bartl.) seeds collected from different regions of Azerbaijan Republic

Temperature	Term	Germination of seeds (in %)				
		Nakhchıvan AR	Khizi	Turyanchay	Shamkir	Guba
5º C	0 weeks	16	21	9	10	12
	4 weeks	31	26	16	14	17
	8 weeks	42	32	39	39	29
	12 weeks	39	22	25	37	21
	16 weeks	28	21	22	25	19
5 º C and scarification*	0 weeks	18	29	13	15	18
	4 weeks	38	31	23	28	25
	8 weeks	51	34	48	45	41
	12 weeks	43	22	17	31	33
	16 weeks	24	15	13	22	29

Summarizing all this, we can note that growing juniper trees for decorative purposes, higher germination can be achieved if the stratification period and temperature are adapted to the area where the seeds are collected, taking into account all these factors.

The germination rates were analyzed using one-way ANOVA ($\alpha = 0.05$). Results were expressed as mean ± SD based on four replicates ($n = 4$). Significant differences were found among populations ($p < 0.001$). The highest germination rate was recorded in seeds collected from Nakhchivan (51.2 ± 3.4%), followed by Turyanchay (48.3 ± 4.1%) and Shamkir (45.5 ± 3.8%), whereas Khizi seeds showed the lowest germination rate (34.0 ± 2.7%). These differences were statistically significant compared with the control ($p < 0.05$). The results indicate that environmental conditions and genetic adaptations significantly affect dormancy-breaking efficiency and germination success across regions

CONCLUSION

Studies have shown that the germination rate of Juniperus communis seeds varies significantly due to a combination of environmental and genetic factors. These factors include temperature, moisture availability, altitude, soil composition, and the specific dormancy mechanisms inherent to different populations of the species. The successful germination of juniper seeds is crucial for the regeneration of natural populations, especially in regions where the species plays a vital ecological role in preventing soil erosion, maintaining biodiversity, and providing habitat for wildlife.

Recent research conducted on *Juniperus communis* seeds collected from the foothills and lowlands of the Republic of Azerbaijan has demonstrated that pre-treatment methods such as scarification and cold stratification can significantly enhance germination rates. Scarification, which involves mechanically or chemically weakening the hard seed coat, facilitates water absorption and gas exchange, effectively breaking dormancy and promoting seedling emergence. Cold stratification—an extended exposure to low temperatures—mimics natural winter conditions and helps trigger the physiological changes necessary for germination. The study found that combining these treatments improved the germination success of juniper seeds from lower-altitude populations, indicating that these methods effectively overcome dormancy in such environmental conditions.

However, there remains a need to optimize stratification methods for Juniperus communis populations distributed in high mountainous regions. Seeds from these areas may exhibit deeper dormancy due to harsher environmental conditions, such as lower temperatures, reduced soil moisture, and shorter growing seasons. Developing tailored stratification techniques—potentially involving longer chilling periods, varying temperature fluctuations, or alternative scarification methods—could be essential for improving germination rates in these high-altitude populations. Further research should also investigate the genetic variability of different juniper populations and how their dormancy-breaking requirements differ across elevation gradients.

Understanding the germination dynamics of Juniperus communis is critical not only for ecological conservation efforts but also for afforestation and reforestation projects aimed at restoring degraded landscapes. By refining seed pre-treatment techniques, researchers and conservationists can enhance seedling establishment rates, thereby supporting the long-term sustainability of juniper forests in Azerbaijan.

J. communis is an excellent choice for the restoration of degraded forests. Effective pre-treatment strategies, including scarification and stratification, play a crucial role in enhancing germination and survival rates. It is imperative to select region-specific seeds to ensure successful restoration outcomes. This study provides definitive guidelines for conservationists and forestry managers to follow.

References

Adams, R. P., Tashev, A. N., & Schwarzbach, A. E. (2014). Variation in *Juniperus communis* L. trees and shrubs from Bulgaria: Analyses of nrDNA and cpDNA regions plus leaf essential oil. *Phytologia, 96*(2), 124–129.

Adams, R. P., Al-Farsi, A., & Schwarzbach, A. E. (2014). Confirmation of the southern-most population of *Juniperus seravschanica* in Oman by DNA sequencing of nrDNA and four cpDNA regions. *Phytologia, 96*(3), 218–224.

Adams, R. P. (2015). *Junipers of the world: The genus Juniperus* (3rd ed.). Bloomington, IN: Trafford Publishing.

Adams, R. P., Farzaliyev, V., Tashev, A. N., & Schwarzbach, A. E. (2015). *Juniperus communis* L. f. pygmaea in Azerbaijan: Analyses of nrDNA and cpDNA regions. *Phytologia, 97*(1), 6–11.

Adams, R. P. (2015). Allopatric hybridization and introgression between *Juniperus maritima* R. P. Adams and *J. scopulorum* Sarg.: Evidence from nuclear and cpDNA and leaf terpenoids. *Phytologia, 97*(1), 55–66.

Adams, R. P., & Thornburg, J. (2015). A survey of percent-filled and empty seeds in multiple years of observations of *Juniperus arizonica* and *J. osteosperma. Phytologia, 98*(3), 164–169.

Alpacar, G. (1988). *Studies on overcoming germination difficulties for Juniperus excelsa Bieb., J. foetidissima Willd., J. oxycedrus L., J. drupacea Labill. seeds and determination of morphological characteristics of juniper cones and seeds.* Orman Araştırma Enstitüsü, No. 197. Bursa, Turkey.

Bewley, J. D., & Black, M. (1994). *Seeds: Physiology of development and germination* (2nd ed.). New York: Plenum Press.

Bonner, F. T., & Karrfalt, R. P. (2008). *The woody plant seed manual.* USDA Forest Service, Agriculture Handbook 727. Washington, D.C.: U.S. Department of Agriculture.

Eckenwalder, J. E. (2009). *Conifers of the world: The complete reference.* Portland, OR–London: Timber Press.

Gurbanov, E. M., & Rzayeva, A. A. (2023). Comparative analysis of *Juniperus communis* L. (Cupressaceae) berry oils in Azerbaijan. In *Proceedings of the International Conference "Chemical Science and Education: Problems and Prospects of Development"* (pp. 150–153). Makhachkala.

Justice, O. L., & Bass, L. N. (1978). *Principles and practices of seed storage.* USDA Handbook 506. Washington, D.C.: U.S. Department of Agriculture.

El-Juhany, L. I., Aref, I. M., & Al-Ghamdi, M. A. (2009). Effects of different pretreatments on seed germination and early establishment of the seedlings of *Juniperus procera* trees. *World Applied Sciences Journal, 7*(5), 616–624.

Milberg, P., & Andersson, L. (1997). Does cold stratification level out differences in seed germinability between populations? *Plant Ecology, 134*(2), 225–234.

Nawaz, M. F., et al. (2022). Germination and seedling performance of *Juniperus excelsa* under different pre-treatments. *Silvae Genetica, 71*, 20–28.

Tigabu, M., Fjellström, J., Christer, P., & Teketay, D. (2007). Germination of *Juniperus procera* seeds in response to stratification and smoke treatments, and detection of insect-damaged seeds with VIS + NIR spectroscopy. *New Forests, 33*, 155–169.

Tilki, F. (2007). Preliminary results on the effects of various pre-treatments on seed germination of *Juniperus oxycedrus* L. *Seed Science and Technology, 35*, 765–770.

Rzayeva, A. A. (2023). Seed propagation of *Juniperus foetidissima* Willd. in Absheron. *Bulletin of Science and Practice,* 55–58.

Willan, R. L. (1985). *A guide to forest seed handling with special reference to the tropics.* FAO Forestry Paper 20/2. Rome: Food and Agriculture Organization of the United Nations.

Yirdaw, E., & Leinonen, K. (2002). Seed germination responses of four afromontane tree species to red/far-red ratio and temperature. *Forest Ecology and Management, 168*(1–3), 53–61

MITIGATING ENVIRONMENTAL IMPACTS WHILE BOOSTING MAIZE YIELD: THE ROLE OF OPTIMIZED PLANT DENSITY AND REDUCED NITROGEN FERTILIZATION

Ghulam Mujtaba Shah[1]|https orcid.org/0000-0002-9525-610X
Abdul Lateef Iesaqi[1]| https orcid.org/0009-0003-8635-0369
Khursheed Ur Rehman[1]| https orcid.org/0009-0004-5982-0764
Fazal Ullah[1]*| https orcid.org/0000-0002-1143-2947
Javanshir Isayev[4]|https orcid.org/0000-0003-1728-4559
Abduraimov Ozodbek[2]|https://orcid.org/0000-0001-9087-8949
Maxmudov Azizbek[2]|https://orcid.org/0000-0003-0783-3788
Murodov Sirojiddin[3]|https://orcid.org/0000-0003-2547-5910

[1]Department of Botany, Hazara University, Mansehra, Pakistan
[2] Institute of Botany, Academy of Sciences of the Republic of Uzbekistan, Tashkent, Uzbekistan
[3] Bukhara State Pedagogical Institute, Bukhara, Uzbekistan
[4]Azerbaijan Medical University, Baku, Azerbaijan

Correspondence: fazalullah.38uoswabi@gmail.com

Article Info
DOI: https://doi.org/10.30546/abc.2025.007
Pages: 10-23
Received: July 12, 2025 | Revised: Augut 16, 2025 | Accepted: September 01, 2025

Abstract

Plant density is one of the most important cultural practices determining grain yield, as well as other important agronomic attributes of this crop. Stand density affects plant architecture, alters growth and development, similarly maize productivity depends upon the external supply of nutrients, therefore application of nitrogen and adequate planting density might be a feasible technology to improve maize yield and yield components. A field study was conducted to determine the effects of plant density and nitrogen fertilization on the growth and yield of maize. The experiment was laid out in a Randomized Complete Block Design with a split-plot arrangement during the Kharif 2022 season. Treatments consisted of three plant populations (60,000, 75,000, and 90,000 plants ha^{-1}) as the main factor and three nitrogen levels (100, 150, and 200 kg N ha^{-1}) as the subplot factor. Results demonstrated that nitrogen application significantly influenced all measured parameters. The highest nitrogen level (200 kg N ha^{-1}) resulted in the greatest biological yield (13,205 kg ha^{-1}), thousand-grain weight (301.6 g), grain yield (5,057 kg ha^{-1}), and delayed physiological maturity. In contrast, plant population had a divergent effect: the highest plant density (90,000 plants ha^{-1}) produced the maximum biological yield (13,455 kg ha^{-1}), while the lowest density (60,000 plants ha^{-1}) optimized grain yield (5,091 kg ha^{-1}) and harvest index (41%). The interaction between plant population and nitrogen was not significant for any parameter. It is concluded that for the maize variety "Jalal" in the agro-climatic conditions of Swabi, a combination of a lower plant population (60,000 plants ha^{-1}) with a high nitrogen rate (200 kg ha^{-1}) is the most effective strategy for maximizing grain yield and harvest index.

Keywords: *plant density, nitrogen management, maize yield, sustainable agriculture, environmental impact, nitrogen use efficiency, harvest index.*

INTRODUCTION

Maize (*Zea mays* L.) Family (poaceae) is the third most important cereal crop after wheat and rice in Pakistan. it is consumed as human and animal food and provides a major raw material for starch industry.it is short duration and quick growing crop and is potentially capable of production very high quantity of grain per unit area. Grain yield is the combined outcome of genetic potential and environment relations. Variability in genetic potential among varieties is a major component of variable yield. average maize yield in Pakistan is an account of suboptimal plant density, inadequate fertilizer use, insufficient water supply, weed infestation, insect pest attack and the selection of unsuitable cultivars under a given set environment (Tahir et al., 2008).

Maize is an important food and feeds crop of the world. In Pakistan, area under maize occupies third position after wheat and rice 98% of which is grown in Pakistan Punjab and Khyber Pakhtunkhwa. In Pakistan, Maize is grown on an area of 1.016 million hectares with an annual production of 3.037-million-hectare tons of grain and average grain yield of about 2864 kg / ha_1 (GOP,2019). Maize grain has high nutritional value as it contains 72% starch ,10% protein,4.8% oil, 8.5% fiber,3% sugar and 1%ash. (Chaudhary, 1983; Mondal et al., 1992).

Its commercial products are corn oils, corn flakes, corn starch, tanning material for leather industry, custard, glucose, jelly, energize etc. improved quantities of corn have been used in the manufacturing compound, soap, varnishes, paints and similar other products (Martin et al., 1975).

Maize is a standout amongst the most potential oats that become all around and is the third after wheat and rice altogether sustenance grain generation. because of its high versatility and profitability. Maize being the most noteworthy yielding grain crop on the planet is of critical significance for nations such as Pakistan. In Pakistan maize is imperative oat after wheat and rice represents 4.8% of the aggregate trimmed territory and 3.5% of the estimation of farming yield. The mass (97%) of the generation originates from two noteworthy areas, KPK, representing 57% of the aggregate range and 68% of aggregate creation and Punjab contributes 38% land with 30% of aggregate maize grain creation. Almost no maize 2-3% is created around Sindh. Additionally, an extremely developing and high yielding segment of maize, the spring maize range and generation in Punjab is not represented, which covers around 0.070 million tons of maize grains being delivered (Shah, et al., 2014).

Stand density affects plant architecture, alters growth and developmental patterns and influence carbohydrate production. At low densities, many modern maize varieties do not tiller effectively and quite often produce only one ear per plant. Whereas, the use of high population increases interplant competition for light, water and nutrients, which may be detrimental to final yield because it stimulates apical dominance, induces barrenness, and ultimately decreases the number of ears produced per plant and kernels set per ear (Sangoi, 2001).

There are several biotic and abiotic factors that affect maize yield considerably; however, it is more affected by variations in plant density than other members of the grass family (Abuzar et al., 2011).

Plant populations affect most growth parameters of maize even under optimal growth conditions and therefore it is considered a major factor determining the degree of competition between plants (Sangakkara et al., 2012). The grain yield per plant is decreased in response to decreasing light and other environmental resources available to each plant (Luque et al., 2006).

Maize is one of Pakistan's main crops, but its production is very limited in Khyber Pakhtunkhwa (KP) Province. (Amanullah et al., 2009, 2016). Among the cereals its ranks third because of its importance. It is short-term plant with the ability to produce large quantities of food grain (Niwamanya et al., 2025). It is becoming popular amongst growers because of its multifunctional uses such as food for humans, raw materials for various industries and animal feed. Maize grain is a good source of fat, minerals, starch, protein, vitamin (Mian et al., 2021). Maize has an important nutrient value with about 72% starch, protein approximately 10%, and fiber up to 12% and oils approximately 3% (Swati et al., 2024). Maize is an important staple cereal crop in Pakistan and is a major source of income and food security for many farmers (Ahmad et al., 2020).

Nitrogen (N) is an important plant yield limiting macronutrient. Plants take N in the form of ammonia and nitrate (Javed et al., 2022). It is an imperative element for proper growth and development of the plant, enhance yield and improve quality by playing a key role in the physiochemical functions of the plant (Leghari et al., 2016). Nitrogen is a key component of chlorophyll, protein, and amino acids, and it plays an important role in maize yield (Mohammed et al., 2025). Large amounts of inorganic nitrogen are lost during crop development, resulting in soil, water and environmental pollution (Mattas et al., 2011). In such scenario, combining organic and inorganic fertilizers improves crop production and yield components while also improving soil structure (Zhang et al., 2016).

Objectives:

To investigate the effect of plant population on yield and yield components of maize crops.

To determine the optimum rate of nitrogen fertilizer for high maize production.

To study the interactive effect of plant population and nitrogen levels for yields and yields components of maize crop

MATERIALS AND METHODS

A field experiment was conducted during the Kharif season of 2022. The experiment was laid out in a Randomized Complete Block Design (RCBD) with a split-plot arrangement, replicated three times. Plant population levels were assigned to the main plots, and nitrogen levels were assigned to the sub-plots.

Factor A *Plant population (ha^{-1}) — Main plot*

P_1 = 60,000

P_2 = 75,000

P_3 = 90,000

Factor B *Nitrogen (kg ha^{-1}) — Subplot*

N_1 = 100

N_2 = 150

N_3 = 200

Each replication consisted of nine treatments (3 x 3 = 9) having three levels of plant population (60,000, 75,000 and 90,000 ha^{-1}) which were allotted to main plot and three levels of nitrogen (100, 150 and 200 kg ha^{-1}) which were allotted to subplot. Plot size of 5m x 3m ($15m^{-2}$) was used accommodating 5 rows for P_1, 4 rows for P_2 and 3 rows for P_3. Plant population (P_1) was maintained by planting 50cm x 20cm, R-R and P-P distance respectively by accommodating 150 plants per plot. Similarly plant population (P_2) was maintained by planting 75cm x 20cm, R-R and P-P distance respectively accommodating 100 plants per plot while for P_3, 75 plants per plot were maintain by keeping 100cm x 20cm R-R and P-P distance respectively. The field was twice ploughed through cultivator and rotavator and then leveled through back leveler. Maize variety (Jalal) was sown in the first week of July 2022. The required nitrogen (N) rates were applied from Urea in two equal splits i.e., half at sowing, and half with first irrigation after emergence. All agronomic and management practices were kept uniformly for each experimental unit.

Data was collected on following parameters during the experiment:

1. Days to physiological maturity

Days to maturity were recorded by counting the number of days from sowing till 75% of plants reached to physiological maturity in each plot indicated by turning yellow the color of spikes (Rajendra, 2017).

2. Biological yield (kg ha^{-1})

Biological yield was recorded by harvesting four central rows in each plot. The harvested materials were then sun dried, weighed and converted into kg ha^{-1}.

$$Biological\ yield = \frac{Biological\ yield\ off\ our\ central\ rows}{No.\ of\ rows\ harvested \times row\ to\ row\ distance \times row\ length} \times 10000\ \mathrm{m}^2 5$$

3. Thousand grains (g)

A sample of thousand grains was counted using electronic grains counting machine and separated for each plot. The grains were then weighed with the help of a sensitive electronic balance, and thousand grains weight was noted.

4. Grain yield (kg ha^{-1})

The harvested material for obtaining biological yield was threshed using a mini wheat thresher and the grains obtained were weighed with the help of a sensitive digital balance and then data were converted to kg ha^{-1}. Formula for grain yield:

$$\text{Grain yield} = \frac{\text{Grain yield of four centralrows}}{\text{No. of rows } \times R - R \text{ distance} \times \text{row length}} \times 10000\ \text{m}^2$$

5. Harvest index (%)

Harvest index for each p1ot was calculated by using the fol1owing formula:

$$\text{Grain yield} = \frac{\text{Grain yield of four centralrows}}{\text{No. of rows } \times R - R \text{ distance} \times \text{row length}} \times 10000\ \text{m}^2$$

Statistical analysis:

Data recorded on each parameter was subjected to analysis of variance (ANOVA) techniques appropriate for a Randomized Complete Block Design (RCBD) with a split-plot arrangement having three replications to compare the meaning differences among different plant populations and to assess the effect of nitrogen on various parameters.

RESULTS AND DISCUSSION

1. Days to physiological maturity

Data regarding number of days to physiological maturity is presented in (Table 1& fig. 1). Analysis of the data showed that nitrogen significantly affected days to physiological maturity of maize, while plant population had no significant effect on days to physiological maturity. Mean data regarding the different levels of nitrogen showed that maturity delayed (103 to 107 days) as nitrogen rate increased from 100 to 200 kg ha^{-1}, respectively. However, the interaction between the different plant populations and nitrogen was also not significant for days to physiological maturity. The reason for delayed maturity due to N might be the better growth and development with the application of N which enhanced the lifecycle of the crop and delayed the maturity. These results are in line with (Imran et al., 2021; Vyas and Gulati. 2009) who reported a significant effect of N on days to maturity of maize.

Table 1. Number of days to physiological maturity of maize as affected by plant population and different levels of nitrogen.

Nitrogen (Kg ha^{-1})	Plant Population (ha^{-1})			Mean
	60,000	75,000	90,000	
100	103	103	103	103 c
150	105	105	105	105 b
200	108	107	107	107 a
Mean	105	105	105	

LSD(P<0.05) for plant population (PP) = NS
LSD(P<0.05) for nitrogen (N) = 1.80
LSD(P<0.05) for PP x N = NS

Means of the levels of each factor are significantly different at P value equal or less than 0.05, presented by various letters (a, b, c) using LSD test.

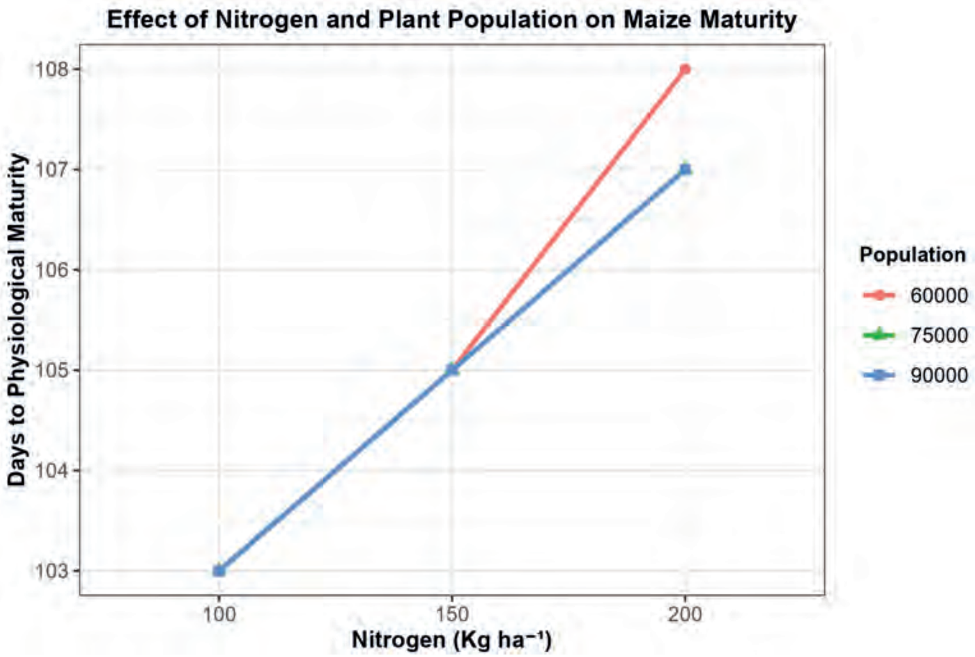

Figure 1. Number of days to physiological maturity of maize as affected by plant population and different levels of nitrogen.

2. Biological yield (kg ha^{-1})

The effect of plant population and nitrogen on biological yield is presented in Table 2. Analysis of the data indicated that plant populations and nitrogen levels significantly affected biological yield of maize. Highest rate of N (200 kg ha^{-1}) resulted in maximum biological yield (13205 kg ha^{-1}), while minimum biological yield (12661 kg ha-1) was recorded with the lowest rate of N (100 kg ha^{-1}). Likewise higher biological yield (13455 kg ha^{-1}) was recorded in the plots where plant population was maintained higher (90,000 ha^{-1}), while lower biological yield (12424 kg ha^{-1}) was noted in the plots where plant population was maintained lower (60,000 ha^{-1}). Similar results were earlier reported (Ali et al., 2012; Imran et al., 2015). Plant density is one of the most important cultural practices determining biological and grain yield, as well as other important agronomic attributes of this crop. Stand density affects plant architecture, alters growth and developmental patterns and influences carbohydrate production and partition (Casal, 1985).

Table 2. Biological yield (kg ha^{-1}) of maize as affected by plant population and different levels of nitrogen

Nitrogen (kg ha^{-1})	Plant Population (ha^{-1})			Mean
	60,000	75,000	90,000	
100	12172	12537	13274	12661 c
150	12474	12828	13249	12850 b
200	12628	13146	13841	13205 a
Mean	12424 b	12837 b	13455 a	

LSD(P<0.05) for plant population (PP) = 217
LSD(P<0.05) for nitrogen (N) = 246
LSD(P<0.05) for PP x N = NS

Means of the levels of each factor are significantly different at P value equal or less than 0.05, presented by various letters (a, b, c) using LSD test.

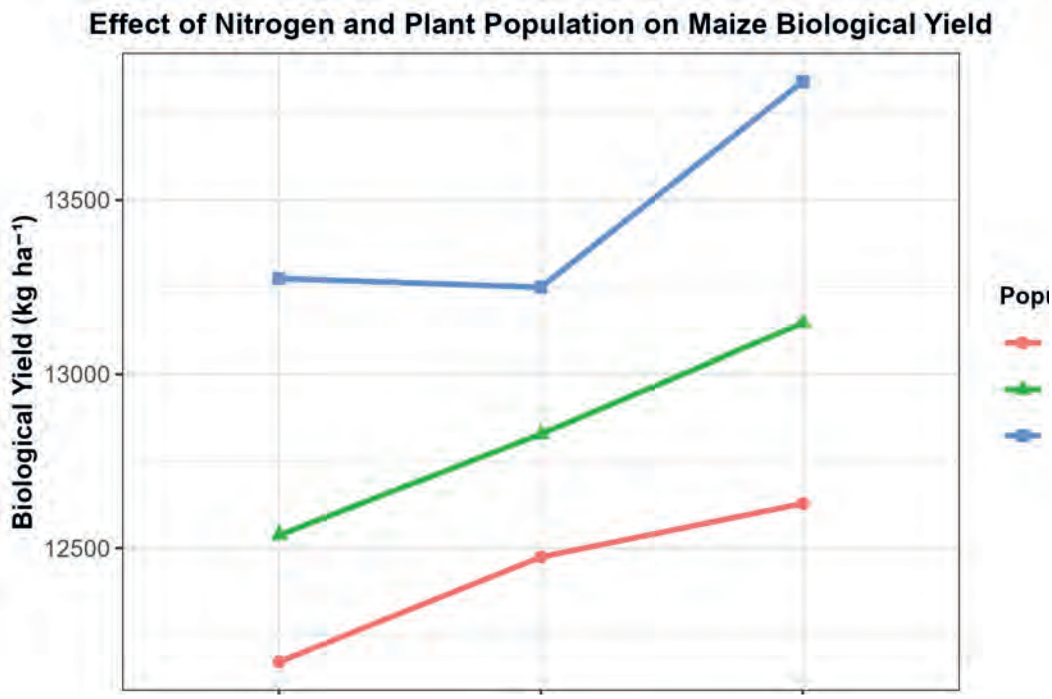

Figure 2. Biological yield (kg ha-1) of maize as affected by plant population and different levels of nitrogen.

Thousand grain weight (g)

Analysis of the data indicated that plant populations and nitrogen levels significantly affected thousand grain weight of maize, while the interaction between the different plant populations and nitrogen was not significant (Table 5). Highest rate of N (200 kg ha^{-1}) resulted highest thousand grain weight (301.6g), followed by 150 kg N ha^{-1} (289.9g), while lowest thousand grain weight (282.1g) was recorded with the lowest rate of N (100 kg ha^{-1}). Likewise higher thousand grain weight (304.8g) was observed in the plots where plant population was kept lower (60,000 ha^{-1}), while minimum thousand grain weight (278.1g) were noted in the plots where plant population was maintained higher (90,000 ha^{-1}). Hossain, (2015) stated that maximum thousand grain weight was produced by planting density of 45000 plants ha^{-1} when compared with other treatments.

Table 3. Thousand grains weight (g) of maize as affected by plant population and different levels of nitrogen.

Nitrogen (kg ha^{-1})	Plant Population (ha^{-1})			Mean
	60,000	75,000	90,000	
100	295.7	286.7	264.1	282.1 c
150	303.2	288.3	278.0	289.9 b
200	315.5	297.0	292.3	301.6 a
Mean	304.8 a	290.7 b	278.1 c	

LSD(P<0.05) for plant population (PP) = 12.40
LSD(P<0.05) for nitrogen (N) = 7.88
LSD(P<0.05) for PP x N = NS

Mean of the levels of each factor are significantly different at P value equal or less than 0.05, presented by various letters (a, b, c) using LSD test.

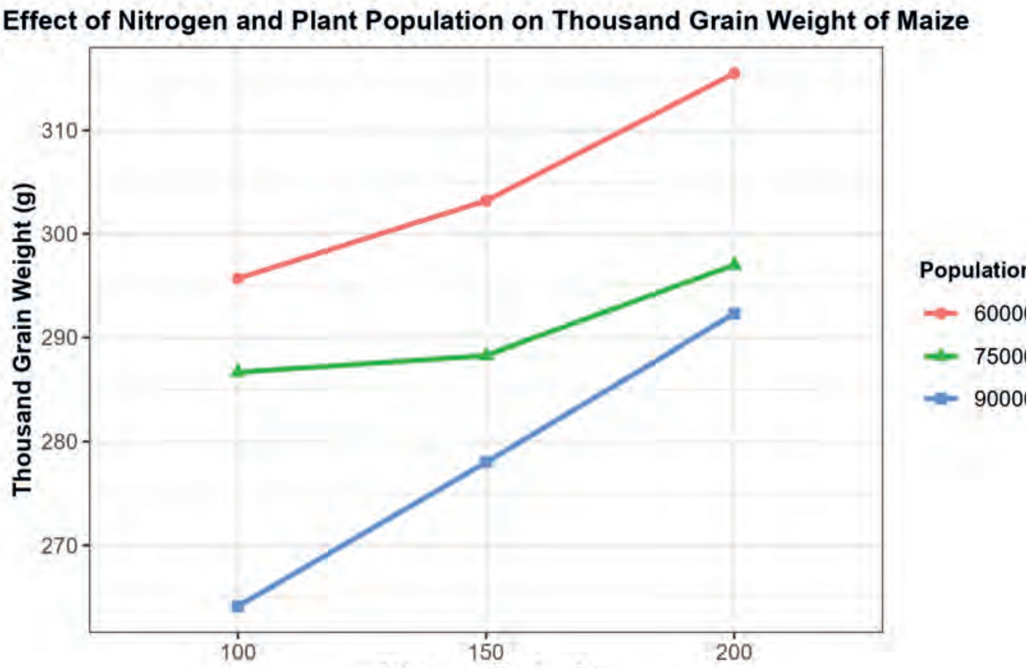

Figure 3. Thousand grains weight (g) of maize as affected by plant population and different levels of nitrogen.

4. Grain yield (kg ha^{-1})

The effect of plant population and nitrogen on grain yield is presented in Table 4. Analysis of the data indicated that plant populations and nitrogen levels significantly affected grain yield of maize, while the interaction between the different plant populations and nitrogen was not significant. Highest rate of N (200 kg ha^{-1}) resulted maximum grain yield (5057 kg ha^{-1}), while minimum grain yield (5003kg ha^{-1}) was recorded with the lowest rate of N (100 kg ha^{-1}). Likewise higher grain yield (5091 kg ha^{-1}) was recorded in the plots where plant population was maintained lower (60,000 ha^{-1}), while lower grain yield (4966 kg ha^{-1}) was noted in the plots where plant population was maintained higher (90,000 ha^{-1}). The increase in grain yield due to combining application of P form organic and inorganic source might be due to the higher yield components like grains ear^{-1} and higher growth with the application of P from combining organic and inorganic sources. These results are in agreement of those reported by (Adamu et al., 2015; Ali et al., 2012) who reported higher grain yield with the combined application of P from organic and inorganic sources. Maize grain yield declines when plant density is increased beyond the optimum plant density primarily because of decline in the harvest index and increased stem lodging (Tollenaar *et al*., 1997).

Table 4. Grain yield (kg ha-1) of maize as affected by plant populsation and different levels of nitrogen.

Nitrogen (kg ha^{-1})	Plant Population (ha^{-1})			Mean
	60,000	75,000	90,000	
100	5059	4995	4953	5003 b
150	5098	5024	4956	5026 b
200	5117	5065	4988	5057 a
Mean	5091 a	5028 b	4966 c	

LSD(P<0.05) for plant population (PP) = 30
LSD(P<0.05) for nitrogen (N) = 29
LSD(P<0.05) for PP x N = NS

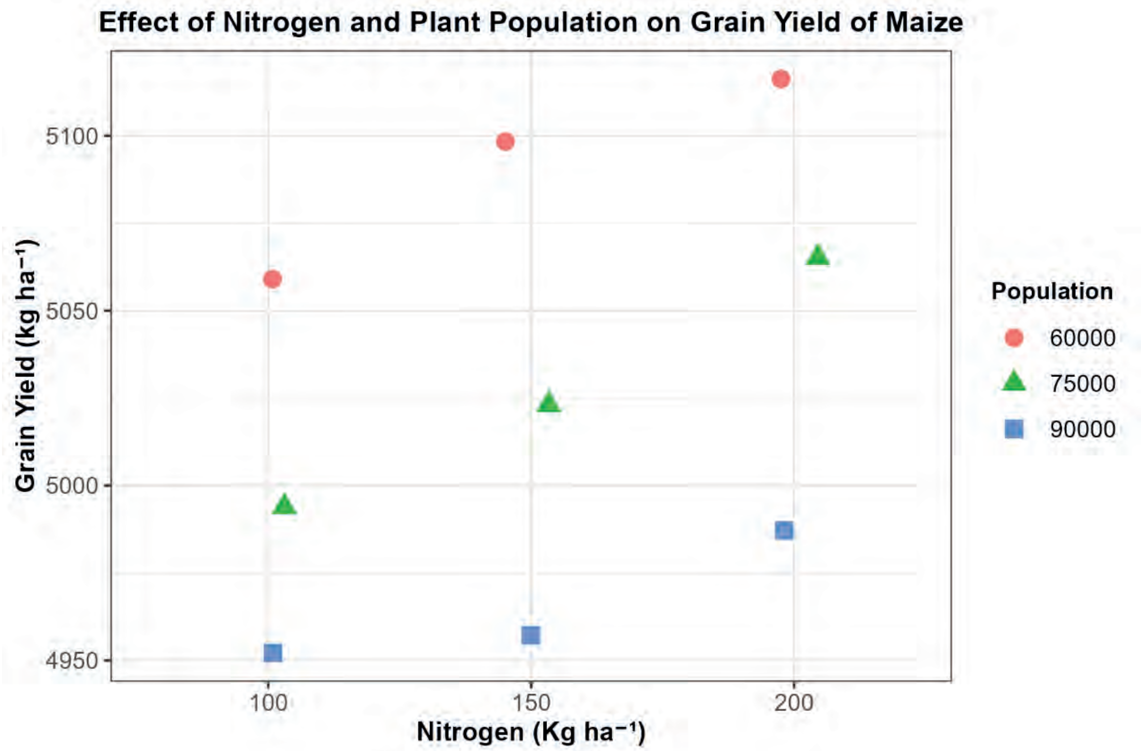

Figure 4. Grain yield (kg ha-1) of maize as affected by plant population and different levels of nitrogen.

5. Harvest index (%)

Data regarding harvest index (%) is presented in Table 5. Analysis of the data showed that plant population and nitrogen significantly affected harvest index of maize. The different levels of nitrogen had a minute effect on harvest index as there was no significant difference observed between the mean values of harvest index. Likewise higher harvest index (41%) was recorded in the plots where plant population was maintained lower (60,000 ha^{-1}) as compared to the plots where plant population (75,000 and 90,000) was maintained higher (39.2 and 36.9%), respectively. The interaction between the different plant populations and nitrogen was not significant. The harvest index is the ratio of grain yield to biological yield which increased with higher grain ratio the probable reason for higher harvest index might be that higher grain to Stover ratio due to combining application of organic and inorganic P similar results were reported earlier by (Ali *et al*., 2019; Ochami, 2021).

Table 5. Harvest index (%) of maize as affected by plant population and different levels of nitrogen.

Nitrogen (kg ha^{-1})	Plant Population (ha^{-1})			Mean
	60,000	75,000	90,000	
100	41.6	39.8	37.3	39.6 a
150	40.9	39.2	37.4	39.2 a
200	40.5	38.5	36.0	38.4 a
Mean	41.0 a	39.2 b	36.9 c	

LSD($P<0.05$) for plant population (PP) = 0.50
LSD($P<0.05$) for nitrogen (N) = 0.87
LSD($P<0.05$) for PP x N = NS

Mean of the levels of each factor are significantly different at P value equal or less than 0.05, presented by various letters (a, b, c) using LSD test.

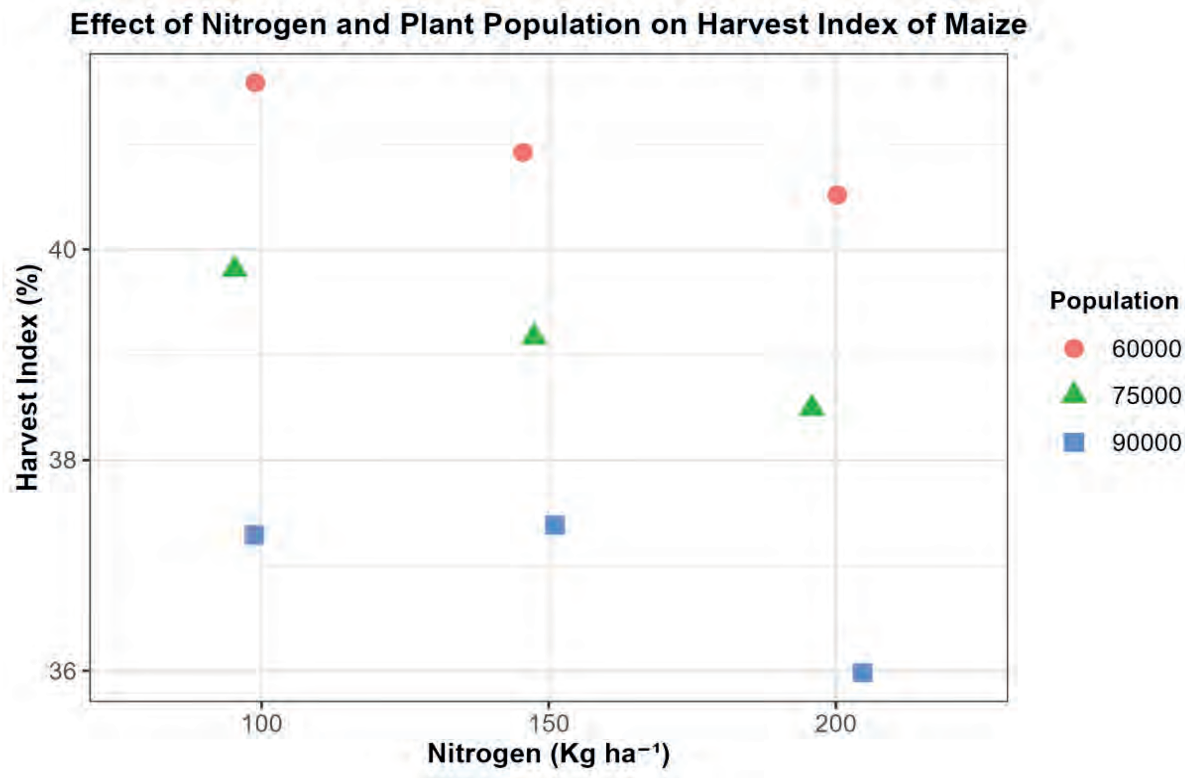

Figure 5. Harvest index (%) of maize as affected by plant population and different levels of nitrogen.

CONCLUSION

Based on the findings of this study, it can be concluded that both nitrogen application and plant population significantly influence the growth and yield of maize. The results demonstrate that a higher nitrogen level of 200 kg ha^{-1} was optimal for enhancing key yield parameters, including biological yield, thousand grain weight, grain yield, and harvest index. Conversely, among the plant populations tested, a lower density of 60,000 plants ha^{-1} proved to be more beneficial for maximizing grain yield, biological yield, and harvest index compared to higher densities. Therefore, for the maize variety 'Jalal' under the agro-climatic conditions of Swabi during the Kharif season, the combination of a lower plant population (60,000 plants ha^{-1}) with a higher nitrogen rate (200 kg ha^{-1}) appears to be the most effective strategy for optimizing yield and yield-related attributes. This suggests that under these experimental conditions, compensating for lower plant density with enhanced nutrient supply per plant is a more productive approach than relying on higher plant populations.

References

Abuzar, M. R., Sadozai, G. U., Baloch, M. S., Baloch, A. A., Shah, I. H., Javaid, T., & Hussain, N. (2011). Effect of plant population densities on yield of maize. *The Journal of Animal & Plant Sciences, 21*(4), 692–695.

Adamu, U. K., Mrema, J. P., & Msaky, J. J. (2015). Growth response of maize (*Zea mays* L.) to different rates of nitrogen, phosphorus and farm yard manure in Morogoro urban district, Tanzania.

Ahmad, I., Ahmad, B., Boote, K., & Hoogenboom, G. (2020). Adaptation strategies for maize production under climate change for semi-arid environments. *European Journal of Agronomy, 115*(12), 60–40.

Ali, W., Ali, M., Kamal, A., Uzair, M., Ullah, N., Khan, M. D., & Khalil, M. K. (2019). Maize yield response under various phosphorus sources and their ratios. *European Journal of Experimental Biology, 9*(1), 5.

Amanullah, Khattak, R. A., & Khalil, S. K. (2009). Plant density and nitrogen effects on maize phenology and grain yield. *Journal of Plant Nutrition, 32*(2), 246–260.

Amanullah, S. A., Iqbal, A., & Fahad, S. (2016). Foliar phosphorus and zinc application improve growth and productivity of maize (*Zea mays* L.) under moisture stress conditions in semi-arid climates. *Journal of Microbial & Biochemical Technology, 8*(5), 433–439.

Casal, J. J., Deregibus, V. A., & Sanchez, R. A. (1985). Variations in tiller dynamics and morphology in *Lolium multiflorum* Lam. vegetative and reproductive plants as affected by differences in red/far-red irradiation. *Annals of Botany, 56*(4), 553–559.

Chaudhary, A. R. (1983). *Maize in Pakistan.* Agriculture Research Coordination Board, University of Agriculture Faisalabad.

Hossain, M. (2015). *Effect of planting configuration on the growth and yield of white maize* [Doctoral dissertation, Department of Agronomy].

Imran, M., Ali, A., & Safdar, M. E. (2021). The impact of different levels of nitrogen fertilizer on maize hybrids performance under two different environments. *Asian Journal of Agriculture and Biology, 2021*(4).

Imran, S., Arif, M., Khan, A., Khan, M. A., Shah, W., & Latif, A. (2015). Effect of nitrogen levels and plant population on yield and yield components of maize. *Advances in Crop Science and Technology, 3*(2), 1–7.

Javed, T., Iqbal, I., Singhal, R. K., Shabbir, R., Shah, A. N., Kumar, P., ... & Siuta, D. (2022). Recent advances in agronomic and physio-molecular approaches for improving nitrogen use efficiency in crop plants. *Frontiers in Plant Science, 13*, 877544.

Leghari, S. J., Wahocho, N. A., Laghari, G. M., Hafeez-Laghari, A., Mustafa-Bhabhan, G., Hussain-Talpur, K., ... & Lashari, A. A. (2016). Role of nitrogen for plant growth and development: A review. *Advances in Environmental Biology, 10*(9), 209–219.

Luque, S. F., Cirilo, A. G., & Otegui, M. E. (2006). Genetic gains in grain yield and related physiological attributes in Argentine maize hybrids. *Field Crops Research, 95*(2–3), 383–397.

Martin, J. H., Leonard, W. H., & Stamp, D. L. (1975). *Principles of field crop production.*

Mattas, K. K., Uppal, R. S., & Singh, R. P. (2011). Effect of varieties and nitrogen management on the growth, yield and nitrogen uptake of durum wheat. *Research Journal of Agricultural Sciences, 2*(2), 376–380.

Mian, I., Anwar, Y., Khan, S., Muhammad, M. W., Mussarat, M., Tariq, M., ... & Ali, J. (2021). Integrated influence of phosphorus and zinc along with farmyard manure on the yield and nutrients uptake in spring maize. *Egyptian Journal of Soil Science, 61*(2), 241–258.

Mohammed, T. A., & Ismaiel, R. R. (2025). Impact of different levels of nitrogen fertilization on physiological traits, forage yield and yield components of some maize (*Zea mays* L.) hybrids. *Journal of Medicinal and Industrial Plants, 3*(1), 16–28.

Mondal, S. S., Verma, D., & Kuila, S. (1992). Effect of organic and inorganic sources of nutrients on growth and seed yield of sesame (*Sesamum indicum*).

Niwamanya, A., Nsanzumukiza, M. V., & Singirankabo, J. (2025). The impact of climate variability on maize production in Rwanda: A case of Nyagatare District from 2015–2023. *Journal of Agriculture & Environmental Sciences, 9*(3), 45–55.

Ochami, F. A. (2021). *Effect of spacing and number of plants per hill on growth and yield of SC Duma 43 in the coastal lowlands* [Doctoral dissertation, KeMU].

Rajendra, M. K. S. (2017). *Assessment of promising genotypes of wheat for quality parameters (Triticum aestivum L.)* [Doctoral dissertation, Mahatma Phule Krishi Vidyapeeth].

Sangakkara, R., Wijesinghe, D., Amarasekera, P., Bandaranayake, S., & Stamp, P. (2012). Growth, yields and nitrogen use of open-pollinated and hybrid maize (*Zea mays* L.) as affected by organic matter and its placement in minor seasons of Asia. *Maydica, 57*(4), 284–292.

Sangoi, L. (2001). Understanding plant density effects on maize growth and development: An important issue to maximize grain yield. *Ciência Rural, 31*, 159–168.

Shah, F. U., Sajid, G. M., & Siddiqui, S. U. (2014). Evaluation of mulching materials as integrated weed management component in maize crop. *Pakistan Journal of Agricultural Research, 27*(2).

Swati, P., Rasane, P., Kaur, J., Kaur, S., Ercisli, S., Assouguem, A., ... & Singh, J. (2024). The nutritional, phytochemical composition, and utilisation of different parts of maize: A comparative analysis. *Open Agriculture, 9*(1), 20220358.

Tahir, M., Tanveer, A., Ali, A., Abbas, M., & Wasaya, A. (2008). Comparative yield performance of different maize hybrids under local conditions of Faisalabad, Pakistan. *Pakistan Journal of Life and Social Sciences, 6*, 118–120.

Tollenaar, M., Aguilera, A., & Nissanka, S. P. (1997). Grain yield is reduced more by weed interference in an old than in a new maize hybrid. *Agronomy Journal, 89*(2), 239–246.

Vyas, P., & Gulati, A. (2009). Organic acid production *in vitro* and plant growth promotion in maize under controlled environment by phosphate-solubilizing fluorescent *Pseudomonas*. *BMC Microbiology, 9*(1), 174.

Zhang, H. Q., Yu, X. Y., Zhai, B. N., Jin, Z. Y., & Wang, Z. H. (2016). Effect of manure. *IOP Conference Series: Earth and Environmental Science, 39*, 12–48.

APPENDICES

Appendix-A

Table 1. Analysis of variance of number of days to physiological maturity of maize as affected by plant population and different levels of nitrogen.

Source of Variation (SOV)	DF	SS	MS	F-Value	Probability	Significance
Replication	2	4.22	2.11	0.66	0.57	NS
Plant Population	2	0.89	0.44	0.14	0.88	NS
Error 1 (Main Plot)	4	12.89	3.22			
Nitrogen	2	80.22	40.11	13.05	0.00	***
PP × N	4	1.56	0.39	0.13	0.97	NS
Error 2 (Sub Plot)	12	36.89	3.07			
Total	26	136.67				

CV_1 (%) = 1.71
CV_2 (%) = 1.67

Table 2. Analysis of variance of biological yield (kg ha^{-1}) of maize as affected by plant population and different levels of nitrogen.

Source of Variation (SOV)	DF	SS	MS	F-Value	Probability	Significance
Replication	2	71 994.74	35 997.37	1.31	0.37	NS
Plant Population	2	4 841 140.07	2 420 570.04	88.08	0.00	***
Error 1 (Main Plot)	4	109 923.70	27 480.93			
Nitrogen	2	1 373 582.74	686 791.37	12.01	0.00	**
PP × N	4	179 243.04	44 810.76	0.78	0.56	NS
Error 2 (Sub Plot)	12	685 964.22	57 163.69			
Total	**26**	**7 261 848.52**				

CV_1 (%) = 1.28
CV_2 (%) = 1.85

Table 3. Analysis of variance of thousand-grain weight (g) of maize as affected by plant population and different levels of nitrogen.

Source of Variation (SOV)	DF	SS	MS	F-Value	Probability	Significance
Replication	2	28.29	14.14	0.16	0.86	NS
Plant Population	2	3 203.95	1 601.97	17.84	0.01	*
Error 1 (Main Plot)	4	359.19	89.80			
Nitrogen	2	1 731.90	865.95	16.76	0.00	***
PP × N	4	251.77	62.94	1.22	0.35	NS
Error 2 (Sub Plot)	12	620.08	51.67			
Total	**26**	**6 195.18**				

CV_1 (%) = 3.25
CV_2 (%) = 2.47

Table 4. Analysis of variance of grain yield (kg ha^{-1}) of maize as affected by plant population and different levels of nitrogen.

Source of Variation (SOV)	DF	SS	MS	F-Value	Probability	Significance
Replication	2	330.30	165.15	0.31	0.75	NS
Plant Population	2	71 316.96	35 658.48	67.10	0.00	***
Error 1 (Main Plot)	4	2 125.70	531.43			
Nitrogen	2	13 212.74	6 606.37	8.25	0.01	**
PP × N	4	1 615.93	403.98	0.50	0.73	NS
Error 2 (Sub Plot)	12	9 612.67	801.06			
Total	**26**	**98 214.30**				

CV_1 (%) = 0.46
CV_2 (%) = 0.56

Table 5. Analysis of variance of harvest index (%) of maize as affected by plant population and different levels of nitrogen.

Source of Variation (SOV)	DF	SS	MS	F-Value	Probability	Significance
Replication	2	0.87	0.44	2.94	0.16	NS
Plant Population	2	74.92	37.46	252.21	0.00	***
Error 1 (Main Plot)	4	0.59	0.15			
Nitrogen	2	6.75	3.37	4.75	0.03	*
PP × N	4	1.06	0.26	0.37	0.82	NS
Error 2 (Sub Plot)	12	8.53	0.71			
Total	**26**	**92.72**				

CV_1 (%) = 0.99
CV_2 (%) = 2.16

Note. *CV_1 and CV_2 represent the coefficients of variation for the main-plot and subplot errors, respectively.*
*NS = non-significant; * = significant ($p < 0.05$); ** = highly significant ($p < 0.01$); *** = very highly significant ($p < 0.001$).*

Appendix B

Table 1. Replicated data of number of days to physiological maturity of maize as affected by plant population and different levels of nitrogen.

Plant population (ha^{-1})	Nitrogen ($kg\ ha^{-1}$)	Rep 1	Rep 2	Rep 3
60 000	100	102	104	104
	150	105	104	106
	200	107	110	106
75 000	100	103	103	102
	150	106	106	104
	200	109	105	106
90 000	100	104	102	103
	150	104	106	105
	200	111	104	107

Table 2. Replicated data of biological yield ($kg\ ha^{-1}$) of maize as affected by plant population and different levels of nitrogen.

Plant population (ha^{-1})	Nitrogen ($kg\ ha^{-1}$)	Rep 1	Rep 2	Rep 3
60 000	100	11 897	12 387	12 231
	150	12 589	12 520	12 312
	200	13 008	12 534	12 341
75 000	100	12 432	12 552	12 627
	150	12 749	13 002	12 734
	200	13 367	13 087	12 984
90 000	100	13 234	13 453	13 134
	150	12 876	13 542	13 330
	200	13 856	13 698	13 970

Table 3. Replicated data of thousand-grain weight (g) of maize as affected by plant population and different levels of nitrogen.

Plant population (ha^{-1})	Nitrogen ($kg\ ha^{-1}$)	Rep 1	Rep 2	Rep 3
60 000	100	290.0	293.0	304.0
	150	298.1	300.4	311.2
	200	310.2	315.6	320.8
75 000	100	290.0	283.0	287.0
	150	281.0	301.0	283.0
	200	307.0	288.0	296.0
90 000	100	264.8	267.5	260.0
	150	278.0	276.0	280.0
	200	289.0	305.0	283.0

Table 4. Replicated data of grain yield (kg ha^{-1}) of maize as affected by plant population and different levels of nitrogen.

Plant population (ha^{-1})	Nitrogen (kg ha^{-1})	Rep 1	Rep 2	Rep 3
60 000	100	5 063	5 054	5 061
	150	5 145	5 084	5 065
	200	5 087	5 143	5 121
75 000	100	4 993	4 983	5 010
	150	5 041	5 022	5 008
	200	5 032	5 043	5 121
90 000	100	4 934	4 950	4 976
	150	4 956	4 960	4 951
	200	4 975	5 002	4 986

Table 5. Replicated data of harvest index (%) of maize as affected by plant population and different levels of nitrogen.

Plant population (ha^{-1})	**Nitrogen (kg ha^{-1})**	**Rep 1**	**Rep 2**	**Rep 3**
60 000	100	42.56	40.80	41.38
	150	40.87	40.61	41.14
	200	39.11	41.03	41.50
75 000	100	40.16	39.70	39.68
	150	39.54	38.62	39.33
	200	37.64	38.53	39.44
90 000	100	37.28	36.79	37.89
	150	38.49	36.63	37.14
	200	35.91	36.52	35.69

ANALYSIS OF THE PHYTOCHEMICAL COMPOSITION OF *SAPONARIA OFFICINALIS* L. SPECIES IN THE FLORA OF THE NAKHCHIVAN AUTONOMOUS REPUBLIC

Enzala Novruzova[1]* / https://orcid.org/0009-0003-3547-6025
Tariyel Talibov[2] / https://orcid.org/0000-0001-6455-8255

[1*,2]Nakhchivan State University, AZ7012, University Campus, Nakhchivan, Azerbaijan

Correspondence: enzale80@gmail.com

Article Info:
DOI: https://doi.org/10.30546/abc.2025.009
Pages: 24-31
Received: July 29, 2025 | Revised: August 06, 2025 | Accepted: September 01, 2025

Abstract

The growing demand for safe, natural alternatives to synthetic antioxidants—many of which are linked to adverse health effects—has intensified interest in plant-derived bioactive compounds. This study investigates the phytochemical composition and antioxidant activity of Saponaria officinalis L. (Caryophyllaceae), cultivated within the cultural flora of the Nakhchivan Autonomous Republic. Chromatographic and spectrophotometric techniques were employed to identify key classes of secondary metabolites, including flavonoids, carotenoids, anthocyanins, alkaloids, and saponins.

Ethanol extracts of leaves and flowers demonstrated strong antioxidant potential, with DPPH radical-scavenging inhibition rates of 87.6% and 86.4% at 50 mg/mL concentration, respectively. Chromatographic analysis revealed the presence of flavone, 3-hydroxyflavone, and β-carotene in leaf extracts, as well as apigenin, flavanones, and hydroxyflavones in flower extracts. Spectrophotometric data identified chlorophyll peaks at 664 nm and carotenoid absorption at 470 nm. The total phenolic content of aerial parts was quantified as 7.12 µg/mg gallic acid equivalents (GAE).

These findings suggest that S. officinalis L. is a potent natural source of antioxidant compounds with potential applications in pharmaceutical, nutraceutical, and cosmetic industries as an alternative to synthetic antioxidants.

Keywords: *Saponaria officinalis L.; antioxidant activity; phytochemicals; flavonoids; DPPH assay; phenolic content; chromatography; spectrophotometry.*

INTRODUCTION

In recent years, scientific and regulatory concerns over the safety of synthetic antioxidants—such as butylated hydroxytoluene (BHT) and butylated hydroxyanisole (BHA)—have driven increased interest in natural alternatives. Oxidative stress, resulting from an imbalance between reactive oxygen species (ROS) and the body's antioxidant defense mechanisms, plays a critical role in the pathogenesis of numerous degenerative conditions, including cardiovascular diseases, cancer, and neurodegenerative disorders. One of the primary manifestations of oxidative stress is lipid peroxidation, wherein ROS attack polyunsaturated fatty acids, leading to membrane damage and the formation of harmful metabolites.

As a result, research into plant-derived antioxidants capable of neutralizing free radicals has intensified. Among promising candidates is *Saponaria officinalis* L., commonly known as soapwort, a perennial species from the Caryophyllaceae family. This plant, cultivated within the cultural flora of the Nakhchivan Autonomous Republic, has historically been used in folk medicine as a cleanser, diuretic, and expectorant. Recent studies (Guliyev & Mansur, 1999; Dönmez & Yılmaz, 2024; Ekşi Bona, 2025) confirm its rich phytochemical profile, including saponins, flavonoids, phenolic acids, carotenoids, and alkaloids—compounds widely recognized for their antioxidant properties.

The present study provides a detailed analysis of the phytochemical composition and antioxidant capacity of *S. officinalis* L., using chromatographic and spectrophotometric techniques. Specific compounds such as flavone, 3-hydroxyflavone, β-carotene, and apigenin were identified, while antioxidant activity was assessed using DPPH free radical scavenging assays and colorimetric reactions. Notably, phenolic content and flavonoid derivatives were found to contribute significantly to antioxidant behavior.

This research contributes to the growing body of evidence supporting the pharmaceutical and nutraceutical relevance of *S. officinalis* L. and highlights its potential role as a natural antioxidant source for industrial applications.

MATERIALS AND METHODS

The species *Saponaria officinalis* L., selected as the object of the study, was prepared for analysis at the *Biochemical Research Laboratory* of Nakhchivan State University. Plant samples were collected and dried to a constant weight, after which their mass was measured.

In the study of the phytochemical composition of the species, modern analytical methods such as chromatography and spectrophotometry were primarily used. Chromatography is one of the most effective and universal physicochemical techniques for separating and analyzing complex mixtures of substances. Today, the chromatographic method is widely applied in various research fields, particularly in the analysis of food product composition and the assessment of their quality parameters (Alpınar, 2015; Mete, 2009; Wu, Raven, & Hong, 2001).

The main purpose of using spectroscopic analysis methods was to identify plant-derived compounds such as flavonoids, carotenoids, anthocyanins, alkaloids, and other classes of bioactive substances.

Spectral analyses were performed using a *Hitachi U-2900 UV-VIS spectrophotometer*, while chromatographic analyses were carried out using a *60108-712 HYPERSEP SI column* (10 g/75 mL/10 PKG) (Figure 1) and *DC-fertigfolien ALUGRAM SIL G/UV254* thin-layer plates. To determine the composition of the extracts, both column and thin-layer chromatography were employed using the following solvent systems:

- Acetic acid + n-butanol + water (1:4:5)
- Petroleum ether + acetone + water (3:1:1) (Mabry, Markham, & Thomson, 1970)

Thin-layer chromatography was performed on standard silica gel plates (Kieselgel G60 F254, Merck). Using a micropipette, 30 µL of the test extract solution and, in parallel, 10 µL of 1% solutions of standard compounds (rutin, quercetin, isoquercitrin, etc.) were applied as spots along the starting line of the plates.

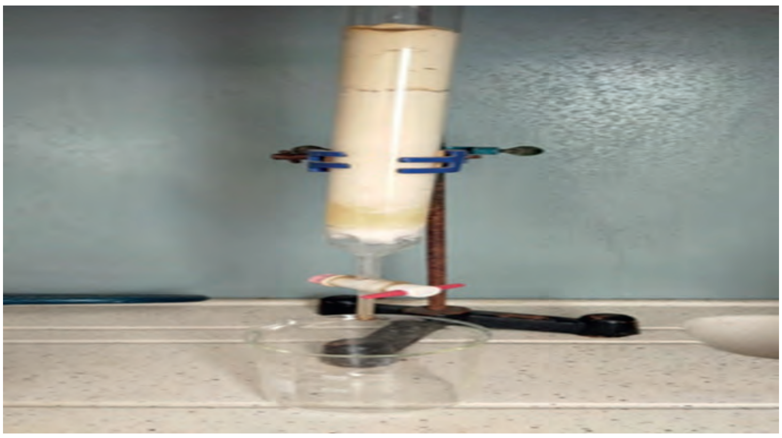

Figure 1. Column chromatography

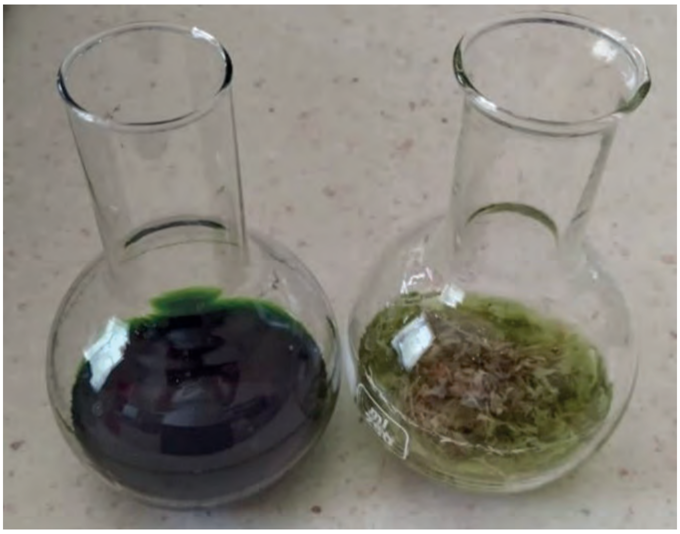

Figure 2. Extraction of Stems and Flowers of Saponaria officinalis L. (1. Leaf extract; 2. Flower extract)

During the chromatographic procedure, the plates were first placed in chambers pre-saturated with eluent vapors. After the solvent front had migrated 11 cm, the plates were removed from the chamber and air-dried until the solvents had completely evaporated. The resulting chromatograms were examined under UV light (Model CM-10A fluorescence analysis cabinet) at wavelengths of 254 nm and 365 nm. The positions and colors of the spots were recorded (Prior, Wu, & Scaich, 2005).

The leaves, flowers, and stems of *Saponaria officinalis* L. were dried separately according to standard methods and ground using a blender. The dried plant materials were extracted with various solvents for 3 hours, in two repetitions, and the resulting extracts were filtered.

The flowers were first extracted with hexane and ethanol, followed by extraction with 0.5% hydrochloric acid in ethanol. The leaves were extracted using hexane and ethanol, while an aqueous extract was prepared from the stems. The extracts were concentrated under vacuum using a rotary evaporator (Figure 2).

The absorbance spectra of the obtained extracts were measured with a UV spectrophotometer, and based on the wavelength values, the compounds present in the extracts were identified.

METHODS FOR THE STUDY OF FLAVONOIDS

The qualitative determination of flavonoids in extracts obtained from different plant organs was carried out using two characteristic reactions: the ferric (III) chloride reaction and the cyanidin reaction. The interaction of flavonoids with ferric (III) chloride produces green-colored complexes for flavonols (rutin, quercetin, kaempferol, etc.) and brown-colored complexes for flavanones.

In the cyanidin reaction, flavonols and flavones are reduced in the presence of magnesium powder and HCl, resulting in the formation of anthocyanidins that produce red or orange coloration (Velioglu, Mazza, Gao, & Omah, 1998).

Chalcones and aurones do not give a reaction in the cyanidin test; however, when concentrated HCl is added to their solutions (without magnesium), red coloration appears due to the formation of oxonium salts. To 2 mL of the extract, 5–7 drops of concentrated HCl and 10–15 mg of magnesium powder are added. After 3–5 minutes, a gradual color change is observed. To accelerate the reaction and enhance color intensity, the reaction tube can be heated in a boiling water bath for 2–3 minutes (Rahimova & Novruzova, 2023; Johnson, Foster, Low, & Kiefer, 2017; Yenigün & Başar, 2024).

METHODS FOR THE STUDY OF SAPONINS

The presence of saponins in extracts was determined by several qualitative tests. The extract was dissolved in 20 mL of distilled water and stirred for 15 minutes. The formation of a 1 cm foam layer indicated the presence of saponins. To the aqueous saponin extract, 1 mL of ethanol, 1 mL of concentrated H_2SO_4, and 1 drop of 10% $FeSO_4$ solution were added. Upon heating, a blue-green color developed (Lafon reaction).

METHODS FOR THE STUDY OF PHENOLIC COMPOUNDS

The total phenolic content of the plant extract was determined using the Folin–Ciocalteu method. For quantification, 0.5 mL of Folin–Ciocalteu reagent (1 N), 7.5 mL of water, 1.5 mL of 10% Na_2CO_3, and 1 mL of the extract were mixed. The mixture was allowed to stand for 90 minutes, and the absorbance was measured at 765 nm. Gallic acid (1 mL) was used as the standard.

RESULTS AND DISCUSSION

Information regarding the qualitative composition and quantitative characteristics of *Saponaria officinalis* L. distributed within the territory of the Nakhchivan Autonomous Republic is limited. Therefore, the present study was undertaken to obtain comprehensive data on the qualitative composition and quantitative indicators of various organs of this species, as well as its overall phytochemical profile.

The leaves, flowers, and stems of the plant were extracted with various solvents, after which the extracts were filtered, concentrated using a rotary evaporator, and analyzed spectrophotometrically. The absorbance spectra were recorded using a UV spectrophotometer, while chromatographic analyses were performed to identify the compounds present in the extracts based on their *Rf* values.

Chromatographic data revealed the presence of flavone, 3-hydroxyflavone, and β-carotene in the leaf extracts of the plant. In the acidified ethanol extract of the flowers, apigenin, flavone, two hydroxyflavone-type compounds (3-hydroxyflavone and 6-hydroxyflavone), as well as flavanone compounds were identified. These findings demonstrate that *Saponaria officinalis* L. possesses a diverse range of flavonoid derivatives, indicating its potential antioxidant and pharmacological activity, consistent with previous research on the Caryophyllaceae family (Velioglu et al., 1998; Prior et al., 2005; Rahimova & Novruzova, 2023). Table 1 presents the chromatographic analysis results of *Saponaria officinalis* L. extracts, showing the *Rf* values obtained for individual compounds.

Table 1. Chromatographic analysis results of *Saponaria officinalis* L. extracts

Extract Type	Identified Compounds	Rf Values
Leaf Extract	Flavone	0.91
	3-Hydroxyflavone	0.56
	β-Carotene	0.97
Flower Extract	Apigenin	0.21
	6-Hydroxyflavone	0.46
	3-Hydroxyflavone	0.56
	Flavanone	0.75

The pigments present in the leaf extracts of *Saponaria officinalis* L. were analyzed using both chromatographic and spectrophotometric techniques. A prominent absorption peak was recorded at **664 nm**, corresponding to **chlorophyll *a***, thereby confirming its presence in the leaf extract (*Figure 3*). This result aligns with the characteristic absorption maxima of chlorophyll *a* in higher plants, as reported in previous studies (Mabry, Markham, & Thomson, 1970; Johnson, Foster, Low, & Kiefer, 2017).

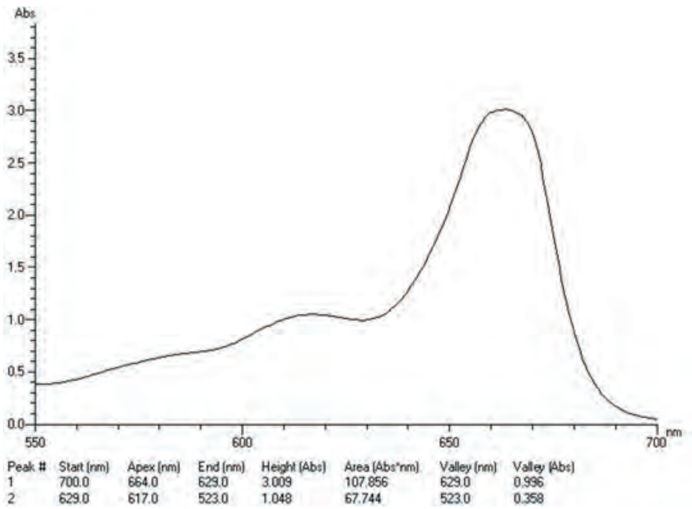

Peak #	Start (nm)	Apex (nm)	End (nm)	Height (Abs)	Area (Abs*nm)	Valley (nm)	Valley (Abs)
1	700.0	664.0	629.0	3.009	107.856	629.0	0.996
2	629.0	617.0	523.0	1.048	67.744	523.0	0.358

Figure 3. UV spectrum of chlorophyll A pigment in the leaf extract of *Saponaria officinalis L.*

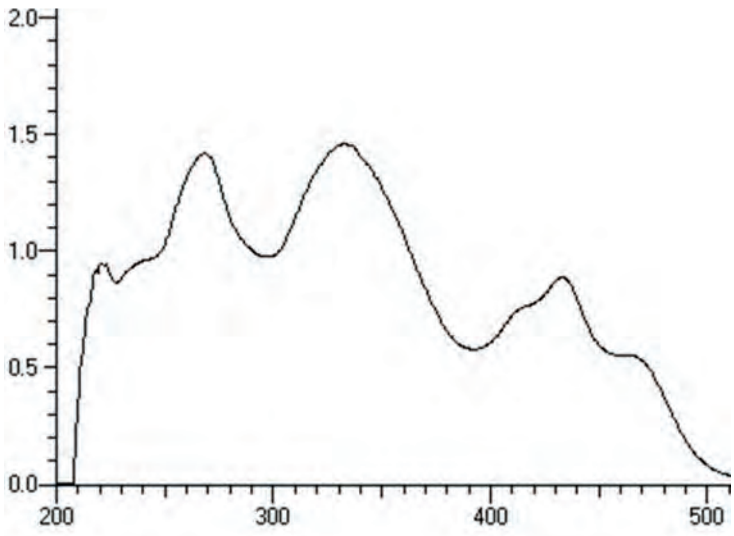

Figure 4. UV spectrum of the ethanol extract of the leaves of Saponaria officinalis L.

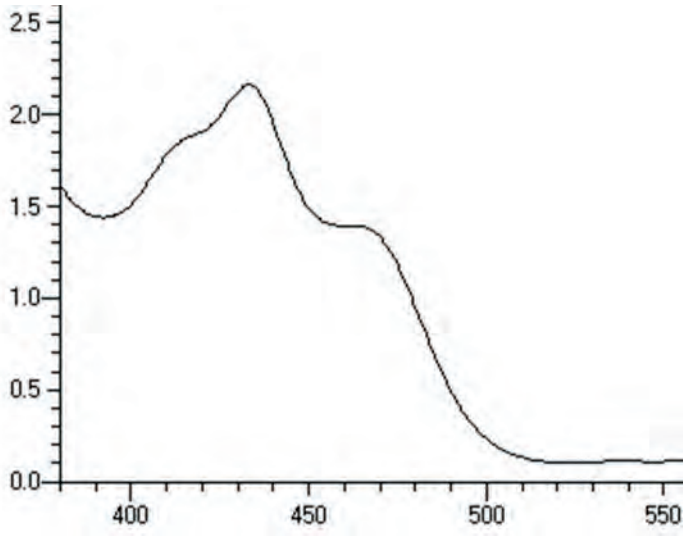

Figure 5. UV spectrum of Saponaria officinalis L. flower extract

Based on the wavelengths obtained with a UV spectrophotometer from the ethanol extract of the plant leaves, the compounds present in the extract were identified, as shown in Figure 4.

The observed wavelengths of 268 nm and 333 nm correspond to flavones, specifically apigenin 7-O-glucoside. Additionally, a wavelength of 280 nm was recorded, which is characteristic of phenolic compounds.

In the flowers of the plant, peaks at a wavelength of 470 nm, corresponding to carotenoid compounds, were recorded, as shown in Figure 4.

Saponaria officinalis L. is rich in flavonoids and phenolic compounds. The total amount of phenolic compounds in the aerial parts of the plant was determined, and the total phenolic content was found to be 7.12 μg/mg in gallic acid equivalents.

The qualitative composition of saponins in the stems of the plant was determined using the Lafon reaction. The formation of a 1 cm foam layer and the appearance of a blue-green color upon heating indicate the presence of saponins in the extract [Güçlü-Üstündağ, Ö.; Mazza, G., 2007; Mehra, N., 2023].

The free radical scavenging activities of the extracts were determined using the 2,2-diphenyl-1-picrylhydrazyl (DPPH) method. During the reaction, the decrease in the amount of DPPH radicals was measured by recording the absorbance of the reaction mixture at a wavelength of 517 nm. A decrease in absorbance indicates a reduction in the amount of DPPH in the reaction medium. The DPPH free radical scavenging activity of the ethanol extract of the leaves of Saponaria officinalis was 87.6% at a concentration of 50 mg/ml, while the DPPH free radical scavenging activity of the flower extract was 86.4% at the same concentration. At the same time, a strong correlation between the total phenolic content and antioxidant activity in the plant was observed (Figure 6).

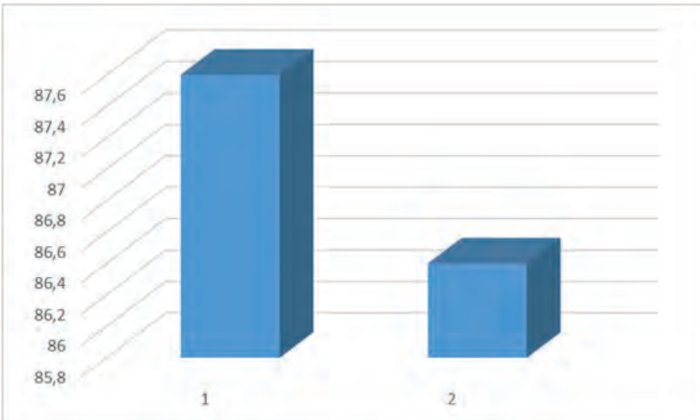

Figure 6. DPPH free radical scavenging activity of leaf and flower extracts of Saponaria officinalis
1. *Free Radical Scavenging Activity of the Leaf Extract*
2. *Free Radical Scavenging Activity of the Flower Extract*

CONCLUSION

Saponaria officinalis L., cultivated in the cultural flora of the Nakhchivan Autonomous Republic, was comprehensively studied under laboratory conditions to determine its phytochemical composition and antioxidant potential. During the study, leaves, flowers, and stems of the plant were extracted using various solvents. The resulting extracts were filtered, concentrated with a rotary evaporator, and subjected to thin-layer and column chromatography. Their absorbance spectra were measured using UV–visible spectrophotometry. Based on Rf values obtained from chromatographic analyses, several phytochemical compounds were identified.

In the leaf extracts, flavone, 3-hydroxyflavone, and β-carotene were detected. In the acidified ethanol extract of the flowers, apigenin, flavone, and two hydroxyflavone-type compounds—3-hydroxyflavone and 6-hydroxyflavone—along with flavanone compounds were identified. The aqueous extract of the stems tested positive for saponins, confirming the presence of triterpenoid glycosides. The total phenolic content in the aerial parts of the plant was quantified as 7.12 µg/mg in gallic acid equivalents (GAE), indicating a significant presence of polyphenolic antioxidants.

The antioxidant activity of the leaves and flowers was assessed using classical qualitative reactions. In the ferric (III) chloride test, the formation of green-colored complexes for flavonols (such as rutin, quercetin, and kaempferol) and brown-colored complexes for flavanones confirmed the presence of structurally diverse flavonoids. In the cyanidin reaction, the reduction of flavones in the presence of magnesium powder and HCl produced red or orange-colored anthocyanidins, further demonstrating the presence of flavonoid derivatives.

Quantitative evaluation of antioxidant capacity was conducted using the DPPH free radical scavenging assay. The ethanol extract of the leaves exhibited 87.6% inhibition at a concentration of 50 mg/mL, while the flower extract showed 86.4% inhibition at the same concentration. These values confirm the strong antioxidant activity of *S. officinalis* L. extracts.

Spectrophotometric analysis revealed a chlorophyll *a* absorption peak at 664 nm in the leaf extract, and characteristic carotenoid peaks at 470 nm in the flower extract. These findings support the presence of photosynthetic pigments alongside bioactive flavonoids and phenolics.

In summary, *Saponaria officinalis* L. demonstrates a rich phytochemical profile, including flavonoids, phenolics, carotenoids, saponins, and chlorophyll pigments, with substantial antioxidant potential. The high levels of radical scavenging activity and phenolic content suggest promising applications in the development of natural antioxidant agents for use in pharmaceutical, nutraceutical, and cosmetic industries. Further research is warranted to isolate individual bioactive compounds and evaluate their specific mechanisms of action in biological systems.

References

Alpınar, K. (2015). *Zeytinburnu Medicinal Plants Garden*. Merkezefendi Traditional Medicine Association.

Ekşi, B. (Ed.). (2025). *Illustrated flora of Turkey* (Vol. 17c, p. 500). ANG Publications.

Guliyev, V. B., & Mansur, H. (1999). *Flavonoids*. Cağaloğlu.

Güçlü-Üstündağ, Ö., & Mazza, G. (2007). Saponins: Properties, applications, and processing. *Critical Reviews in Food Science and Nutrition, 47*(3), 231–258. https://doi.org/10.1080/10408390600698197

Mabry, T., Markham, K., & Thomson, M. (1970). *The systematic identification of flavonoids*. Springer-Verlag.

Dönmez, C., & Yılmaz, B. (2024). Endemic *Achillea* species in Turkey: Phytochemical contents and pharmacological activities. *Current Perspectives on Medicinal and Aromatic Plants, 7*(1), 73–84. https://doi.org/10.38093/cupmap.1479696

Mete, O. (2009). *Encyclopedia of Medicinal Plants*. Kabalcı Publishing.

Mehra, N. (2023). A comparative study on conventional and advanced techniques for plant extraction and effect on the extract yield: Review. *Current Perspectives on Medicinal and Aromatic Plants, 6*(2), 108–116. https://doi.org/10.38093/cupmap.1365128

Prior, R. L., Wu, X., & Scaich, K. (2005). Standardized methods for the determination of antioxidant capacity and phenolics in foods and dietary supplements. *Journal of Agricultural and Food Chemistry, 53*(8), 3110–3113. https://doi.org/10.1021/jf047573w

Rahimova, S. A., & Novruzova, E. S. (2023). Anthocyanins of *Morus nigra* L. fruit growing in the territory of Nakhchivan Autonomous Republic. *International Journal of Bioscience and*

Biochemistry, 5(2), 17–19. https://doi.org/10.33545/26646536.2023.v5.i2a.45

Johnson, R., Foster, S., Low, T., & Kiefer, D. (2017). *Encyclopedia of Medicinal Plants*. Hürriyet Gazetecilik.

Huseynova, H.Z. (2021) The classification of desert and semi-desert vegetation of the Caspian coast (Azerbaijan). Bulletin of Science and Practise 7/11: 43–50.
https://doi.org/10.33619/2414-2948/72/05

Huseynova, H. Z. Vegetation of the southern part of the Caspian Coast and its nutritional value. Biosystems Diversity, v. 30, n. 3, p. 205-212, 2022. https://doi.org/10.15421/012222

Velioglu, Y. S., Mazza, G., Gao, L., & Omah, B. D. (1998). Antioxidant activity and total phenolics in selected fruits, vegetables and grain products. *Journal of Agricultural and Food Chemistry, 46*(10), 4113–4117. https://doi.org/10.1021/jf9801973

Wu, Z., Raven, P. H., & Hong, D. (Eds.). (2001). *Flora of China: Caryophyllaceae through Lardizabalaceae* (Vol. 6). Science Press; Missouri Botanical Garden Press.

World Flora Online. (n.d.). Retrieved November 4, 2025, from https://about.worldfloraonline.org/

Yenigün, S., Başar, Y., Yılmaz, S., & Demirtaş, İ. (2024). Phytochemical contents and antioxidant activity of *Paliurus spina-christi* Miller leaf and seed extracts: PASS predictions and in silico studies on xanthine oxidase and cytochrome P450 1A1. *Current Perspectives on Medicinal and Aromatic Plants, 7*(2), 96–106. https://doi.org/10.38093/cupmap.1516991

IMPACTS OF CLIMATE CHANGE ON ORIENTAL SPRUCE (*PICEA ORIENTALIS*) ECOSYSTEMS IN THE EASTERN BLACK SEA REGION OF TURKEY

Aydın Tufekcioglu [1]*| https://orcid.org/0000-0003-0835-2839
Cengizhan Yildirim[2]| https://orcid.org/0000-0003-1525-3265

[1*2] Faculty of Forestry, Artvin Çoruh University, Artvin, Turkey

Correspondence: atufekci@artvin.edu.tr

Article Info
DOI: https://doi.org/10.30546/abc.2025.0014
Pages: 32-36
Received: September 12, 2025 | Revised: October 01, 2025 | Accepted: October 15, 2025

Abstract

Climate change has recently gained increased attention from the global scientific community due to its widespread and accelerating impacts on ecosystems. The Eastern Black Sea Region of Turkey is expected to be significantly affected by these changes, as projected by the RegCM3 regional climate model.

Oriental spruce (Picea orientalis), an ecologically and economically important tree species endemic to this region, is highly sensitive to climatic shifts. Recent observations indicate that global warming has contributed to severe bark beetle outbreaks, resulting in the death of over 200,000 trees.

This study evaluates the current status and future vulnerability of Oriental spruce ecosystems using field observations and existing literature on regional climate projections. According to Dalfes et al. (2007), regional temperatures are expected to rise by 2–4 °C over the next century. Precipitation is projected to increase by 200–300 mm in the eastern part of the region, while no significant change is expected in the western areas.

Temperature increases, particularly in the western zone, are likely to intensify drought stress, elevate bark beetle infestations, and increase wildfire risk. A potential upward altitudinal shift of 400–800 meters in the spruce distribution zone is anticipated, along with a general upward movement of the treeline across both eastern and western parts of the region.

These findings highlight the urgent need for adaptive forest management and conservation strategies to mitigate the projected impacts of climate change on Oriental spruce ecosystems.

Keywords: *Climate change; oriental spruce (Picea orientalis); Eastern Black Sea region; forest ecosystems; bark beetle; Turkey*

INTRODUCTION

Global warming has been receiving increasing attention from both the public and scientific communities in Turkey and worldwide. Weather anomalies, extreme temperatures, frequent flooding events, sea-level rise, and glacial melting represent key phenomena that the scientific community strongly associates with ongoing climate warming (IPCC, 2007).

The period from 1995 to 2006 included eleven of the twelve warmest years in the instrumental record of global surface temperature since 1850. Oceanographic observations since 1961 indicate that the average temperature of the global ocean has increased to depths of at least 3000 m, with the ocean absorbing over 80% of the additional heat introduced into the climate system. This thermal expansion of seawater contributes significantly to sea-level rise (IPCC, 2007).

Atmospheric concentrations of carbon dioxide, methane, and nitrous oxide have increased markedly due to human activities since 1750, now substantially exceeding pre-industrial levels documented through ice core records spanning millennia. The rise in atmospheric CO_2 primarily results from fossil fuel combustion and land-use changes, while increased methane and nitrous oxide concentrations are largely attributable to agricultural practices (IPCC, 2007).

The global atmospheric CO_2 concentration has risen from approximately 280 ppm in pre-industrial times to 379 ppm by 2005. This current level dramatically exceeds the natural range of 180-300 ppm observed over the past 650,000 years in ice core records. Notably, the annual growth rate of atmospheric CO_2 was higher during the recent decade (1995-2005 average: 1.9 ppm/year) compared to the long-term average since continuous monitoring began (1960-2005 average: 1.4 ppm/year), despite interannual variability (IPCC, 2007).

These documented changes provide compelling evidence that climate warming is occurring, predominantly driven by fossil fuel consumption. However, research examining how global warming will specifically affect Turkey's climate and ecosystems remains limited. Analysis of meteorological data from 1951-2004 by Dalfes et al. (2007) revealed significant decreases in winter precipitation across western Turkey over recent decades, while autumn precipitation increased at stations primarily in northern central Anatolia. Their most prominent finding was the widespread increase in summer temperatures throughout the country. Using the RegCM3 climate model, Dalfes et al. (2007) projected temperature increases of 4-6°C in western Turkey and 2-4°C in eastern regions for future climate scenarios. Precipitation projections generally indicated decreases along Aegean and Mediterranean coasts, with increases anticipated along the Black Sea coast.

Picea orientalis represents an ecologically significant conifer species endemic to the eastern Black Sea region of Turkey. As spruce genera typically dominate boreal ecosystems characterized by cold winters and cool summers, these spruce-dominated ecosystems are likely to be among the first to manifest detectable responses to climate change. This investigation utilizes current scientific literature and field observations to evaluate this hypothesis systematically.

MATERIALS AND METHODS

The genus *Picea* comprises 35 species across the Northern Hemisphere, with *Picea orientalis* representing the only naturally occurring species in Turkey. Oriental spruce forests cover approximately 297,396 hectares of Turkey's forested areas (Anonymous, 2006). This species demonstrates preference for humid climates, areas experiencing summer fog events, and north-facing slopes where precipitation is limited. It forms mixed stands with several species including *Pinus sylvestris*, *Abies nordmanniana*, *Fagus sylvatica*, and *Quercus* species. *Picea orientalis* becomes the dominant canopy species in mixed stands at elevations around 1000 meters, maintaining dominance up to 2400 meters, and frequently forms pure stands within this elevational range (Anonymous, 2001).

Climatic conditions within the species' distribution range feature mean annual temperatures of 5-10°C, though extreme temperatures can reach -20°C in winter and 30°C in summer. Mean temperatures during the growing season range between 10-20°C (Tüfekçioğlu, 2008). Annual precipitation across the species' distribution varies substantially from 700-3000 mm.

Fog precipitation plays a crucial role in the distribution and persistence of spruce ecosystems within these warm temperate regions. Despite its importance, no scientific studies have quantified fog water input to these ecosystems in the region. For comparison, an 18-week investigation in a *Picea sitchensis*/*Tsuga heterophylla* stand in Oregon recorded 290 mm of fog drip alongside 640 mm of rainfall (Kimmins, 1997). Additionally, fog provides shading from direct solar radiation while fog drip cools needle surfaces. We hypothesize these mechanisms represent key factors enabling spruce ecosystem persistence in this humid temperate region.

This study employs comprehensive literature review and systematic field observations to address our research questions regarding climate change impacts on Oriental spruce ecosystems.

RESULTS AND DISCUSSION

Global Climate Change and Spruce Ecosystems

Spruce ecosystems predominantly occur within the boreal zone, characterized by short, moderately warm, moist summers and prolonged, cold, dry winters, with mean annual temperatures ranging from –5 to 3°C (Perry, 1994). The boreal forest spans over 1.2 billion hectares across North America and Eurasia, representing the largest terrestrial carbon reservoir (30-35% of global terrestrial carbon), primarily stored in organic soils of the forest floor (Soja et al., 2007). Spruce forests also extend into high-elevation areas of temperate regions.

Scientific consensus acknowledges increasing global mean temperatures, with the most pronounced warming occurring in northern high-latitude and high-elevation regions where spruce forests predominantly exist (Soja et al., 2007; Tüfekçioğlu, 2008). Predicted ecological indicators of climate change in these regions include: (1) intensified fire regimes (increased frequency, severity, burned area, and extended fire seasons); (2) enhanced insect infestations (greater frequency, duration, and spatial extent); (3) treeline altitudinal shifts; and (4) stand- and landscape-level alterations in forest composition (age structure, and species composition) (Soja et al., 2007).

Fire represents the primary ecological driver influencing structure, age distribution, and species composition in spruce forests, playing a vital role in maintaining biodiversity. Research conducted across North American and Russian boreal forests demonstrates increased fire frequency that is projected to accelerate with continued climate change (Soja et al., 2007).

Bark beetle outbreaks have emerged as a significant threat to spruce ecosystems worldwide. Enhanced bark beetle activity has been directly linked to climate warming, as elevated temperatures enable completion of the insect life cycle in one year rather than two, dramatically increasing population growth (Berg et al., 2006; Weissbacher, 2004). In Germany, bark beetles caused extensive mortality across 3,700 hectares of spruce forest in Bavaria National Park, primarily driven by elevated temperatures, windthrow events, and drought stress (Heurich et al., 2001; Nusslein et al., 2000).

Climate change-induced treeline shifts have been documented globally (Soja et al., 2007). Altitudinal treeline advances have been recorded across the southern Urals, Altai, Sayan, and Kuznetsky Alatau mountain ranges. In the southern Urals, the forest treeline ascended 20-40 meters, reducing adjacent tundra area by approximately half.

Climate-mediated growth responses in spruce forests demonstrate complex patterns. Contrary to expectations, increased productivity at treeline due to warming may not be straightforward. Lloyd and Fastie (2002) examined tree growth responses at boreal forest margins to 20th-century climate variability, finding regional differences in climate sensitivity. Post-1950, warmer temperatures correlated with growth declines except in the most humid regions, indicating drought stress may accompany warming in many boreal forests (Soja et al., 2007).

Complementary research by Barber et al. (2000, 2004) documented negative growth responses in Alaskan *Picea glauca* to drought conditions. Dendrochronological and $\delta^{13}C$ isotope analyses near Fairbanks revealed moisture-stress-mediated effects during warmer decades, consistent with model predictions.

Climate Change Impacts on Turkey's Spruce Ecosystems

Turkey is projected to experience significant climate change impacts (UNDP Turkey, 2007). Analysis of 18 meteorological stations (1939-1989) identified a 0.63°C increase in Turkey's mean annual temperature (Asan, 1995). Regional analysis of Eastern Black Sea stations (1951-2004) by Dalfes et al. (2007) showed increased winter and spring precipitation in Artvin, decreased spring precipitation in Trabzon, and surprisingly, decreased mean annual temperature in Artvin. Regional climate modeling using RegCM3 projects temperature increases of 2-4°C in the region during the coming century (Dalfes et al., 2007). Precipitation scenarios indicate increases of 200-300 mm in the eastern Black Sea region, while western areas show no substantial precipitation changes.

These projected changes may cause upward shifts of 400-800 meters in the spruce distribution belt in western regions. Eastern areas will likely experience treeline ascent without significant lower-elevation boundary changes due to compensatory precipitation increases. Consequently, spruce forest area may decrease in western regions while expanding in eastern areas.

Temperature increases will likely induce physiological stress in spruce trees, potentially increasing susceptibility to bark beetle attacks. Approximately 100,000 spruce trees experienced mortality from bark beetle outbreaks in Hatilla National Park, Artvin (Tüfekçioğlu et al., 2005). Dendroecological analysis of 200 tree-ring samples (100 live, 100 dead) revealed that beetle-killed trees exhibited greater mean annual diameter increment over two decades, suggesting these rapidly growing trees experienced significant stress in their final decade.

Fire may emerge as a novel threat in western regions under projected climate change. Currently, fire represents an insignificant disturbance agent in Oriental spruce ecosystems due to humid summer conditions. However, fire plays a crucial ecological role in maintaining structure, diversity, and health in boreal spruce ecosystems globally (Soja et al., 2007).

Climate change will likely trigger drought-induced mortality and growth reduction in Oriental spruce ecosystems. Similar drought-mediated growth declines have been documented in Alaskan spruce forests (Barber et al., 2000). Mortality events in low-elevation spruce and pine forests during dry years have already been observed in the Black Sea region (Tüfekçioğlu et al., 2005).

Climate change will fundamentally alter the structure, stability, and biodiversity of Oriental spruce ecosystems. Fire-mediated secondary succession may become established in western regions, while insect outbreak-driven succession events will likely increase in frequency. Such changes may increase plant diversity through replacement of shade-tolerant *Picea orientalis* with shade-intolerant species, which typically support richer understory communities (Kılınç & Kutbay, 2004). Conversely, treeline advance and replacement of alpine grasslands by spruce forest would likely decrease plant diversity at high elevations.

CONCLUSIONS

Climate change will significantly influence distribution, diversity, structure and stability of the oriental spruce ecosystems. According to RegCM3 regional climate model, the temperatures will increase 2-4 °C in the region in the next century. Future climate scenarios predict 200-300 mm increases in precipitation in the eastern part of the region while the western part won't have any increase in precipitation in the next century. Temperature increases in the western part of the region will put more stress on spruce trees and will probably increase bark beetle attacks. Also, fire could become an important threat in the western part of the region. It is possible to observe 400-800 m upward shift in the spruce belt in the western part. Treeline of spruce and scotch pine stands will probably move upward both in western and eastern part of the region.

References

Anonymous. (2001). *Doğu Ladini El Kitabı* [Oriental spruce handbook]. Orman Araştırma Enstitüsü Yayınları, No: 58. Bahçelievler, Ankara. *(In Turkish)*

Anonymous. (2006). *Orman varlığımız* [Forest resources of Turkey]. T.C. Çevre ve Orman Bakanlığı, Orman Genel Müdürlüğü Yayınları. Ankara. *(In Turkish)*

UNDP Turkey. (2007). Climate change & Turkey: Impacts, sectoral analyses, socio-economic dimensions. UNDP Türkiye Office Publications. Ankara.

Asan, Ü. (1995). Global iklim değişimi ve Türkiye ormanlarında karbon birikimi [Climate change and carbon sequestration in forests in Turkey]. *İstanbul Üniversitesi Orman Fakültesi Dergisi*, 45(1–2), 23–37. *(In Turkish)*

Barber, V. A., Juday, G. P., & Finney, B. P. (2000). Reduced growth of Alaskan white spruce in the twentieth century from temperature-induced drought stress. *Nature*, 405, 668–673.

Barber, V. A., Juday, G. P., Finney, B. P., & Wilmking, M. (2004). Reconstruction of summer temperatures in interior Alaska from tree-ring proxies: Evidence for changing synoptic climate regimes. *Climatic Change*, 63(1–2), 30–59.

Berg, E. E., Henry, J. D., Fastie, C. L., De Volder, A. D., & Matsuoka, S. M. (2006). Spruce beetle outbreaks on the Kenai Peninsula, Alaska, and Kluane National Park and Reserve, Yukon Territory: Relationship to summer temperatures and regional differences in disturbance regimes. *Forest Ecology and Management*, 227(3), 219–232.

Dalfes, N., Karaca, M., & Şen, Ö. L. (2007). Climate change scenarios for Turkey. In Ç. Güven (Ed.), *Climate change & Turkey: Impacts, sectoral analyses, socio-economic dimensions*. UNDP Turkey Office Publications.

Goudie, A. (1993). *The nature of the environment* (pp. 227–230). Oxford University Press.

Heurich, M., Reinelt, A., & Fahse, L. (2001). Die Buchdruckermassenvermehrung im Nationalpark Bayerischer Wald. In M. Heurich (Ed.), *Waldentwicklung im Bergwald nach Windwurf und Borkenkäferbefall* (Vol. 14, pp. 9–48). Bayerische Staatsforstverwaltung, Wissenschaftliche Reihe.

Intergovernmental Panel on Climate Change. (2007). *Climate change 2007: The physical science basis. Contribution of Working Group I to the Fourth Assessment Report of the IPCC*. Geneva: IPCC.

Kılınç, M., & Kutbay, H. G. (2004). *Bitki ekolojisi* [Plant ecology] (No. 275). Palme Yayıncılık. *(In Turkish)*

Kimmins, J. P. (1997). *Forest ecology* (2nd ed.). Prentice Hall.

Lloyd, A. H., & Fastie, C. L. (2002). Spatial and temporal variability in the growth and climate response of treeline trees in Alaska. *Climatic Change*, 52(4), 29–49.

Nusslein, S., Faisst, G., Weissbacher, A., Moritz, K., Zimmermann, L., Bittersol, J., Kennel, M., Troycke, A., & Adler, H. (2000). *Zur Waldentwicklung im Nationalpark Bayerischer Wald 1999* (Vol. 25). Bayerische Landesanstalt für Wald und Forstwirtschaft.

Perry, D. A. (1994). *Forest ecosystems*. Johns Hopkins University Press.

Soja, A. J., Tchebakova, N. M., French, N. H. F., Flannigan, M. D., Shugart, H. H., Stocks, B. J., Sukhinin, A. I., Parfenova, E. I., Chapin, F. S., & Stackhouse, P. W. (2007). Climate-induced boreal forest change: Predictions versus current observations. *Global and Planetary Change*, 56(3–4), 274–296.

Tüfekçioğlu, A. (2008). Küresel ısınmanın ülkemiz ladin ormanları üzerine olası etkilerinin irdelenmesi [Potential effects of global warming on Oriental spruce forests in Turkey]. In *IV. Atmosfer Bilimleri Sempozyumu* (pp. 399–407). İstanbul. *(In Turkish)*

Tüfekçioğlu, A., Kalay, H. Z., Küçük, M., Kahriman, A., & Özbayram, A. K. (2005). Artvin-Hatilla Milli Parkı'nda böcek zararı sonucu görülen kurumalar ve bunu tetikleyen ekolojik nedenler [Bark beetle–induced tree mortality in Artvin-Hatilla National Park and contributing ecological factors]. In *I. Çevre ve Ormancılık Şurası* (pp. 1430–1438). Antalya. *(In Turkish)*

Weissbacher, B. (2004). Ecology and management of the spruce bark beetle: *Ips typographus*—A review of recent research. *Forest Ecology and Management*, 202, 67–82.

STUDY OF THE MORPHOLOGICAL AND ANATOMICAL STRUCTURE OF *EPILOBIUM ANGUSTIFOLIUM* RAW MATERIAL FROM THE AZERBAIJANI FLORA

Tahir Suleymanov[1]|https://orcid.org/0009-0005-4680-4025
Kamala Huseynova[1]|https://orcid.org/0009-0004-4550-1324
Yusif Karimov[1]|https://orcid.org/0000-0002-2792-3687
Eldar Gasimov[2]|https://orcid.org/0000-0002-5104-4260
Fuad Rzayev[2]|https://orcid.org/0000-0002-8128-1101

[1] Azerbaijan Medical University, Department of Pharmaceutical Chemistry, Baku, Azerbaijan
[2] Azerbaijan Medical University, Department of Histology, Embryology and Cytology, Baku, Azerbaijan

Correspondence: tahir.suleymanov@amu.edu.az

Article Info
DOI: https://doi.org/10.30546/abc.2025.0019
Pages: 37-42
Received: September 02, 2025 | Revised: September 26, 2025 |Accepted: October 01, 2025

Abstract

This study aimed to characterize the morphological and anatomical diagnostic features of Epilobium angustifolium L. raw material, a widely distributed species in the Azerbaijani flora, to establish identification criteria for quality control purposes.

Plant material was collected during the flowering stage in August 2021 from Malham village, Shamakhi district, Azerbaijan. The investigation utilized the entire herb, including both aerial (stem, leaves, flowers) and subterranean (root) parts. Anatomical examination was performed using light microscopy on semi-thin sections prepared from specimens processed with standard histological fixation and embedding techniques.

The anatomical study revealed several distinctive diagnostic characteristics: the leaves exhibit a dorsoventral structure with an astomatous upper epidermis; the lower epidermis contains anomocytic stomatal complexes; the floral pedicel and the base of the calyx are densely covered with non-glandular trichomes; and the sepals are pigmented, with a lilac-colored, glabrous basal interior.

The identified morphological and anatomical features represent reliable taxonomic and pharmacognostic markers for authenticating E. angustifolium raw material. These characteristics will support the standardization and quality control of herbal preparations and provide a foundational reference for compiling a comprehensive Pharmacopoeia monograph for this medicinal plant.

Keywords: *Epilobium angustifolium, fireweed, anatomy, morphology, pharmacognosy, diagnostic features, Azerbaijani flora, quality control*

INTRODUCTION

Epilobium (*Chamerion*) *angustifolium* belongs to the Onagraceae family, which comprises 22 genera and approximately 650 species. *Chamerion* (Raf.) Raf. ex Holub (syn. *Chamaenerion* Seg.) represents a genus of eight species within the subfamily Onagroideae and tribe Epilobieae, distributed predominantly across the Northern Hemisphere, particularly in Eurasia (Artur et al., 2019). Although frequently classified under *Epilobium* L., the largest genus of Onagraceae, *Chamerion* is morphologically distinct—especially in terms of floral architecture and leaf arrangement. Molecular phylogenetic analyses further support the recognition of *Chamerion* as a monophyletic lineage separate from *Epilobium* (Artur et al., 2019).

Species of *Epilobium* have been traditionally used in various ethnomedicinal systems, and modern pharmacological research identifies them as promising sources for phytopharmaceuticals. Studies on the dynamics of secondary metabolite accumulation have shown that the mass flowering stage yields the highest flavonoid content (11.12 ± 0.34 mg/g) and free radical scavenging activity (8.71 ± 0.29 mg/g) (Audrius et al., 2014).

Epilobium angustifolium L. is employed in the treatment of prostate, kidney, and urinary tract disorders, as well as dermatological conditions. A comprehensive phytochemical analysis of methanol-aqueous extracts from the aerial parts revealed 121 secondary metabolites, including acetic acids, gallotannins, ellagitannins, flavonoids, and glycosylated phenolic acids (Gevrenova et al., 2025). Among these, 46 compounds were identified for the first time in this species. The total phenolic and flavonoid contents were reported as 85.04 ± 0.18 mg GAE/g and 27.71 ± 0.74 mg QE/g, respectively (Gevrenova et al., 2025).

Despite growing evidence regarding the clinical safety and efficacy of *E. angustifolium* in managing benign prostatic hyperplasia, its application in mainstream medicine remains limited (Renata et al., 2020). In traditional medicine, it is primarily used for its antihemorrhagic, dermatological, and analgesic properties. Pharmacological studies confirm a wide spectrum of therapeutic activities—including antioxidant, anti-inflammatory, antiproliferative, antibacterial, and anti-aging effects—mainly attributed to bioactive compounds such as Oenothein B and ellagitannins (Schepetkin et al., 2016).

Furthermore, extracts of *E. angustifolium* have shown potential benefits in breast cancer therapy (Audrius et al., 2017). However, despite the presence of flavonoids with anti-inflammatory potential, their mechanisms of action remain insufficiently elucidated. The analgesic effects of its dry extract have been validated through standard hot plate and writhing tests (Vitalone et al., 2001).

Given the genus *Epilobium*'s rich profile of biologically active substances, it constitutes a valuable natural source for pharmaceutical development. This relevance is particularly pronounced in the flora of Azerbaijan, where *Epilobium* L. species are naturally distributed (Suleymanov et al., 2023). Nevertheless, the morphological and anatomical features of *E. angustifolium* raw material have not been adequately studied. Therefore, the aim of this study is to characterize the morphological and anatomical diagnostic features of *E. angustifolium* collected from the Azerbaijani flora, to support its quality control and pharmacognostic standardization.

MATERIALS AND METHODS

The *Epilobium angustifolium* (Fig. 1) raw material used for this study was collected during the flowering stage of the plant in August 2021 from Malham village in the Shamakhi district of the Republic of Azerbaijan. The entire herb, including roots, stems, leaves, and flowers, was used as the research object. The plant samples selected for investigation were freshly prepared. Samples intended for microscopic examination were fixed in a solution composed of 2.5% glutaraldehyde, 2% paraformaldehyde, 4% sucrose, and 0.1% picric acid, prepared in 0.1 M phosphate buffer (pH = 7.4). The fixed materials were processed and examined at the Electron Microscopy Laboratory of Azerbaijan Medical University.

After fixation, the samples were rinsed three times in 0.1 M phosphate buffer (pH = 7.4) for 15 minutes each (total 45 minutes). Subsequently, post-fixation was carried out by immersing the samples in a mixture containing 1% osmium tetroxide (OsO_4), 0.1 M phosphate buffer, and 1.5% potassium ferricyanide (red blood salt) for 1.5 hours. After post-fixation, the samples were washed again in 0.1 M phosphate buffer for 15 minutes and subjected to dehydration.

Figure 1. Epilobium angustifolium

The dehydration process involved immersing the samples sequentially in 50%, 70%, and 96% ethyl alcohol for 15 minutes each (total 45 minutes). In the next stage, samples were treated in a 1:1 solution of 96% ethyl alcohol and acetone for 15 minutes, followed by pure acetone for 15 minutes, repeated three times (total 45 minutes).

Following dehydration, embedding blocks were prepared using an araldite-epon mixture composed of five components: Epon-812, DDSA (dodecenyl succinic anhydride), Araldite M, dibutyl phthalate, and DMP-30 (2,4,6-tris(dimethylaminomethyl)phenol).

The samples were placed in pre-labeled molds and polymerized in a thermostat at 37°C, 45°C, and 60°C, each for 24 hours (a total of 3 days). After polymerization, the solidified blocks were removed from the molds, and semi-thin sections (1 µm) were cut using a Leica EM UC7 ultramicrotome.

The sections were stained using a double-staining method:

Solution A: 0.5% methylene blue, 0.5% azure II, 0.5% borax

Solution B: 5% ethanol, 0.1% fuchsin

Stained sections were examined under a **Latimet (Leitz)** light microscope. Photomicrographs of the relevant anatomical features were captured using **Pixera (USA)** and **Canon (Japan)** digital imaging systems (D'Amico, 2005; Kuo, 2008).

RESULTS AND DISCUSSION

Morphological Characteristics

Epilobium angustifolium L. is a perennial herbaceous plant characterized by a thick, creeping rhizome system and erect stems reaching up to 1 meter in height. The stems display fine pubescence in the upper regions, transitioning to glabrous and bark-like textures in the lower parts. The leaves are primarily alternate in arrangement, with rare spiral occurrences. They are oblong to lanceolate in shape, possess acute apices, and have entire or finely serrated margins. Leaf surfaces are sessile or short-petiolate, with a dark green, glossy adaxial (upper) surface and a lighter abaxial (lower) surface.

ANATOMICAL FEATURES

Leaf Anatomy. Microscopic examination revealed a dorsoventral (bifacial) leaf structure (Figure 2). The upper epidermis is astomatous, whereas the lower epidermis contains **anomocytic-type** stomatal complexes. The mesophyll consists of 1–2 layers of palisade parenchyma cells beneath the upper epidermis and a spongy parenchyma region occupying the central area. The vascular system is represented by a single, large **collateral-type**, crescent-shaped vascular bundle. Sclerenchyma tissue is notably absent in the foliar structure.

Stem Anatomy. In cross-section, the stem displays a pentagonal shape (Figure 3). Below the epidermis lies a layer of both angular and plate-like collenchyma. The vascular system comprises a circular arrangement of collateral bundles. The **xylem** is composed of vessel elements and parenchyma cells, while the **phloem** consists of sieve tubes and companion cells. A well-developed **cambial layer** is present between the xylem and phloem (Figure 4).

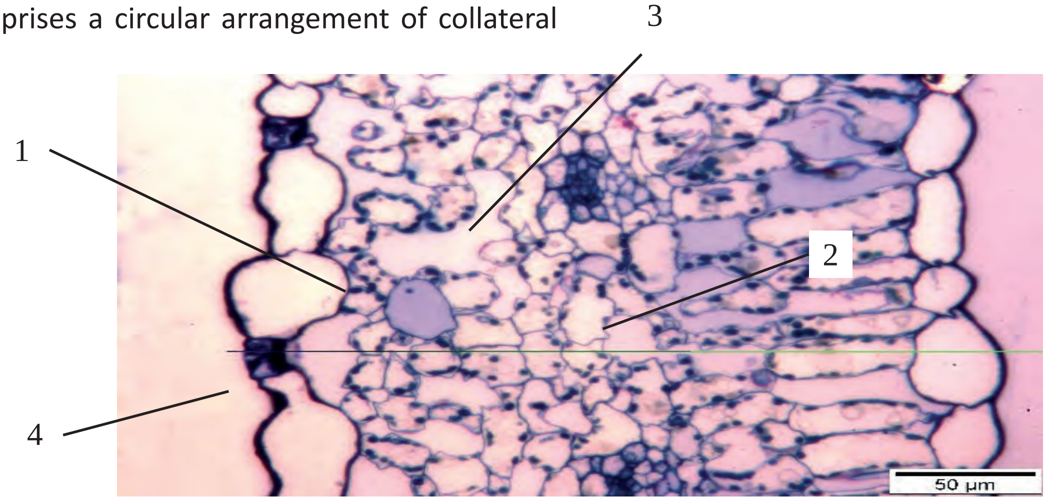

Figure 2. Cross-section of Epilobium angustifolium leaf 1 – Epidermal cells; 2 – Palisade parenchyma cells; 3 – Spongy parenchyma; 4 – Stomata of the lower epidermis.

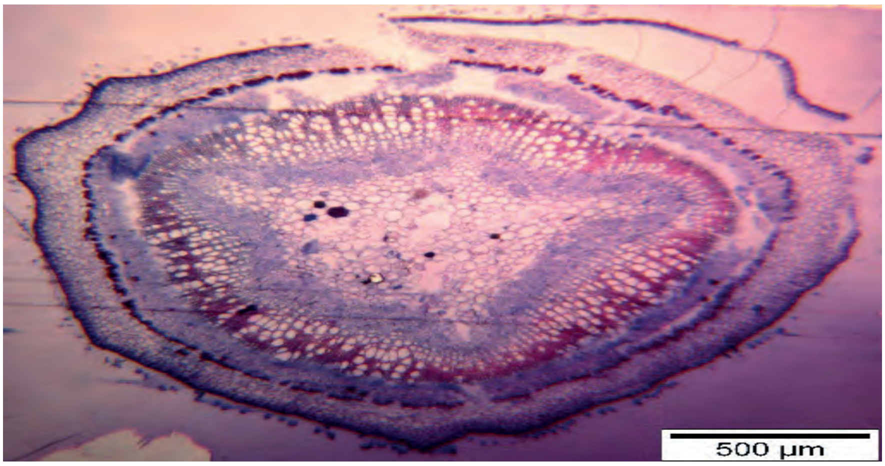

Figure 3. Cross-section of a pentagonal-shaped stem

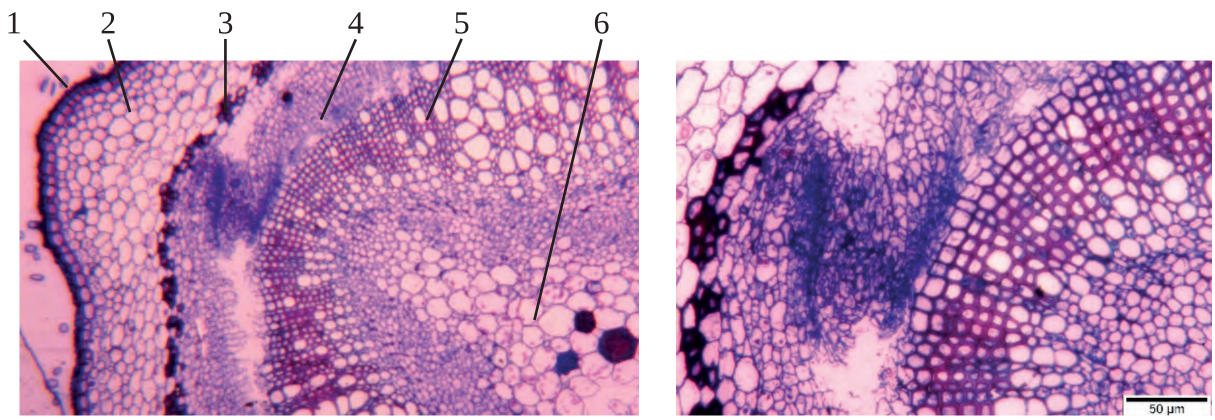

Figure 4. Cross-section of stem vascular tissue
1 – Epidermis; 2 – Collenchyma; 3 – Sclerenchyma; 4 – Phloem; 5 – Cambium; 6 – Xylem.

DISCUSSION

The anatomical investigation revealed several diagnostically significant features of *E. angustifolium* raw material. The dorsoventral leaf organization, with a stomata-free upper epidermis and anomocytic stomata confined to the lower epidermis, serves as a key diagnostic marker. Likewise, the presence of trichomes on floral organs—particularly on the pedicel and calyx base—as well as the pentagonal stem shape and characteristic vascular arrangement, provide reliable morphological criteria for species identification.

These features are not only taxonomically valuable but also reflect **adaptive responses** to the plant's environmental conditions. The bifacial leaf structure enhances photosynthetic efficiency under varying light intensities, while the stomatal positioning limits transpiration, which may be crucial in temperate habitats. The supporting tissues—collenchyma and phloem-associated sclerenchyma—contribute to the mechanical stability required for the plant's upright growth.

Overall, these detailed anatomical and morphological traits can be employed in pharmacognostic standardization, aiding in the **authentication**, **quality control**, and **regulatory classification** of *E. angustifolium* as a medicinal raw material.

Conclusion

The anatomical examination of *Epilobium angustifolium* raw material revealed several key diagnostic features essential for its accurate identification and quality evaluation. These include:

- A dorsoventral leaf structure with an astomatous upper epidermis;
- Presence of anomocytic stomata in the lower epidermis;
- Dense trichome coverage on the flower stalk and base of the calyx;
- Pigmented sepals with a glabrous, lilac-colored interior at the base.

These distinct anatomical markers are characteristic of *E. angustifolium* specimens naturally distributed in the flora of Azerbaijan. The findings provide a scientific foundation for establishing reliable quality control criteria and will be instrumental in the development of a Pharmacopoeial monograph for the raw material.

References

Audrius, M., Rasa, U., Danguolė, R., et al. (2017). Analysis of antiproliferative effect of Chamerion angustifolium water extract and its fractions on several breast cancer cell lines. Advances in Medical Sciences, 62, 158–164.

Audrius, M., To Him, R., Ovidius, V., et al. (2014). Flavonoids of willow herb (Chamerion angustifolium (L.) Holub) and their radical scavenging activity during vegetation. Advances in Medical Sciences, 59(1), 136–141.

D'Amico, F. (2005). A polychromatic staining method for epoxy embedded tissue: A new combination of methylene blue and basic fuchsine for light microscopy. Biotech Histochemistry, 80(5–6), 207–210. https://doi.org/10.1080/10520290600560897

Gevrenova, R., Zengin, G., Ozturk, G., & Zheleva-Dimitrova, D. (2025). Exploring the phytochemical profile and biological insights of Epilobium angustifolium L. herb. Plants, 14(3), 415.

Gurbanov E., Ibrahimov Sh, Huseynova H. (2022). Plant ecological research for the bioremediation from pollution by oil and oil products in Absheron peninsula (Azerbaijan). Bulletin of Science and Practice. Vol. 8. №12. https://doi.org/10.33619/2414-2948/85

Kuo, J. (2008). Electron microscopy. In Springer Protocols Handbooks (pp. 975–1008). Springer. https://doi.org/10.1007/978-1-60327-375-6_54

Renata, S., Giulia, M., Valeria, K., et al. (2020). Inventing a herbal tradition: The complex roots of the current popularity of Epilobium angustifolium in Eastern Europe. Journal of Ethnopharmacology, 247, Article 112356.

Schepetkin, I., Ramstead, A., & Kirpotina, N. L. (2016). Therapeutic potential of polyphenols from Epilobium angustifolium (fireweed): Polyphenols from fireweed. Phytotherapy Research, 30(8), 1287–1297.

Suleymanov, T. A., Huseynova, K. A., & Balayeva, E. Z. (2023). Spectrophotometric determination of flavonoids in Epilobium angustifolium raw material and validation of the method. Azerbaijan Journal of Pharmacy and Pharmacotherapy, 2, 5–10.

Vitalone, A., Mazzanti, G., Tita, B., et al. (2001). Analgesic properties of Epilobium angustifolium, evaluated by the hot plate test and the writhing test. Il Farmaco, 56(4), 341–343.

Zagórska-Marek, B., Artur, A., Mariola, M., Katarzyna, S., et al. (2019). Fireweed (Epilobium angustifolium L.): Botany, phytochemistry and traditional uses. Journal of Natural Fibers and Medicinal Plants, 65(3), 51–63.

EFFECTS OF IAA AND IAA–GRAPHENE OXIDE NANOENSEMBLE ON DROUGHT STRESS IN DURUM WHEAT (*TRITICUM DURUM*)

Elshan Aliyev[1,2]* |https://orcid.org/0009-0008-2125-4153
Nurlan Amrahov[1] |https://orcid.org/0000-0002-6916-7672
Faig Khudayev[2] |https://orcid.org/0009-0004-5385-885X
Ziyaddin Mammadov[1] |https://orcid.org/0000-0001-8009-194X
Sibel Hasanova[3] |https://orcid.org/0009-0009-5239-3081
Amin Valiyev[1] |https://orcid.org/0009-0006-6076-918X
Ulviyya Hasanova[1] |https://orcid.org/0000-0003-1502-4227

[1]Baku State University, Baku, Azerbaijan
[2]Azerbaijan Research Institute of Crop Husbandry, Ministry of Agriculture, Baku, Azerbaijan
[3]Azerbaijan State Oil and Industry University, Baku, Azerbaijan

[1*]Correspondence: aliyevelshan2002@gmail.com

Article Info:
DOI: https://doi.org/10.30546/abc.2025.0022
Pages: 43-51
Received: September 5, 2025 | Revised: September 25, 2025 |Accepted: October 2, 2025

Abstract

Wheat (Triticum durum) is one of the world's most important crops, supplying essential nutrients and serving as a key source of food and livestock feed. Drought stress is a major challenge that hampers wheat growth and yield by disrupting its physiological and biochemical processes. Recent developments in nanotechnology present new opportunities to boost plant resilience and productivity. In this study, we examined the effects of a newly developed indole-3-acetic acid–graphene oxide (IAA–GO) nanoensemble on wheat seedlings under both normal and drought conditions. Seeds of the Yasaman variety were treated with IAA and IAA–GO and grown under controlled phytotron settings. We evaluated seedling growth, photosynthetic pigment levels, and activities of antioxidant enzymes, including catalase and guaiacol peroxidase. The results revealed that IAA alone significantly improved germination, root and shoot growth, and catalase activity. In contrast, the IAA–GO nanoensemble showed mixed effects, slightly enhancing catalase activity but reducing peroxidase activity and chlorophyll b content. Under drought stress, both treatments positively affected photosynthetic pigments, indicating an adaptive response. These findings suggest that IAA–GO complexes could be a valuable tool for enhancing drought tolerance in wheat by supporting growth, photosynthesis, and antioxidant defense systems.

Key words: *wheat, graphene oxide, nanotechnology, antioxidant system, phytohormones, plant protection*

INTRODUCTION

Plant-based products play a crucial role in ensuring human nutrition, accounting for approximately 90 % of the total food sources. A significant portion of these, around 60 % comes from cereal crops. On a global scale, about 75 % of the human dietary demand is met by wheat (Hajiyeva et al., 2019). Wheat demonstrates remarkable ecological adaptability compared to other cereal crops and stands as the most widely cultivated grain globally. It is also recognized as one of the primary sources of plant-derived protein essential for human nutrition (Hasanova et al., 2019; Vilayet & Boyukkhanim, 2024). Wheat undergoes extensive processing and serves as a key raw material in producing a variety of food products such as pasta, flour, pastries, starch, beer and alcoholic beverages. Moreover, cereal grains play a vital role in providing the main feed source for livestock and poultry (Mirzayeva et al., 2022). According to the data provided in the *Food Balances of Azerbaijan* compendium published by the State Statistical Committee of the Republic of Azerbaijan, the total wheat reserves in 2024 amounted to 3,343,240 tons. Of this amount, 111,447 tons were allocated for seed, 695,681 tons for livestock and poultry feed, 1,822,312 tons for flour and groats production, 34,779 tons for alcohol production, and 31 tons for beer production (Food balances of Azerbaijan, 2025).

Drought stress is among the most significant abiotic challenges that farmers across thr globe encounter due to the impacts of climate change (Mammadova et al., 2025; Mansour et al., 2020). Drought stress profoundly affects wheat by altering its physiology, morphology and biochemical processes, which in turn slows down its growth and lowers overall yield (Jafarzadeh et al., 2025; Nyaupane et al., 2024).

Recent studies highlight the great potential of nanotechnology to transform agriculture by boosting the effiency of inputs and offering innovative solutions to the environmental and farming challenges, ultimately supporting higher good production and improved food security (Hasanova et al., 2022; Usman et al., 2020). Nanotechnology holds diverse applications in agroecosystems and is an emerging technique contributing to sustainable agricultural development with various potential functions. In recent years, graphene oxide (GO) and similar nanomaterials have been increasingly utilizied to efficiently deliver agrochemicals and nutrients to plants. They possess distinctive physicochemical properties, such as a very high specific surface area (2620 m^2/g) excellent resistance to the chemical and thermal breakdown, and a strong ability to adsorb both agrochemicals and micronutrients (Zhang et al., 2020). The way nanomaterials interact with and influence plants is complex and constantly changing, depending on factors such as the type of nanoparticle, how it is applied (including concentration, duration, and method), and the balance of plant hormones (Cheng et al., 2016). Plants respond to GO mainly through the reactive oxygen species (ROS) pathway. While ROS are naturally produced during normal cellular metabolism, stress can trigger their excessive accumulation, leading to oxidative damage and cell death. Research indicates that nanomaterials can affect plant growth and development by modulating this ROS metabolism (Rashid et al., 2021; Siddiq & Husen, 2017). GO can be used to deliver a range of substances, including plant hormones, which helps improve nutrient availability for plants while reducing losses due to leaching, breakdown by light, or hydrolysis (Amrahov at el., 2025). One example of such a phytohormone is IAA, a natural auxin that is essential for controlling plant growth, boosting stress resistance, and activating antioxidant defenses. IAA helps plants produce more energy by promoting the accumulation of photosynthetic products and also strengthens their antioxidant defenses when they face stressful conditions. IAA lowers the buildup of reactive oxygen species (ROS), helping to prevent oxidative damage and boosting the plant's ability to withstand stress. (Wang et al., 2024). This study focused on exploring how a newly synthesized IAA–graphene oxide complex influences the growth and immune system components of one of the most important wheat species (*Triticum durum*).

MATERIALS AND METHODS

The study was carried out using the Yasaman (Triticum durum) wheat variety, with seeds sourced from the Azerbaijan Research Institute of Crop Husbandry. Before sowing, the wheat seeds were sterilized in a 0.1% potassium permanganate solution for one minute. Then they were planted in plastic pots filled with cocopeat substrate.

Graphene oxide (GO) nanolayers were prepared using a modified Hummer method (Taghiyeva et al ., 2024). IAA (1 μM) and IAA-GO (1 μM) were applied continuously throughout the growth period, starting from the earliest seedling stage. To simulate drought stress, polyethylene glycol (PEG-6000) was used; a 15% solution was prepared by adding 150 g of PEG-6000 to 1 liter of Steiner hydroponic solution.

The experiments were carried out using wheat seedlings that had been grown for two weeks.

Enzymatic activity analysis. The activity of the catalase enzyme was determined using the Mosheva gasometric method (Mosheva, 1982).

Guaiacol peroxidase activity was determined based on the method developed by Chance and Maehly (Chance & Maehly, 1955).

Chlorophyll a, chlorophyll b, and carotenoid contents were measured according to the procedure established by Wellburn and Lichtenthaler (Wellburn & Lichtenthaler, 1984).

Statistical analyses. All adsorption experiments were carried out in triplicate, and the results are presented as the mean ± standard deviation (SD). Regression parametres (R^2) for the isotherm, kinetic models were generated using the statistical measures in Microsoft Excel (Office 11, Microsoft Corporation, USA).

RESULTS

The impact of IAA and the IAA-GO nanoensemble on wheat seedling germination and growth and is illustrated in Figure 1 and summarized in Table 1.

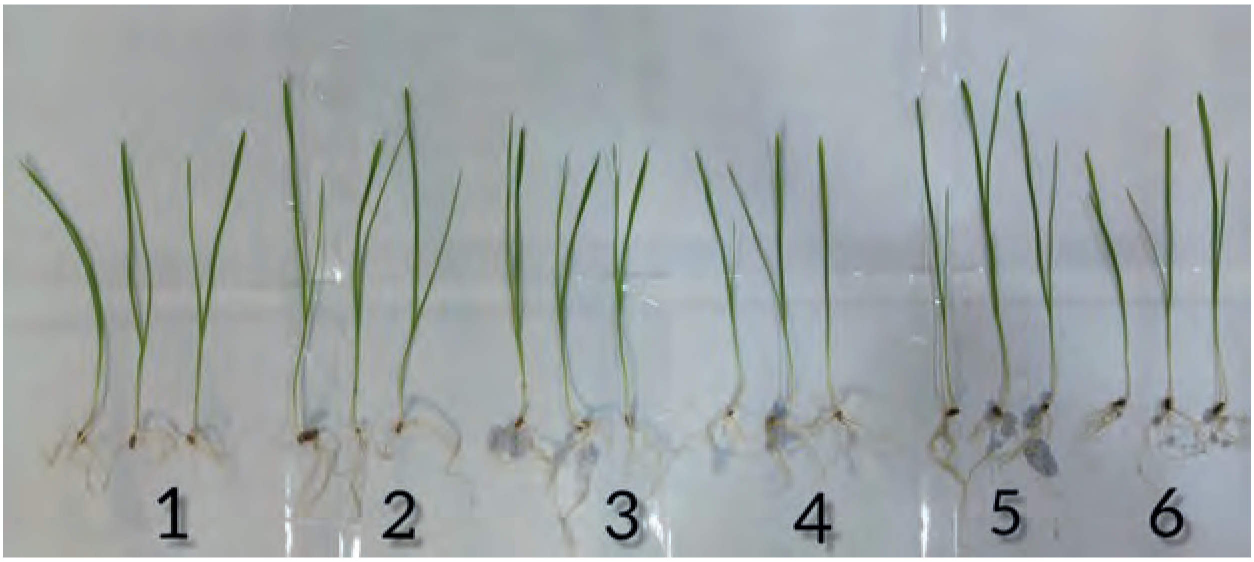

Figure 1. Effect of İAA and İAA-GO nanoensembles on the development of 14 day old Yasemen wheat genotype under drought stress. 1.Control. 2. 1 µM IAA. 3. 1 µM + GO. 4. 15 % PEG. 5. 15 % PEG + 1 µM IAA. 6. 15 % PEG + 1 µM IAA + GO

Table 1.
Germination percentage, root, and stem lengths of the Trititucum durum Desf. Yasemen variety exposed to IAA and IAA + graphene oxide under drought stress

Samples	Number of seedlings (total number of seeds – 72)	Germination percentage, %	Stem length (sm)	Root length (sm)
Control	59	81.9	17.5±1,01	4.11±0.22
1 µM IAA	65	90.2	19.26±1.22	7.68±1.21
1 µM IAA+ GO	54	75	16.79±0,49	6.17±1.36
15 % PEG	49	68.05	16.34±1.57	6.45±1.35
15% PEG+ 1 µM IAA	58	80.5	19.28±0.21	10.06±2,01
15 % PEG +1 µM IAA + GO	53	73.61	16.73±0.48	4.77±0.85

According to the results of the comparative germination analysis, the 1 µM IAA + GO treatment exhibited a minimal effect compared to the control variant. Although this treatment increased root length by 50%, it reduced leaf length by 4%. In contrast, the application of 1 µM IAA alone enhanced both leaf and root elongation by 10% and 86%, respectively. Under drought stress conditions, the 1 µM IAA + GO treatment slightly improved germination by 8.17% and leaf length by 2.38%. Regarding primary root development, compared with the 15% PEG variant, the nanoensemble caused a 26% reduction in root length, whereas 1 µM IAA exerted a positive influence on all three measured parameters, increasing germination by 18.29%, leaf length by 17.9%, and root length by 55.96%.

As a result of treating wheat seedlings with the IAA–GO phytohormone complex, a decrease in GPX enzyme activity was observed compared to the control variant (Figure 2). A similar inhibitory effect on the enzyme activity was also recorded during the application of the IAA–graphene oxide nanoensemble under drought stress conditions — with a 12.9% reduction before stress application and a 24.59% reduction afterward. IAA alone, however, did not affect peroxidase activity in either case. These data indicate that IAA exerted a stable (non-significant) effect, while the IAA–graphene oxide nanoensemble demonstrated an inhibitory effect on this enzymatic component of the antioxidant system in wheat plants.

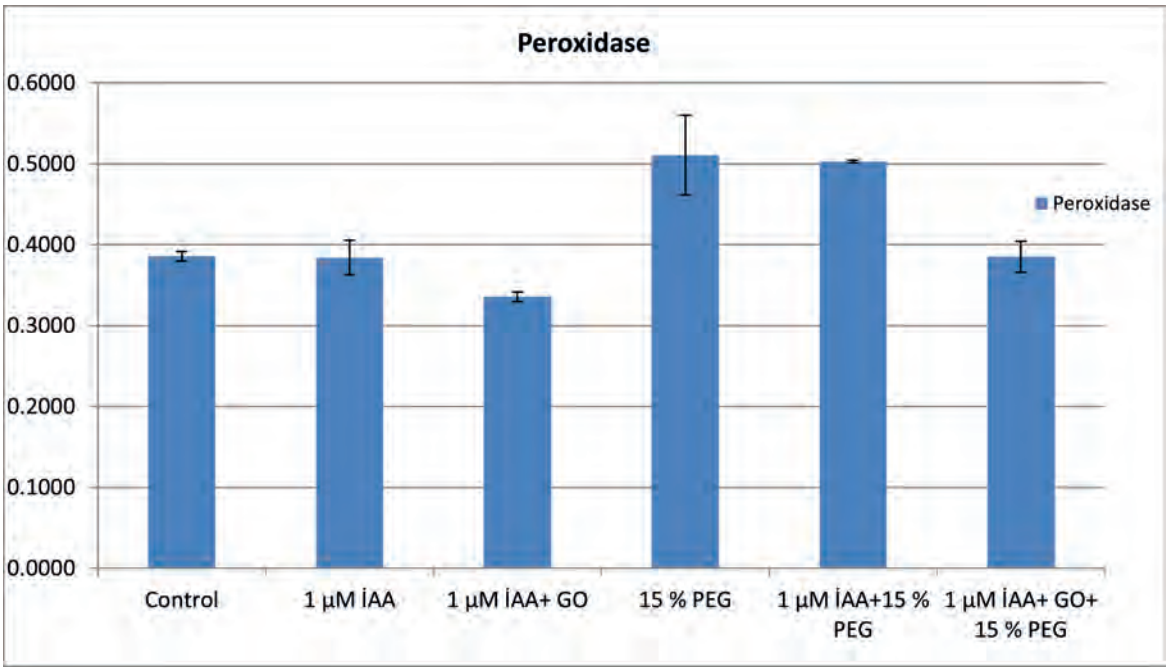

Figure 2. Guaiacol Peroxidase (GPX) activity in the leaves of Triticum durum Desf. Yasemen genotype treated by concentrations of İAA and İAA-GO nanoensemble**.**

The conducted analyses showed that, under normal conditions, treatment with the IAA+GO complex caused a 36.54% reduction in chlorophyll b content compared to the control group (Figure 3). This finding suggests that IAA–GO suppresses chlorophyll b synthesis, negatively affecting the plant's photosynthetic machinery by weakening the production of key photosynthetic pigments and diminishing its activity. When applied under drought stress, both IAA and the IAA–GO nanoensemble complex influenced the synthesis of all three components of the photosynthetic system. In particular, IAA treatment resulted in 0.3, 2.3, and 2.5 times increases, while IAA–GO treatment led to 3.25%, 31.28%, and 16.96% increases, respectively. However, these effects appear to be primarily associated with the influence of drought stress.

Overall, the results highlight the importance of further studies to better understand the interaction mechanisms between nanoensembles and drought stress in the regulation of photosynthetic activity in plants.

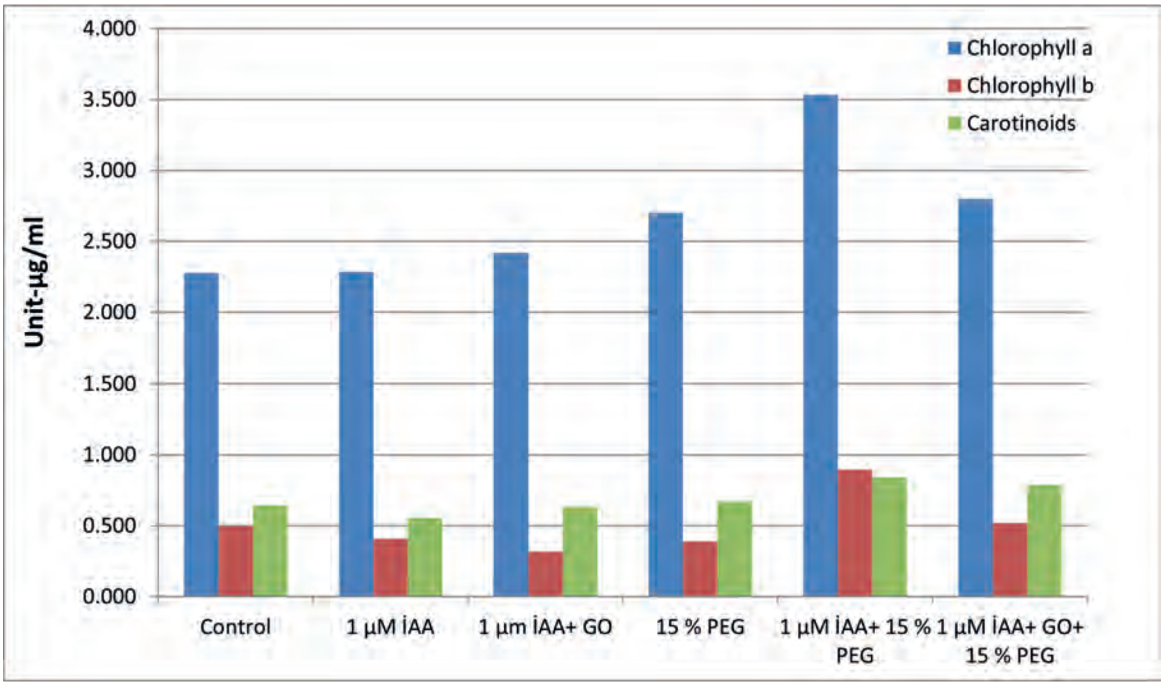

Figure 3. The impact of IAA and IAA-graphene oxide nanoensemble on the levels of chlorophyll a, b, and carotenoids in the leaves of Triticum durum Desf. Yasemen genotype.

Catalase is a vital antioxidant enzyme responsible for breaking down hydrogen peroxide into water and oxygen, thus helping to protect cells by preventing the accumulation of harmful reactive molecules. Under both normal and drought conditions, treatment with IAA enhanced catalase activity by 20% and 8.2%, respectively. Although the IAA–GO nanoensemble showed slightly lower catalase activity than IAA alone, it still caused a modest increase compared to the control group (Figure 4).

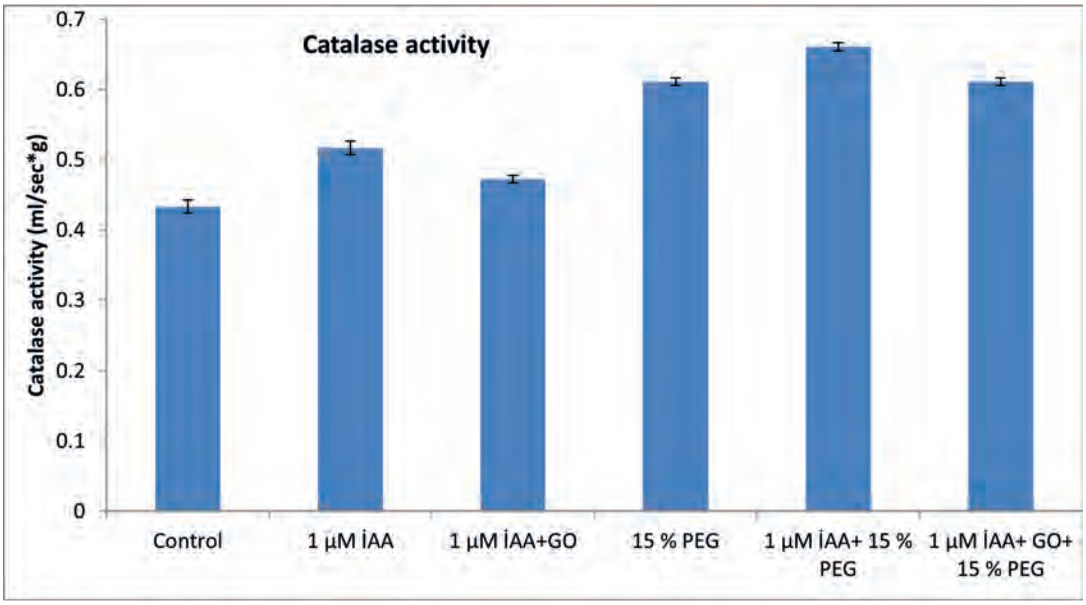

Figure 4. The effect of IAA and IAA-GO nanoensemble on catalase activity in the leaves of Triticum durum Desf., Yasemen genotype

DISCUSSION

Auxins are key regulators of vegetative development and growth, controlling nearly all aspects of these processes, as well as mediating resistance to various stress factors (Amrahov et al., 2023). In addition to regulating fundamental aspects of cell division, cell elongation, and cell differentiation, they play a crucial role in diverse plant physiological processes (Zhang et al., 2022). Indole-3-acetic acid (IAA), as a member of the auxin group of phytohormones, possesses the characteristic properties described above. In previous studies, a single exogenous application of IAA resulted in a theoretical yield increase of 48.53% in *Pinus yunnanensis* (Zhu et al., 2025). In our research, exogenous IAA was also found to have an inductive effect on both leaf and root length, as well as seed germination, in wheat plants.

In recent years, numerous studies have explored the effects of nanoensemble structures on plant development. In particular, the use of nanomaterials such as carbon nanotubes, graphene, and graphene oxide has shown significant results. Recent research has demonstrated that graphene holds considerable potential in agricultural applications, including the delivery of plant nutrients and crop protection agents, as well as in post-harvest management processes (Bhattacharya et al., 2023). However, to ensure the safe development of nanotechnology, it is essential to investigate the potential negative effects of nanoparticles (Rzayev et al., 2022).

Recent studies have reported that a graphene oxide-based nanoensemble, non-covalently combined with kinetin, did not enhance stem growth in cotton plants, but accelerated seed germination by 13.3%, providing clear evidence of the positive effects of graphene oxide (Amrahov et al., 2025; Olatunbosun et al., 2023). In contrast, in our study, a graphene oxide-based nanoensemble combined with IAA negatively affected both seed germination and stem and root growth. This may be explained by the fact that graphene oxide can interfere with the distinct metabolic pathways of mono- and dicotyledonous plants through different mechanisms.

Plants in their natural environments are exposed to various abiotic stresses that trigger the production of reactive oxygen species (ROS), leading to oxidative stress and potential cellular damage. ROS perform a dual function in plant systems: while their excessive accumulation can cause oxidative damage, they also act as key signaling molecules, transmitting stress signals to the nucleus via redox-mediated activation of mitogen-activated protein kinase (MAPK) cascades (Agbektas et al., 2023). ROS can oxidize specific redox-sensitive proteins and initiate MAPK signaling. Through these mechanisms, ROS play a central role in plant acclimation to environmental stress and function as primary signal transducers interacting with multiple pathways (Rao et all, 2023). Studies on wheat and rapeseed seedlings have shown that modified graphene oxide can slightly enhance catalase activity (Wang et al., 2022). In our study, both IAA and the IAA–graphene oxide nanoensemble slightly increased catalase activity, suggesting that the nanoensemble may exert a synergistic effect on the antioxidant system.

Alongside catalase, peroxidases also play a crucial role in the antioxidant defense of plant cells, making it important to determine how the activity of these enzymes is affected by nanoensembles. In our study, a decrease in guaiacol peroxidase activity was observed, and this effect remained consistent under drought stress when plants were treated with the IAA–graphene oxide nanoensemble. Under 15% PEG-induced drought stress, PEG itself increased peroxidase activity due to the generation of reactive oxygen species, which lead to oxidative stress. The reduction in peroxidase activity under combined drought stress and IAA–graphene oxide treatment appears to be a direct effect of graphene oxide. Graphene oxide possesses a redox-active surface and can influence intracellular electron transfer processes. This interaction alters the redox environment and cofactor balance, indirectly affecting the active site of peroxidase and consequently weakening its overall activity.

Chlorophylls a and b, the main components of the photosynthetic apparatus, provide plants with energy and carbon for organic matter synthesis. In our study, the IAA–graphene oxide nanoensemble alone inhibited chlorophyll b formation. However, under drought stress, both IAA and the IAA–graphene oxide nanoensemble increased the levels of photosynthetic components. Previous studies have also reported that graphene oxide (GO) alone stimulated photosynthetic pigments in certain tolerant species, such as *Iris pseudacorus*, where chlorophyll a + b and carotenoid levels increased by 26–178% depending on GO concentration (Zhou et all, 2023). This effect has been associated with improved light capture, electron transport, and other photophysical processes, although it is strongly dependent on plant species and GO dosage (Aliyeva et al., 2025; Nahida, 2020).

CONCLUSION

The results of this study indicate that the IAA–graphene oxide (IAA–GO) phytohormone complex plays a significant role in enhancing drought tolerance in wheat plants. Under drought stress, it stimulates the components of the photosynthetic apparatus and regulates the activity of antioxidant enzymes such as catalase and peroxidase, thereby improving the plants' resistance to stress. Future research should further explore these mechanisms on a broader scale and compare the effects of the complex across different plant species.

References

Agbektas, T., Zontul, C., Ozturk, A., Huseynzada, A., Ganbarova, R., Hasanova, U., ... & Silig, Y. (2023). Effect of azomethine group containing compounds on gene profiles in Wnt and MAPK signal patterns in lung cancer cell line: In silico and in vitro analyses. *Journal of Molecular Structure*, *1275*, 134619. https://doi.org/10.1016/j.molstruc.2022.134619

Aliyeva, N. K., Aliyeva, D. R., Suleymanov, S. Y., Rzayev, F. H., Gasimov, E. K., & Huseynova, I. M. (2025). Comparative Analysis of Mesophyll and Bundle Sheath Chloroplasts from Maize Plants Subjected to Salt Stress. *Biochemistry (Moscow)*, *90*(4), 522-533. https://doi.org/10.1134/S0006297924603162

Amrahov, N., Hasanova, U., Aliyeva, G., Aghazada, G., Mammadova, R., Alizade, Sh., Gakhramanova, Z., Hasanova, S., Mukhtarova, N., Mammadov, Z. (2025). Effect of kinetin-graphene oxide nanoensemble on the development and antioxidant system of cotton. *Acta Botanica Caucasica*, 4(1), 55–66. https://doi.org/10.30546/abc.2025.4.1.612

Amrahov, N. R., Allahverdiyev, V. Y., Agharzayeva, Y. I., Mammadova, R. B., Omarova, S. N., Khudayev, F. A., ... & Mammadov, Z. M. (2023). Effect of Verticillium wilt on the antioxidant system and formation of iron nanoparticles in cotton genotypes. *JAPS: Journal of Animal & Plant Sciences*, *33*(6). 1322-1332. https://doi.org/10.36899/JAPS.2023.6.0672

Amrahov, N.R., Mammadova, R.B., Allahverdiyeva, S.N., Aliyev E.I., Alizada Sh.R., Aghazada G.A., Ojagverdiyeva, S.Y. & Mammadov Z.M. (2023). Effect of *indole*-3- butyric acid on the antioxidant enzymes, no and chlorophyll content of Agdash-3 and AP-317 genotypes of upland cotton (*Gossypium Hirsutum* L.). *Advances in Biology & Earth Sciences,* 8(2), 147-156.

Bhattacharya, N., Cahill, D. M., Yang, W., & Kochar, M. (2023). Graphene as a nano-delivery vehicle in agriculture – current knowledge and future prospects. *Critical Reviews in Biotechnology*, 43(6), 851–869. https://doi.org/10.1080/07388551.2022.2090315

Chance, B., & Maehly, A. C. (1955). Assay of catalases and peroxidases. *Methods in Enzymology*, 2, 764–775. https://doi.org/10.1016/S0076-6879(55)02300-8

Cheng, F., Liu, Y. F., Lu, G. Y., Zhang, X. K., Xie, L. L., Yuan, C. F., & Xu, B. B. (2016). Graphene oxide modulates root growth of *Brassica napus* L. and regulates ABA and IAA concentration. *Journal of Plant Physiology*, 193, 57–63. https://doi.org/10.1016/j.jplph.2016.02.011

Hajiyeva, S. K., Fatullayeva, M. H., & Hasanov, F. A. (2019). The study of hybrid lines of wheat under the conditions of the Nakhchivan Autonomous Republic. *Collection of Scientific Works of the Azerbaijan Research Institute of Crop Husbandry*, Vol. XXX, 28–31.

Hasanova, G. M., Huseynov, S. I., & Asadova, S. A. (2019). Dependence of flour output and test weight on growing conditions and species in bread wheat. *Collection of Scientific Works of the*

Azerbaijan Research Institute of Crop Husbandry, Vol. XXX, 44–46.

Hasanova, U. A., Aliyev, A. R., Hasanova, I. R., Gasimov, E. M., Hajiyeva, S. F., Israyilova, A. A., ... & Amrahov, N. R. (2022). Functionalization of surgical meshes with antibacterial hybrid Ag@ crown nanoparticles. *Digest Journal of Nanomaterials & Biostructures (DJNB)*, 17(1). doi.org/10.15251/djnb.2022.171.11

Jafarzadeh, B., Abdiyev, V., Ismayilova, S., & Aliyeva, N. (2025). Determination of Proline Content in Bread Wheat Varieties Under Iso-Cation Sodium Salinity Conditions. *Nature & Science* International Scientific Journal. Vol: 7 (6), 14-19. DOI: https://doi.org/10.36719/2707-1146/57/14-19

Mammadova, R., Akparov, Z., Amri, A., Bakhsh, A., Alo, F., Alizade, S., Amrahov N. & Yunisova, F. (2025). Genetic diversity analysis of Azerbaijani bread wheat (Triticum aestivum L.) genotypes with simple sequence repeat markers linked to drought tolerance. *Genetic Resources and Crop Evolution,* 72(1), 315-323. https://doi.org/10.1007/s10722-024-01977-6

Mansour, H. A., El Sayed Mohamed, S., & Lightfoot, D. A. (2020). Molecular studies for drought tolerance in some Egyptian wheat genotypes under different irrigation systems. *Open Agriculture*, 5(1), 280–290. https://doi.org/10.1515/opag-2020-0030

Mirzayeva, G., Ibrahimov, E., & Ahmedova, F. (2022). Studying the resistance of introduced wheat samples to diseases and other parameters, selecting the primary material for breeding. In *Biotehnologii avansate–realizări şi perspective* (pp. 196–198). https://doi.org/10.53040/abap6.2022.66

Mosheva, V. (1982). Determination of the catalase activity in plant species. 134.

Nahida, A. (2020). Activities of antioxidant enzymes in mesophyll and bundle sheath cell chloroplasts of maize plants (zea mays l.) exposed to salt stress. *Бюллетень науки и практики*, *6*(11), 47-56. https://doi.org/10.33619/2414-2948/60/05

Nyaupane, S., Poudel, M. R., Panthi, B., Dhakal, A., Paudel, H., & Bhandari, R. (2024). Drought stress effect, tolerance, and management in wheat – a review. *Cogent Food & Agriculture*, 10(1), 2296094. https://doi.org/10.1080/23311932.2023.2296094

Olatunbosun, A., Nigar, H., Rovshan, K., Nurlan, A., Boyukhanim, J., Narmina, A., & Ibrahim, A. (2023). Comparative impact of nanoparticles on salt resistance of wheat plants. *MethodsX*, *11*, 102371. https://doi.org/10.1016/j.mex.2023.102371

Rao, M. J., Duan, M., Zhou, C., Jiao, J., Cheng, P., Yang, L., ... & Zheng, B. (2025). Antioxidant defense system in plants: Reactive oxygen species production, signaling, and scavenging during abiotic stress-induced oxidative damage. *Horticulturae*, 11(5), 477. https://doi.org/10.3390/horticulturae11050477

Rashid, A. N., Janda, M., Mahmud, M. Z., Valentová, O., Burketová, L., & Alekber, Q. A. (2021). Influence of salt stress on the Flg22-induced ROS production in *Arabidopsis thaliana* leaves. *Pak. J. Bot*, *53*(5), 1605-1610. http://dx.doi.org/10.30848/PJB2021-5(16)

Rzayev, F. H., Gasimov, E. K., Agayeva, N. J., Manafov, A. A., Mamedov, C. A., Ahmadov, I. S., ... & Choi, K. C. (2022). Microscopic characterization of bioaccumulated aluminium nanoparticles in simplified food chain of aquatic ecosystem. *Journal of King Saud University–Science*, 34(1), 101666. https://doi.org/10.1016/j.jksus.2021.101666

Siddiqi, K. S., & Husen, A. (2017). Plant response to engineered metal oxide nanoparticles. *Nanoscale Research Letters*, 12(1), 92. https://doi.org/10.1186/s11671-017-1861-y

State Statistical Committee of the Republic of Azerbaijan. (2025). "Food balances of Azerbaijan". "Narıncı Publishing House LLC"

Taghiyeva, N., Hasanova, U., Millet, M., Gardiennet, C., Gakhramanova, Z., Mirzayev, M. H., ... & Akhundzada, H. V. (2024). Synthesis and characterization of novel adsorbents based on functionalization of graphene oxide with Schiff base and reduced Schiff base for pesticide removal. *Materials*, 17(16), 4096. https://doi.org/10.3390/ma17164096

Usman, M., Farooq, M., Wakeel, A., Nawaz, A., Cheema, S. A., ur Rehman, H., ... & Sanaullah, M.

(2020). Nanotechnology in agriculture: Current status, challenges and future opportunities. *Science of the Total Environment*, 721, 137778. DOI: 10.1016/j.scitotenv.2020.137778

Vilayet, A., & Boyukkhanim, J. (2024). The activity of peroxidase and superoxide dismutasein plant seedlings under salt stress. *Acta Botanica Caucasica*, *3*(2), 21–29. https://doi.org/10.30546/abc.2024.3.2.315

Wang, J., Liu, L., Zhang, H., Zhang, D., Dai, Z., Luo, X., ... & Lin, L. (2024). Exogenous indole-3-acetic acid promotes the plant growth and accumulation of selenium in grapevine under selenium stress. *BMC Plant Biology*, 24(1), 426. https://doi.org/10.1186/s12870-024-05105-5

Wang, J., Xie, H., Han, J., Li, J., Lin, X., & Wang, X. (2022). Effect of graphene oxide–glyphosate nanocomposite on wheat and rape seedlings: Growth, photosynthesis performance, and oxidative stress response. *Environmental Technology & Innovation*, 27, 102527. https://doi.org/10.1016/j.eti.2022.102527

Wellburn, A. R., & Lichtenthaler, H. (1984). Formulae and program to determine total carotenoids and chlorophylls. *Advances in Photosynthesis Research*, 9–12. https://doi.org/10.1007/978-94-017-6368-4_3

Zhang, M., Gao, C., Xu, L., Niu, H., Liu, Q., Huang, Y., ... & Li, M. (2022). Melatonin and indole-3-acetic acid synergistically regulate plant growth and stress resistance. *Cells*, 11(20), 3250. doi: 10.3390/cells11203250

Zhang, P., Guo, Z., Luo, W., Monikh, F. A., Xie, C., Valsami-Jones, E., ... & Zhang, Z. (2020). Graphene oxide-induced pH alteration, iron overload, and subsequent oxidative damage in rice (*Oryza sativa* L.): A new mechanism of nanomaterial phytotoxicity. *Environmental Science & Technology*, 54(6), 3181–3190. DOI: 10.1021/acs.est.9b05794

Zhou, Z., Li, J., Li, C., Guo, Q., Hou, X., Zhao, C., ... & Wang, Q. (2023). Effects of graphene oxide on the growth and photosynthesis of the emergent plant *Iris pseudacorus*. *Plants*, 12(9), 1738. https://doi.org/10.3390/plants12091738

Zhu, M., Cheng, S., Tang, G., Hu, Z., Chen, L., Tang, J., ... & Cai, N. (2025). Effects of spraying exogenous hormones IAA and 6-BA on sprouts of *Pinus yunnanensis* seedlings after stumping. *Forests*, 16(1), 92. https://doi.org/10.3390/f16010092

BIODIVERSITY OF MICROORGANISMS IN ISTISU (MASALLI) THERMAL SPRINGS, AZERBAIJAN

Sabina Jafarzadeh[1,2]*|https://orcid.org/0000-0002-1649-9542
Fatma Shahbazova[3]|https://orcid.org/0009-0007-2244-1172
Elman Iskender[2]|https://orcid.org/0009-0004-0790-2784

[1]Karabakh University, Khankendi, Azerbaijan
[2] Institute of Microbiology, Ministry of Science and Education of the Republic of Azerbaijan, Baku, Azerbaijan
[3] Baku State University, Z. Khalilov Street 23, AZ1148, Baku, Azerbaijan

Correspondence: sabina.jafarzade@karabakh.edu.az

Article Info:
DOI: https://doi.org/10.30546/abc.2025.0025
Pages: 52-59
Received: July 12, 2025 | Revised: August 06, 2025 | Accepted: September 23, 2025

Abstract

The Masalli Istisu thermal springs in southern Azerbaijan represent a unique geothermal ecosystem characterized by mineral-rich waters with temperatures ranging from 45–60°C. Such conditions provide an ideal environment for thermophilic and thermotolerant microorganisms with ecological and biotechnological significance. This study investigated the microbial diversity of Masalli Istisu, with a focus on Bacillus spp. and filamentous fungi, during spring (April–May 2025) and autumn (September–October 2025). Water and sediment samples were collected from four representative sites, and microorganisms were isolated on Maltose Peptone Agar (MPA) and Potato Dextrose Agar (PDA). Morphological, Gram staining, and colony enumeration analyses were conducted to assess microbial composition and seasonal variation. Results demonstrated that Bacillus spp. were the dominant microbial population, consistently detected at high colony-forming unit (CFU) counts (1.1 × 10^5–1.4 × 10^5 CFU/ml) across both seasons. Gram staining confirmed their Gram-positive rod-shaped morphology, occurring singly or in short chains. Filamentous fungi, including Alternaria, Aspergillus*, and* Penicillium *species, were isolated at lower abundances, with slightly higher counts in spring compared to autumn. Seasonal fluctuations in fungal abundance are likely influenced by environmental factors such as temperature shifts, nutrient availability, and hydrological conditions, whereas Bacillus populations remained relatively stable. The findings highlight the ecological resilience of Bacillus spp. in thermophilic environments and the complementary role of fungi in ecosystem stability. Both groups possess biotechnological potential: Bacillus strains for thermostable enzyme production, antimicrobial compounds, and bioremediation, and fungi for bioactive metabolites and industrial enzyme applications. Overall, Masalli Istisu represents a promising geothermal habitat for future molecular and metagenomic exploration of novel thermophilic microorganisms.*

Keywords: *Masalli Istisu, Thermal springs, Azerbaijan, Thermophilic microorganisms, Microbial diversity*

INTRODUCTION

Masalli Istisu, located in southern Azerbaijan, represents a unique geothermal ecosystem characterized by hot, mineral-rich waters with temperatures ranging between 45–60°C. These conditions create a selective environment for thermophilic and thermotolerant microorganisms, including bacteria and fungi capable of surviving under high temperature and mineral stress. Previous studies of Azerbaijan's geothermal springs have reported microbial diversity, particularly of *Bacillus spp.,* Thermus spp., and thermotolerant fungi. However, comprehensive studies on Masalli Istisu are lacking, especially regarding seasonal microbial fluctuations, morphology, and ecological roles. Azerbaijan is endowed with abundant mineral and thermal water resources, which have been investigated with respect to their hydrogeological formation, physicochemical composition, and therapeutic potential (Aslanov, Akhundov, & Ahmedova, 1997). These waters not only serve as valuable natural health resources but also represent an important component of the country's economic and ecological assets. More recent studies provide a comprehensive evaluation of the present state of mineral water reserves, emphasizing issues related to uneven distribution, intensive exploitation, and environmental pressures, while also proposing rational management strategies to ensure their sustainable and efficient use in the future (Babayev & Taghiyev, 2018). Understanding the microbial composition of these springs is critical for ecological monitoring and offers potential biotechnological applications. Thermophilic *Bacillus* strains are of particular interest for their production of thermostable enzymes, antimicrobial compounds, and potential use in bioremediation. Similarly, thermotolerant fungi can be valuable in biotechnology for bioactive metabolites and industrial enzymes. This study aims to characterize ***Bacillus spp.*** and filamentous **fungi** in Masalli Istisu thermal springs across spring and autumn seasons, analyzing their morphology, Gram characteristics, colony counts, and ecological significance.

Extremophilic microorganisms, which thrive under extreme environmental conditions such as high temperatures, salinity, pH variations, and pressure, represent a rich source of novel enzymes with unique biochemical properties. These enzymes, often termed extremozymes, are highly stable and active under conditions that typically denature conventional enzymes, making them particularly valuable for diverse industrial applications. The exploration of extremophilic communities has gained significant attention in recent years due to their potential in biotechnological processes, including biofuel production, food processing, pharmaceutical synthesis, and waste management (Jafarzadeh et al., 2025). Despite their promising applications, the diversity and functionality of industrially relevant enzymes from extremophiles remain largely underexplored. This study focuses on isolating and characterizing novel enzymes from extremophilic microbial communities, aiming to expand the repertoire of biocatalysts available for industrial use and to enhance sustainable biotechnological practices.

Thermophilic microorganisms are key inhabitants of geothermal ecosystems, thriving under high-temperature conditions that are inhospitable to most life forms. These microbes possess specialized physiological and biochemical adaptations, such as thermostable enzymes and heat-resistant cellular structures, which allow them to maintain metabolic activity under thermal stress. Previous studies have documented the diversity and ecological significance of thermophiles in various extreme environments. For example, thermophilic bacteria from Moroccan hot springs, salt marshes, and desert soils demonstrate the ability to survive extreme temperature and salinity conditions, highlighting their potential for industrial and biotechnological applications (Aanniz et al., 2015). Similarly, thermophilic bacterial strains from the Soldhar (Tapovan) hot springs in the central Himalayan region show morphological and physiological traits adapted to geothermal habitats (Arya et al., 2015). Thermophiles are also valued for their practical applications; thermophilic hydrolases play important roles in biocatalysis, industrial enzyme production, and biotechnological processes (Ghosh et al., 2020). Wide-ranging applications of thermophiles include pharmaceuticals, environmental bioremediation, and the production of bioactive compounds (Mehta et al., 2016). Beyond applied significance, extremophiles provide crucial insights into microbial ecology, evolution, and the limits of life, both on Earth and potentially on extraterrestrial environments (Von Hegner, 2019). Recent work further emphasizes the exploration of novel industrial enzymes from extremophilic communities, demonstrating their potential to expand the repertoire of biocatalysts available for industrial and biotechnological applications (Jafarzadeh et al., 2025). Collectively, these studies highlight the ecological resilience, biotechnological potential, and scientific value of thermophilic microorganisms, underscoring the importance of studying geothermal habitats such as the Masalli Istisu thermal springs in Azerbaijan.

MATERIALS AND METHODS

1.Collection and Environmental Measurements

Water and sediment samples were collected from four representative sites within Masalli Istisu thermal springs during spring (April–May 2025) and autumn (September–October 2025). Water samples were collected in sterile 50 ml polypropylene tubes, while sediment samples were obtained using sterile spatulas and transferred into sterile containers (Ortega-Villar et al., 2024).

2.Isolation and Cultivation of Microorganisms

- **Bacillus spp.:** Samples were serially diluted (10^{-1}–10^{-6}) in sterile saline solution, spread-plated on Maltose Peptone Agar (MPA), and incubated at 50 °C for 24–48 h. Colonies with distinct morphology were repeatedly streaked to obtain pure cultures (Mohammad et al., 2017).
- **Fungi:** Samples were directly inoculated onto Potato Dextrose Agar (PDA) supplemented with chloramphenicol (50 µg/ml) to inhibit bacterial growth, and incubated at 28 °C for 5–7 days. Distinct fungal colonies were sub-cultured to purity (Ortega-Villar et al., 2024).

3.Gram Staining and Morphology

Bacterial isolates were Gram-stained using standard microbiological protocols (ASM, 2023) and examined under oil immersion at 1000× magnification. Cell shape, arrangement, and Gram reaction were recorded. Determinants of bacterial morphology were considered in the analysis (American Society for Microbiology, n.d.; Van Teeseling et al., 2017; Young, 2007). Fungal isolates were stained with lactophenol cotton blue and examined microscopically to assess hyphal morphology, spore type, and reproductive structures (Smith, 2002).

4.Microbial Enumeration

Colony-forming units (CFU/ml) for Bacillus spp. were determined from countable dilution plates and expressed as mean values from triplicate assays. Fungal CFU/ml was recorded from PDA plates, with colony counts expressed per gram of sediment or per ml of water sample (Ortega-Villar et al., 2024).

5.Data Analysis

Morphological and enumeration data were compared across spring and autumn seasons. Seasonal variation trends were assessed descriptively, and dominant genera were identified based on recurring morphological characteristics (Parkhurst & Appelo, 2013).

RESULTS AND DISCUSSION

Bacillus spp. were **Gram-positive rods**, occurring as single cells or short chains. Fungi were **filamentous with spore-producing hyphae**, including *Alternaria spp.*, *Aspergillus spp.*, and *Penicillium spp.* Morphological characteristics were consistent across spring and autumn.

The Table 1. summarizes the morphological features and Gram staining results of microorganisms isolated from Masalli (Istisu) hot spring during spring and autumn. Bacterial cells were observed as **Gram-positive rods** arranged singly or in short chains, while filamentous microorganisms displayed **spore-producing hyphae**. All isolates were cultured on **MPA medium**, and their GPS coordinates are provided for precise sampling location reference.

Table 1. Gram Staining and Morphology of Microorganisms

№	Season	Sample Name	Color	Shape	Arrange-ment	Gram Stain / Result	Growth Medium	GPS Coordinates
1	Spring	Istisu-1/2	Purple	Rods	Single/Short chains	Gram-positive	MPA	39.0206°N, 48.6681°E
2	Spring	Istisu-1/3	Purple	Filamentous hyphae	Spore-producing	—	MPA	39.0206°N, 48.6681°E
3	Autumn	Istisu-2/2	Purple	Rods	Single/Short chains	Gram-positive	MPA	39.0206°N, 48.6681°E
4	Autumn	Istisu-2/3	Purple	Filamentous hyphae	Spore-producing	—	MPA	39.0206°N, 48.6681°E

The Gram staining and microscopic examination of isolates revealed that Bacillus spp. were the dominant bacterial population across both sampling seasons. These isolates appeared as Gram-positive rods, either singly or arranged in short chains, consistent with the typical morphology of thermophilic *Bacillus* species. In contrast, fungal isolates exhibited filamentous hyphae with spore-producing structures, representing genera such as *Alternaria*, *Aspergillus*, and *Penicillium*. No significant morphological variation was observed between spring and autumn isolates, indicating that microbial communities in Masalli Istisu remain stable under seasonal temperature fluctuations. However, slight differences in fungal abundance suggest environmental factors such as nutrient input and water flow may influence fungal growth dynamics. All isolates were obtained from Maltose Peptone Agar (MPA) and Potato Dextrose Agar (PDA) plates and correspond to GPS coordinates 39.0206°N, 48.6681°E. This consistent morphological profile across seasons highlights the ecological stability of *Bacillus spp.* within the thermophilic ecosystem, while the presence of filamentous fungi reflects the adaptability of eukaryotic microorganisms under geothermal stress conditions.

The microscopic image shows bacterial cells isolated from the Masalli (Istisu) hot spring sample. The cells appear as **Gram-positive occi and bacilli**, occurring both singly and in short chains. Their morphology indicates the presence of spore-forming bacteria, likely belonging to the ***Bacillus spp.,*** which are commonly associated with thermal environments due to their heat resistance and ability to form endospores (Fig.1).

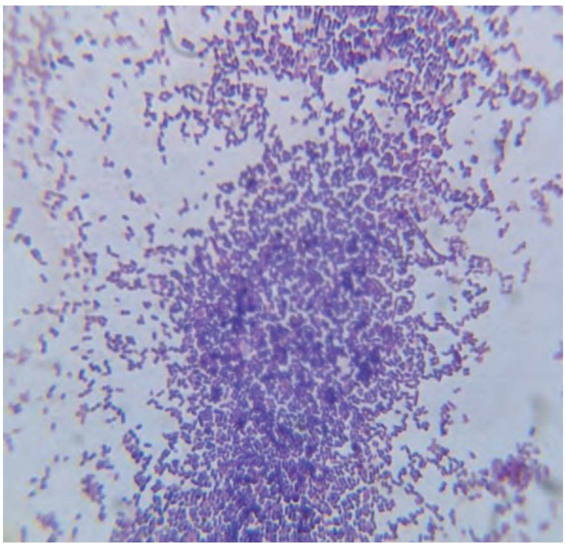

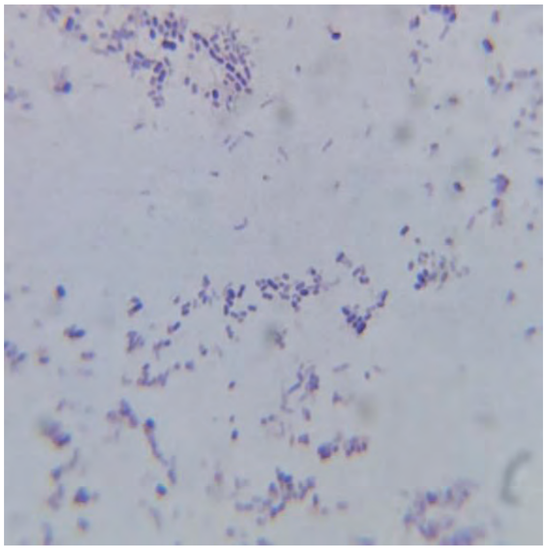

Figure 1. Microscopic view of the bacterium isolated from the Masalli (Istisu) sample

In all samples, Gram-positive bacilli were observed. Based on morphological appearance and arrangement characteristics, the bacteria correspond to the genera *Bacillus* spp. (bacillus-shaped). (Table 2).

Table 2. Ecological Roles and Potential Health Risks of *Bacillus spp.* in the Masallı - Istisu Thermal Hot Spring

Aspect	***Bacillus spp.* in Masallı- Istisu Thermal Hot Spring**
Ecological Role	- **Thermotolerance & Adaptation:** Many *Bacillus* spp. are thermophilic or thermotolerant, contributing to microbial diversity in hot springs.
- **Nutrient Cycling:** Participate in decomposition of organic matter and recycling of carbon, nitrogen, and phosphorus.	
- **Enzyme Production:** Secrete thermostable enzymes (amylases, proteases, lipases) useful for biotechnology and industry.	
- **Antimicrobial Activity:** Some strains produce antibiotics and antimicrobial peptides that regulate microbial community balance.	
Bioremediation Potential: Capable of degrading hydrocarbons and heavy metals, which may help in detoxifying geothermal waters.	
Risks	- **Opportunistic Pathogenicity:** Certain *Bacillus* spp. (e.g., *B. cereus*) can cause food poisoning or opportunistic infections in immunocompromised individuals.
- **Spore Formation:** Resistant spores may persist in extreme conditions, increasing their survival and dispersal potential.	
- **Water Contamination Risk:** If thermal water is used for bathing or drinking (after cooling), pathogenic strains may pose a health hazard.	
- **Antibiotic Resistance:** Some environmental *Bacillus* strains carry resistance genes, potentially transferable to pathogenic bacteria.	
- **Toxin Production:** *B. cereus* group can produce enterotoxins and emetic toxins harmful to humans.	

Quantitative enumeration revealed that *Bacillus* spp. were the dominant microbial group across both sampling seasons. In spring, *Bacillus* populations reached **1.4×10^5 CFU/ml**, while in autumn they remained comparably high at **1.1×10^5 CFU/ml**, demonstrating remarkable stability and adaptation to thermophilic conditions of the springs. These consistently high counts indicate that *Bacillus* spp. form the core microbial community in Masalli Istisu, maintaining ecological dominance regardless of seasonal shifts.

Fungal populations were comparatively scarce. In spring, fungal CFUs were approximately **3.0×10^2 CFU/ml**, representing a minor but detectable component of the community. In autumn, however, fungal colonies dropped to **$<10^2$ CFU/ml**, indicating seasonal suppression. The higher fungal abundance in spring may be associated with increased organic nutrient input and slightly more favorable growth conditions, while their reduced numbers in autumn reflect the sensitivity of fungi to geothermal stress factors such as temperature fluctuations and water flow variability. Overall, the data suggest that *Bacillus* spp. exhibit strong ecological resilience, whereas fungi show clear seasonal dynamics. These patterns highlight the dominance of thermophilic bacteria in sustaining geothermal microbial ecosystems, with fungi playing a secondary but potentially ecologically significant role (Tab. 3).

Table 3. Microbial Enumeration in Masalli-Istisu Thermal Springs

№	Season	Sample Name	*Bacillus* CFU/ml	Fungi CFU/ml	Notes
1	Spring	Istisu-1/2	1.4×10^5	–	*Bacillus spp.* dominant
2	Spring	Istisu-1/3	–	3.0×10^2	Fungi – *Alternaria spp.*, *Aspergillus spp.*, *Penicillium spp.*
3	Autumn	Istisu-2/2	1.1×10^5	–	*Bacillus spp.* dominant
4	Autumn	Istisu-2/3	–	$<10^2$	Fungi – *Alternaria spp.*, *Aspergillus spp.*, *Penicillium spp.*

The microbial diversity of Masalli -Istisu thermal springs demonstrates both ecological resilience and potential industrial value. Thermotolerant *Bacillus* spp. dominate the ecosystem and are well-recognized as sources of thermostable enzymes such as proteases, amylases, cellulases, and lipases, which retain catalytic activity at elevated temperatures and are highly sought after in food, pharmaceutical, detergent, and biofuel industries. In addition, *Bacillus* strains are known for producing antimicrobial peptides and lipopeptides, making them promising candidates for novel biocontrol agents and pharmaceutical applications. Their high CFU counts and persistence across spring and autumn indicate strong ecological stability, suggesting these organisms are well-adapted to geothermal stress and capable of maintaining essential ecosystem functions such as organic matter turnover. Although less abundant, filamentous fungi represent an important complementary microbial group. Genera such as *Aspergillus*, *Penicillium*, and *Alternaria* are notable for producing bioactive metabolites, pigments, and enzymes that could be exploited for industrial and medical applications. Their seasonal fluctuations reflect ecological sensitivity to environmental parameters, but their continued presence indicates a role in nutrient cycling and maintaining microbial community balance.

Taken together, the Masalli- Istisu thermal springs host a thermophilic microbial consortium with considerable ecological significance and biotechnological promise. The dominance of *Bacillus* spp. provides a stable platform for exploring thermostable biocatalysts, while the presence of fungi expands the potential for discovering novel secondary metabolites. These findings highlight the springs as a valuable natural reservoir for future molecular, biochemical, and metagenomic studies aimed at developing innovative applications in biotechnology, environmental management, and industrial microbiology.

CONCLUSION

The Masalli Istisu hot springs harbor a thermophilic microbial ecosystem primarily dominated by *Bacillus* spp., with filamentous fungi occurring at comparatively lower abundance. The consistently high colony counts of *Bacillus* across both spring and autumn highlight their strong ecological adaptation to geothermal conditions and their ability to maintain stability despite seasonal environmental fluctuations. In contrast, fungal populations display greater variability, with higher abundance in spring, reflecting their sensitivity to changes in temperature, nutrient availability, and hydrological factors. From an applied perspective, the microbial community of Masalli Istisu represents a valuable biological resource. Thermophilic *Ba-*

cillus strains are potential producers of thermostable enzymes, antimicrobial metabolites, and bioremediation agents, while filamentous fungi may serve as sources of bioactive secondary metabolites and industrially relevant enzymes. Together, these microbial groups contribute to the ecological resilience of the springs while offering diverse opportunities for biotechnological exploitation.

Future research should employ molecular, biochemical, and metagenomic approaches to complement culture-based findings. Such studies will allow for a deeper understanding of microbial diversity, enable the identification of novel thermophilic strains, and uncover bioactive compounds with industrial, medical, and environmental applications. Overall, Masalli Istisu springs stand out as an underexplored geothermal habitat with significant ecological importance and considerable promise for biotechnology.

References

Aanniz, T., Ouadghiri, M., Melloul, M., Swings, J., Elfahime, E., Ibijbijen, J., Ismaili, M., & Amar, M. (2015). Thermophilic bacteria in Moroccan hot springs, salt marshes and desert soils. *Brazilian Journal of Microbiology, 46*(2), 443–453. https://doi.org/10.1590/S1517-838246220140512

Aslanov, A. D., Axundov, V. J., & Ahmedova, O. M. (1997). *Mineral and thermal waters* (p. 150). Baku University Press.

American Society for Microbiology. (n.d.). *Gram stain protocols*. https://asm.org/protocols/gram-stain-protocols (Accessed April 25, 2023)

Arya, M., Joshi, G. K., Kumar Gupta, A., Kumar, A., & Raturi, A. (2015). Isolation and characterization of thermophilic bacterial strains from Soldhar (Tapovan) hot springs in central Himalayan region, India. *Annals of Microbiology, 65*, 1457–1464. https://doi.org/10.1007/s13213-014-0955-0

Babayev, N. I., & Tagiyev, I. I. (2018). *Modern state of mineral water resources of Azerbaijan and prospects for their efficient use* (p. 239). ASOIU Publishing House, Baku.

Ghosh, S., Lepcha, K., Basak, A., & Mahanty, K. A. (2020). Thermophiles and thermophilic hydrolases. In R. Salwan & V. Sharma (Eds.), *Physiological and Biotechnological Aspects of Extremophiles* (pp. 219–236). Academic Press. https://doi.org/10.1016/B978-0-12-819156-7.00011-2

Jafarzadeh, S. A., Bakhshaliyeva, K. F., Iskender, E. O., Muradov, P. Z., Leyla, A., & Muradova, S. M. (2025). Exploration of novel industrial enzymes from extremophilic communities for biotechnological applications. *International Journal of Agriculture and Biosciences, 14*(5), 944–954. https://doi.org/10.47278/journal.ijab/2025.066

Mehta, R., Singhal, P., Singh, H., Damle, D., & Sharma, A. K. (2016). Insight into thermophiles and their wide-spectrum applications. *3 Biotech, 6*, 2–9. https://doi.org/10.1007/s13205-015-0321-7

Mohammad, T. B., Al Daghistani, I. H., Jaouani, A., Abdel-Latif, S., & Kennes, C. (2017). Isolation and characterization of thermophilic bacteria from Jordania hot springs: *Bacillus licheniformis* and *Thermomonas hydrothermalis* isolates as potential producers of thermostable enzymes. *International Journal of Microbiology, 2017*, 6943952. https://doi.org/10.1155/2017/6943952

Ortega-Villar, R., Escalante, A., Astudillo-Melgar, F., Lizárraga-Mendiola, L., Vázquez-Rodríguez, G. A., Hidalgo-Lara, M. E., & Coronel-Olivares, C. (2024). Isolation and characterization of thermophilic bacteria from a hot spring in the state of Hidalgo, Mexico, and geochemical analysis of the thermal water. *Microorganisms, 12*(6), 1066. https://doi.org/10.3390/microorganisms12061066

Parkhurst, D. L., & Appelo, C. A. J. (2013). *Description of input and examples for PHREEQC Version 3—A computer program for speciation, batch-reaction, one-dimensional transport, and inverse geochemical calculations* (Techniques and Methods). U.S. Geological Survey. https://pubs.usgs.gov/tm/06/a43/pdf/tm6-A43.pdf

Smith, J. M. (2002). Cultural characteristics. In *Microbiological applications: Laboratory manual in* *general microbiology* (8th ed., pp. 157–160). McGraw Hill Higher Education.

Van Teeseling, M. C. F., de Pedro, M. A., & Cava, F. (2017). Determinants of bacterial morphology: From fundamentals to possibilities for antimicrobial targeting. *Frontiers in Microbiology, 8*, 278838. https://doi.org/10.3389/fmicb.2017.02788

Von Hegner, I. (2019). Extremophiles: A special or general case in the search for extra-terrestrial life? *Extremophiles, 24*, 167–175. https://doi.org/10.1007/s00792-019-01090-5

Young, K. D. (2007). Bacterial morphology: Why have different shapes? *Current Opinion in Microbiology, 10*, 596–600. https://doi.org/10.1016/j.mib.2007.10.003.

IN-SILICO EVALUATION OF BIOACTIVE CONSTITUENTS OF *TERMINALIA ARJUNA* AGAINST PROTEINS OF THE HAEMOGLOBIN DEGRADATION PATHWAY

Archana Sharma[1]|https://orcid.org/0009-0004-1420-233X
Sandhya Kumari[1]|https://orcid.org/0009-0003-9685-3218
Ashima Nehra[1]|https://orcid.org/0000-0003-4765-9374
Radha Jangra[1]|https://orcid.org/0009-0003-8051-0966
Natarajan Gopalan[2]| https://orcid.org/0000-0002-3330-4778
Sarvajeet Singh Gill[1*]| / https://orcid.org/0000-0002-8953-7714
Ritu Gill[1*]|https://orcid.org/0000-0002-6837-0281

[1]Centre for Biotechnology, Maharshi Dayanand University, Rohtak – Haryana, India
[2]Department of Epidemiology and Public Health, School of Life Sciences, Central University of Tamil Nadu, Thiruvarur, India

Correspondence: ssgill14@mdurohtak.ac.in ritu_gill@mdurohtak.ac.in

Article Info
DOI: https://doi.org/10.30546/abc.2025.0034
Pages: 60-76
Received: June 12, 2025 | Revised: July 06, 2025 | Accepted: September 21, 2025

Abstract

Malaria, a life-threatening disease caused by Plasmodium parasite, spread by the bite of Anopheles mosquito. The emergence and rapid spread of drug-resistant strains against frontline treatments prompted the need for novel antimalarial drugs. In the present study, phytochemicals from the Terminalia arjuna were evaluated using computational tools to assess their drug likeliness, pharmacokinetic properties and potential inhibitory activity against key enzymes of the heme degradation pathway- Falcipain-2, Falcipain-3 and Plasmepsin-2. On the basis of ADME and toxicity assessment, 24 compounds were shortlisted for molecular docking study, out of these several compounds exhibited strong binding affinities towards the target proteins, with binding energies surpassing that of the reference drug-chloroquine. Notably, Friedelin showed good interaction with Falcipain-2, displaying a binding energy of -10.2kcal/mol, indicating its potential as promising lead compound. These findings supports the therapeutic potential of T. arjuna metabolites and highlights its value for future experimental validation and antimalarial drug development.

Keywords: *Malaria, Plasmodium falciparum, Terminalia arjuna, Falcipain-2, Falcipain-3 and Plasmepsin-2*

INTRODUCTION

Malaria a life-threatening parasitic disease belonging to genus *Plasmodium*, affecting millions of people every year. In 2023, an estimated 263 million new cases were reported globally, that were higher when compared to 2022 (WHO, 2024). Despite the rise in malaria cases, deaths remained nearly stable trend when compared to the previous year. The WHO African region bears the highest burden and accounted for 94% of total cases and 95% of total deaths. Drug resistance to front line treatments, especially to artemisinin increased the difficulty of controlling the severity of the diseases (Basu et al., 2025; Abebe et al., 2025; Dakorah et al., 2025). Disruption imposed by COVID 19 pandemic, environmental changes, further hampered the malaria control programmes (WHO, 2024).

Haemoglobin degradation is an important catabolic process for the intraerythrocytic development of the *Plasmodium* parasite and take place in acidic food vacuole where parasite degrade all the host haemoglobin to acquire amino acids using multiple proteases(Flage et al., 2023; Garnie et al., 2025) Mishra et al., 2024). The degradation process is initiated by aspartic proteases- Plasmepsin 1, which cleave and disrupt the native structure of the molecule and expose it for further proteolysis (Nasamu et al., 2020; Tehlan et al., 2023). After this another aspartic protease plasmepsin 2 progress the haemoglobin breakdown (Nasamu et al., 2020; Mishra et al., 2019). Third key enzyme is cysteine proteases-Falcipain, which does not cleave native haemoglobin but efficiently degrade denatured globulin protein and act synergistically with aspartic protease to ensure complete cleavage of haemoglobin (Mishra et al., 2019; Patra et al., 2023; Pandey et al., 2025). The district specificities of proteases, their order and synergistic action make the pathway an excellent target for malaria chemotherapy. The digestive vacuole proteases are also sensitive to antimalarial drug like chloroquine (Wiser et al., 2024; Moura et al., 2009). Thus, designing of drugs that can target these proteases can serve as important antimalarials.

Herbal medicines are not only cost effective but also have fewer side effects compared to the chemically synthesized compounds. *Terminalia arjuna* is a member of family Combretaceae and is known as 'Arjun tree'. Bark, fruits and leaves of the tree have medicinal importance (Amalraj et al., 2016; Kumar et al., 2023). Diverse bioactive phytochemicals such as flavonoids, tannins, terpenoids have been isolated from the plant (Ramesh et al., 2023; Padmavathy et al., 2024). Thus, integrating the phytochemical components of *Terminalia* with *in silico* techniques enables the identification and optimization of potential inhibitors of *Plasmodium*'s proteases and novel therapies can be developed to combat malaria.

MATERIALS AND METHODS

The selection of bioactive compounds from *T. arjuna* was carried out through extensive literature search. Only those compounds with well-defined chemical structures available on PubChem were considered for the study. A total of 37 compounds were used for the further analysis and ADMET properties were predicted.

Drug likeness and ADMET screening of the compounds

Pharmacokinetic properties of the drug compounds such as absorption, distribution, metabolism and toxicity (ADMET), play crucial role during drug discovery and development process (Lai et al., 2022). Drug likeness of the compounds under study were evaluated via SwissADME webserver (http://www.swissadme.ch/). The physiological parameters of the compounds that were analysed include number of hydrogen bond acceptor and donor, molecular weight, topological surface area, skin permeation, blood brain barrier permeability, gastrointestinal absorption, solubility, topological surface area, molar refractivity, partition coefficient. Toxicity was evaluated using online tool ProTox 3.0 (https://tox.charite.de/protox3/). The SMILES strings of the compounds structure were used as input file for ADMET analysis.

Preparation of ligands and receptor

The 3D chemical structure of 37 compounds of *T. arjuna* were retrieved from the PubChem database in SDF (Structure data file) format. Later, the SDF structure of the compounds was converted into PDB format using Open babel 2.3.2. Autodock 4.2 software was used for the energy minimization and ligand file saved in PDBQT format. The crystal structure of proteins-Falcipain-2 (PDB ID: 3bpf, resolution 2.90 Aº), Falcipain-3 (PDB ID: 3bpm, resolution 2.50Aº) and Plasmepsin-2 (PDB ID: 4z22, resolution 2.62 Aº) were obtained from RCSB protein data bank (https://www.rcsb.org/) and used molecular docking. For molecular docking, chain A from each target protein were selected based on its completeness and biological relevance

(Nkungli et al., 2023; Rajguru et al., 2022). In case of Falcipain-2 (3bpf), the crystallographic structure contains four chains (A, B, C, D), among which chain A consisted of 241 amino acid residues. Both Falcipain-3 (3bpm) and Plasmepsin-2 (4z22) contained two chains (A, B). Chain A of Falcipain-3 comprised 243 amino acid residues, whereas chain A of 4z22 comprised 329 amino acid residues. The native ligands of proteins such as E64 (3bpf), Leupeptin (3bpm), DR718A (4z22) were eliminated. Further, the missing amino acids residues were added followed by removal of water molecules and heteroatoms. Hydrogen atoms were added to the protein structures. After modifications, the proteins were converted into PDBQT file by Autodock4.2. The 3D structures of chain A of each protein represented in figure 1.

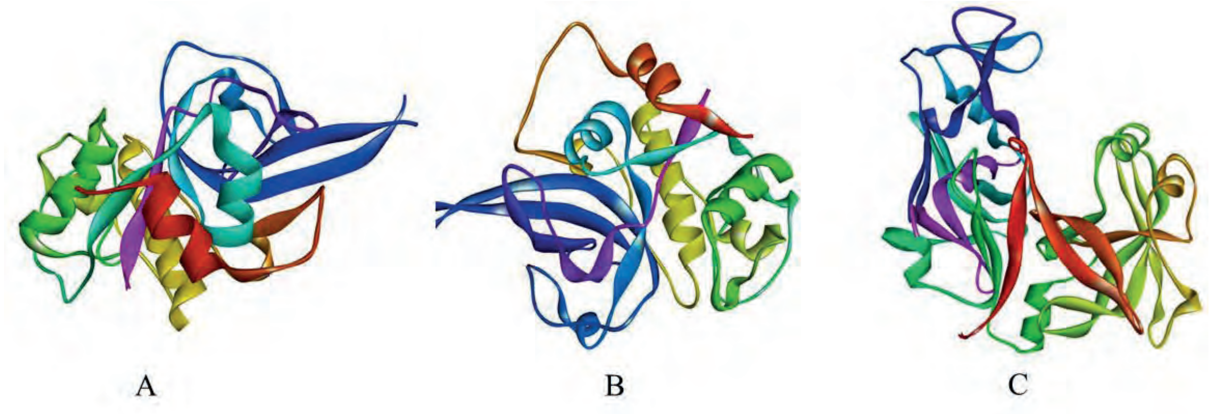

Figure 1. Crystal structure of chain A of *P. falciparum* proteins **(A)** Falcipain-2 (PDB-3bpf) **(B)** Falcipain-3 (PDB-3bpm) **C)** Plasmepsin-2 (PDB-4z22)

Molecular docking process

Autodock 4.2 software was utilized to explore the potential inhibitor among the selected compounds, targeting active site of FP-2, FP-3 and Plm-2. Preparation of ligand and protein were conducted in accordance with the standard protocol of AutoDock 4.2. During docking process, all the amino acids were kept rigid while ligands were treated flexible. The grid box parameters were defined to encompass the entire binding region of each target protein. For FP-2 and Plm-2, grid dimensions were set to 70×70×70 points and for FP-3 60×60×60 points with a grid spacing of 0.375 angstrom. The grid box were centred at co-ordinates corresponding to the active sites of the respective proteins to which the native ligand bind: FP-2 (-54.226, -10.064, and -14.691), FP-3 (6.015, 19.606, and 21.104) and Plm-2 (2.374, -0.648, and 27.950). Lamarckian Genetic Algorithm was selected as docking engine with 100 docking runs per ligand. The resulting conformations were ranked based on binding energy and lowest energy pose for each protein-ligand complex was selected for further analysis. Visualization of binding interactions were carried out using Discovery Studio Visualizer. The docking score (binding free energy) served as primary criteria for evaluating ligand affinity and selecting the best ligand pose.

RESULTS AND DISCUSSION

A total 37 metabolites from *T. arjuna* were selected based on literature search and structure availability. These compounds were assessed for their drug-likeliness and pharmacokinetic properties using ADMET screening, followed by molecular docking to evaluate their binding affinity towards key enzymes involved in haemoglobin degradation. Table 1 lists selected phytochemicals used in the study along with their molecular weight, CID and 2D structure, providing an overview of the chemical diversity included in the present article.

Table 1. Compounds of *T. arjuna* with CID, structures and molecular weight.

S. No	Compound Name	CID	Structure	Molecular weight
1	Arjunone	14034821	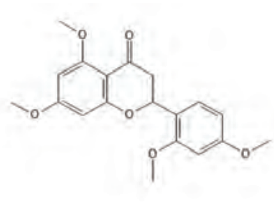	344.4 g/mol
2	Epicatechin	72276	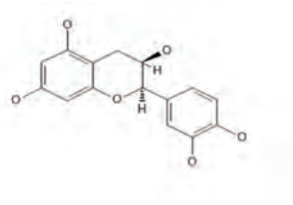	290.27 g/mol
3	Catechin	9064	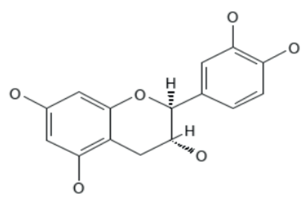	290.27 g/mol
4	Epigallocatechin	72277	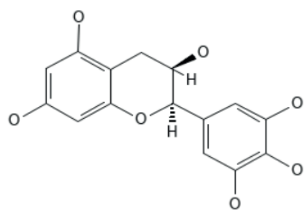	306.27 g/mol
5	Gallocatechin	65084	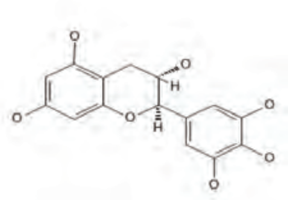	306.27 g/mol
6	Apigenin	5280443	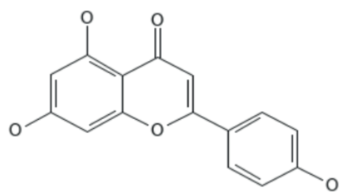	270.24 g/mol

S. No	Compound Name	CID	Structure	Molecular weight
7	Arjunetin	21152828	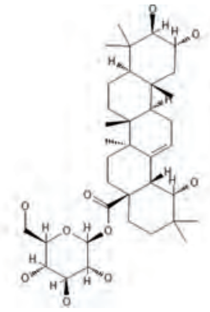	650.8 g/mol
8	Arjungenin	12444386	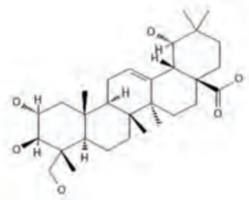	504.7 g/mol
9	Arjunic acid	15385516	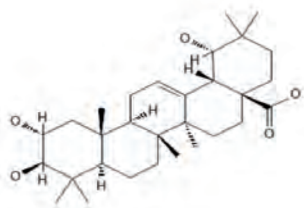	488.7 g/mol
10	Arjunolic acid	73641	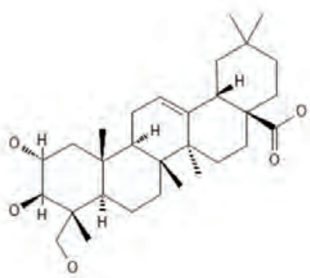	488.7 g/mol
11	Baicalein	5281605	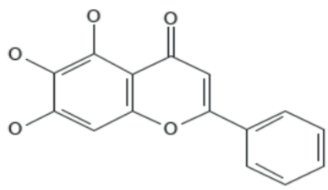	270.24 g/mol

S. No	Compound Name	CID	Structure	Molecular weight
12	Betulinic acid	64971	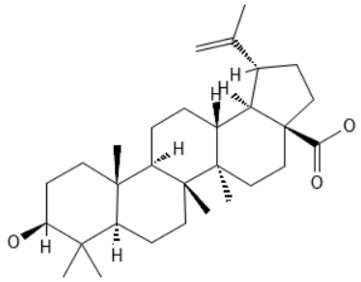	456.7 g/mol
13	Cerasidin	14034812	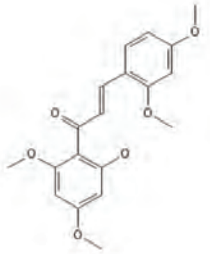	344.4 g/mol
14	Corilagin	73568	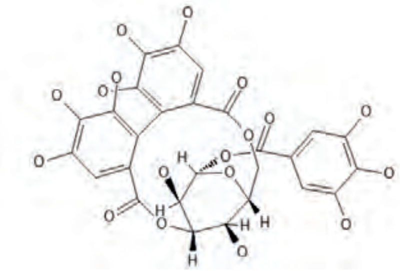	634.5 g/mol
15	Cyanidin	128861	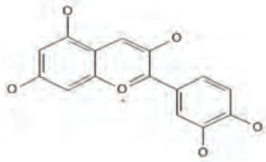	287.24 g/mol
16	Ellagic acid	5281855	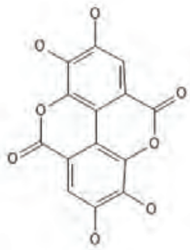	302.19 g/mol
17	Embelin	3218	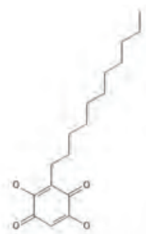	294.4 g/mol

S. No	Compound Name	CID	Structure	Molecular weight
18	Ethyl gallate	13250	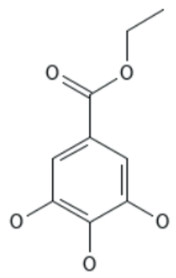	198.17 g/mol
19	Friedelin	91472	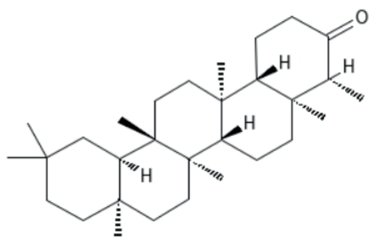	426.7 g/mol
20	Galactose	6036	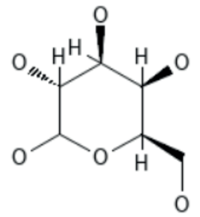	180.16 g/mol
21	Gallic acid	370	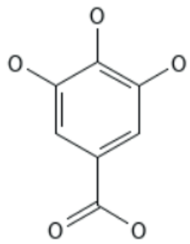	170.12 g/mol
22	Glycyrrhetic acid	10114	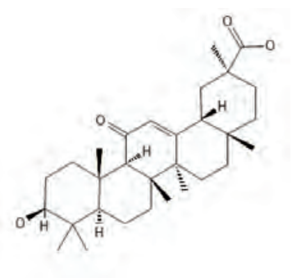	470.7 g/mol
23	Kaempferol	5280863	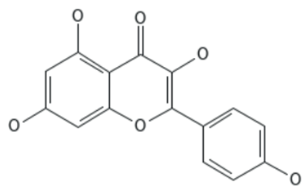	286.24 g/mol

S. No	Compound Name	CID	Structure	Molecular weight
24	Kajiichigoside F1	14019178	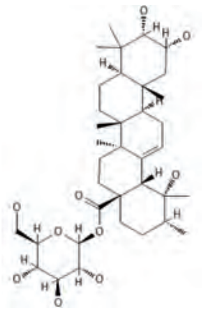	650.8 g/mol
25	Leucocyanidin	71629	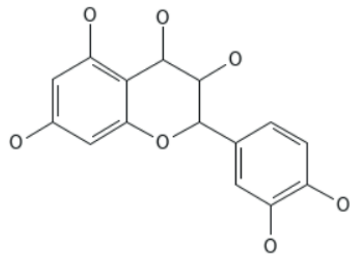	306.27 g/mol
26	Lupeol	259846	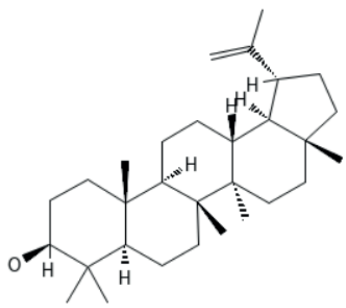	259846
27	Luteolin	5280445	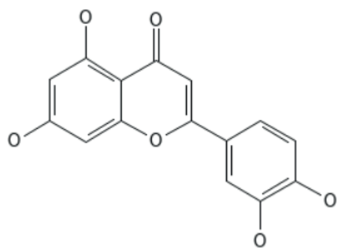	286.24 g/mol
28	Luteolin-7-Glucuro-nide	5280601	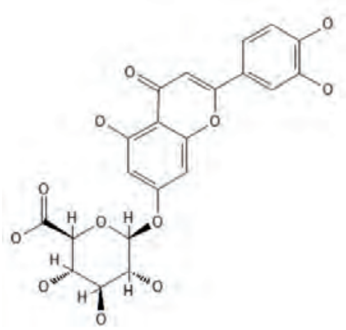	462.4 g/mol

S. No	Compound Name	CID	Structure	Molecular weight
29	Methyl 3,4,5-trihydroxybenzoate	7428	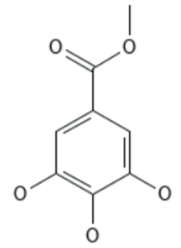	184.15 g/mol
30	Oleanolic acid	10494	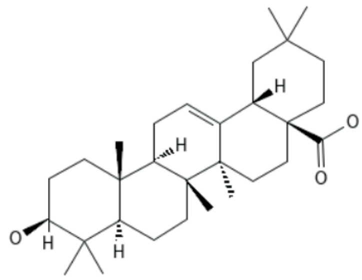	456.7 g/mol
31	Pelargonic acid	8158	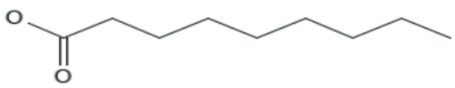	158.24 g/mol
32	Pelargonidin	440832	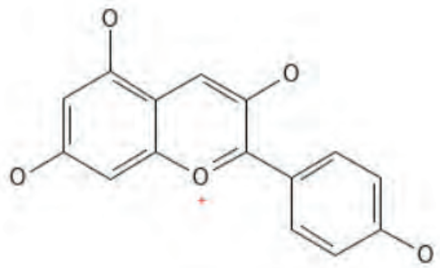	271.24 g/mol
33	Procyanidin	107876	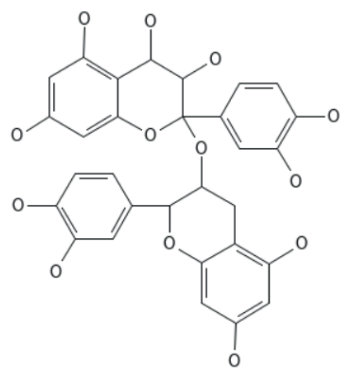	594.5 g/mol

S. No	Compound Name	CID	Structure	Molecular weight
34	Pyrocatechol	289	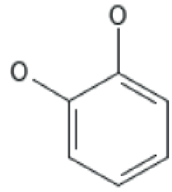	110.11 g/mol
35	Quercetin	5280343	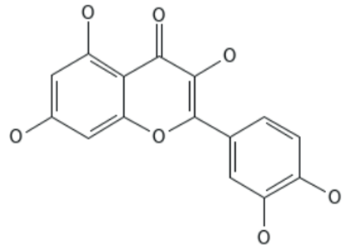	302.23 g/mol
36	Sericoside	76972524	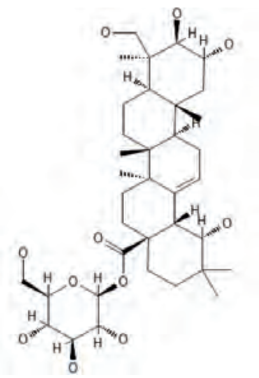	666.8 g/mol

ADMET analysis

ADMET analysis was carried by using Lipinski's rule of five to evaluate the drug likeness of the metabolites of *T. arjuna*, which include less than 10 and 5, hydrogen bond acceptors and hydrogen bond donors respectively, also less than 500g/mol molecular weight. In addition, molar refractivity of 40-130 and less than 10 rotatable bonds, which further supports the drug likeliness. Based on these physiochemical criteria, several metabolites were excluded from the study. Compounds failing to meet three or more of the parameters were filtered out. The remaining, which satisfied the majority of the parameters, were selected for further docking analysis. . The ADME and toxicity profiling of the metabolites are listed in table 2. After analysis 24 compounds were selected for docking analysis.

Table 2. ADMET properties of phytochemicals of T. arjuna

Compound	CID	Formula	NHBA (Number H-bond acceptors)	NHBD (Number H-bond donors)	MR (Molar Refractivity)	TPSA (Å²) (Topological Polar Surface Area)	Log S (ESOL) Solubility	Water Solubility Class(ESOL)	GIA(Gastro-intestinal absorption)	BBB-P(Blood Brain barrier Permeability)	P-gp substrate	Log Kp (skin permeation)	LV (Lipinski Violation)	Bioavailability Score	LD$_{50}$	Predicted toxicity class
Arjunone	14034821	C19H20O6	6	0	91.47	63.22 Å²	-3.84	Soluble	High	Yes	No	-6.33 cm/s	Yes; 0	0.55	2000mg/kg	4
Epicatechin	72276	C15H14O6	6	5	74.33	110.38 Å²	-2.22	Soluble	High	No	Yes	-7.82 cm/s	Yes; 0	0.55	10000mg/kg	6
Catechin	9064	C15H14O6	6	5	74.33	110.38 Å²	-2.22	Soluble	High	No	Yes	-7.82 cm/s	Yes; 0	0.55	10000mg/kg	6
Epigallocatechin	72277	C15H14O7	7	6	76.36	130.61 Å²	-2.08	Soluble	High	No	No	-8.17 cm/s	Yes; 1	0.55	10000mg/kg	6
Gallocatechin	65084	C15H14O7	7	6	76.36	130.61 Å²	-2.08	Soluble	High	No	No	-8.17 cm/s	Yes; 1	0.55	10000mg/kg	6
Apigenin	5280443	C15H10O5	5	3	73.99	90.90 Å²	-3.94	Soluble	High	No	No	-5.80 cm/s	Yes; 0	0.55	2500mg/kg	5
Arjunetin	21152828	C36H58O10	10	7	170.95	177.14 Å²	-5.73	Moderately soluble	Low	No	Yes	-7.88 cm/s	No; 2	0.17	3220mg/kg	5
Arjungenin	12444386	C30H48O6	6	5	140.14	118.22 Å²	-5.67	Moderately soluble	High	No	Yes	-6.18 cm/s	Yes; 1	0.56	2000mg/kg	4
Arjunic acid	15385516	C30H48O5	5	4	138.98	97.99 Å²	-6.06	Poorly soluble	High	No	Yes	-5.61 cm/s	Yes; 0	0.56	2000mg/kg	4
Arjunolic acid	73641	C30H48O5	5	4	138.98	97.99 Å²	-6.42	Poorly soluble	High	No	Yes	-5.13 cm/s	Yes; 0	0.56	2000mg/kg	4
Baicalein	5281605	C15H10O5	5	3	73.99	90.90 Å²	-4.03	Moderately soluble	High	No	No	-5.70 cm/s	Yes; 0	0.55	3919mg/kg	5
Betulinic acid	64971	C30H48O3	3	2	136.91	57.53 Å²	-7.71	Poorly soluble	Low	No	No	-3.26 cm/s	Yes; 1	0.85	2610mg/kg	5
Cerasidin	14034812	C19H20O6	6	1	94.24	74.22 Å²	-4.24	Moderately soluble	High	Yes	No	-5.72 cm/s	Yes; 0	0.55	2000mg/kg	4
Corilagin	73568	C27H22O18	18	11	141.85	310.66 Å²	-3.92	Soluble	Low	No	Yes	-10.12 cm/s	No; 3	0.17	2260mg/kg	5
Cyanidin	128861	C15H11O6+	6	5	76.17	114.29 Å²	-2.6	Soluble	High	No	Yes	-7.51 cm/s	Yes; 0	0.55	5000mg/kg	5
Ellagic acid	5281855	C14H6O8	8	4	75.31	141.34 Å²	-2.94	Soluble	High	No	No	-7.36 cm/s	Yes; 0	0.55	2991mg/kg	4
Embelin	3218	C17H26O4	4	2	84.31	74.60 Å²	-4.42	Moderately soluble	High	Yes	No	-4.25 cm/s	Yes; 0	0.85	2000mg/kg	4

Ethyl gallate	13250	C9H10O5	5	3	48.6	86.99 Å²	-2.01	Soluble	High	No	No	-6.59 cm/s	Yes; 0	0.55	5810mg/kg	6
Friedelin	91472	C30H50O	1	0	134.39	17.07 Å²	-8.66	Poorly soluble	Low	No	No	-1.94 cm/s	Yes; 1	0.55	500mg/kg	4
Galactose	6036	C6H12O6	6	5	35.74	110.38 Å²	1.15	Highly soluble	Low	No	Yes	-9.70 cm/s	Yes; 0	0.55	23000mg/kg	6
Gallic acid	370	C7H6O5	5	4	39.47	97.99 Å²	-1.64	Very soluble	High	No	No	-6.84 cm/s	Yes; 0	0.56	2000mg/kg	4
Glycyrrhetic acid	10114	C30H46O4	4	2	136.85	74.60 Å²	-6.15	Poorly soluble	High	No	Yes	-5.27 cm/s	Yes; 1	0.85	560mg/kg	4
Kaempferol	5280863	C15H10O6	6	4	76.01	111.13 Å²	-3.31	Soluble	High	No	No	-6.70 cm/s	Yes; 0	0.55	3919mg/kg	5
Kajiichigoside F1	14019178	C36H58O10	10	7	171.25	177.14 Å²	-5.6	Moderately soluble	Low	No	Yes	-8.03 cm/s	No; 2	0.17	3220mg/kg	5
Leucocyanidin	71629	C15H14O7	7	6	75.5	130.61 Å²	-1.6	Very soluble	High	No	No	-8.70 cm/s	Yes; 1	0.55	2500mg/kg	5
Lupeol	259846	C30H50O	1	1	135.14	20.23 Å²	-8.64	Poorly soluble	Low	No	No	-1.90 cm/s	Yes; 1	0.55	2000mg/kg	4
Luteolin	5280445	C15H10O6	6	4	76.01	111.13 Å²	-3.71	Soluble	High	No	No	-6.25 cm/s	Yes; 0	0.55	3919mg/kg	5
Luteolin-7-Glucuronide	5280601	C21H18O12	12	7	108.74	207.35 Å²	-3.41	Soluble	Low	No	Yes	-8.43 cm/s	No; 2	0.11	5000mg/kg	5
Methyl 3,4,5-trihydroxybenzoate	7428	C8H8O5	5	3	43.79	86.99 Å²	-1.73	Very soluble	High	No	No	-6.81 cm/s	Yes; 0	0.55	1190mg/kg	4
Oleanolic acid	10494	C30H48O3	3	2	136.65	57.53 Å²	-7.32	Poorly soluble	Low	No	No	-3.77 cm/s	Yes; 1	0.85	2000mg/kg	4
Pelargonic acid	8158	C9H18O2	2	1	47.15	37.30 Å²	-2.51	Soluble	High	Yes	No	-4.84 cm/s	Yes; 0	0.85	900mg/kg	4
Pelargonidin	440832	C15H11O5+	5	4	74.15	94.06 Å²	-3.49	Soluble	High	No	Yes	-6.33 cm/s	Yes; 0	0.55	3919mg/kg	5
Procyanidin	107876	C30H26O13	13	10	147.52	229.99 Å²	-4.9	Moderately soluble	Low	No	No	-8.54 cm/s	No; 3	0.17	2170mg/kg	5
Pyrocatechol	289	C6H6O2	2	2	30.49	40.46 Å²	-1.63	Very soluble	High	Yes	No	-6.35 cm/s	Yes; 0	0.55	100mg/kg	3
Quercetin	5280343	C15H10O7	7	5	78.03	131.36 Å²	-3.16	Soluble	High	No	No	-7.05 cm/s	Yes; 0	0.55	159mg/kg	3
Sericoside	76972524	C36H58O11	11	8	172.11	197.37 Å²	-5.34	Moderately soluble	Low	No	Yes	-8.46 cm/s	No; 3	0.17	3220mg/kg	5

Docking interactions

Docking results showed that binding energy ranged from -4.70kcal/mol to -10.25kcal/mol (Figure 2). The lowest binding energy pose of each ligand-protein complex was considered as best docking pose for all docked molecules. The stability of ligands has inverse relation with the binding energy. The ligand with the minimum binding energy will be most stable (Gogoi et al., 2021). The compound-Friedelin showed best binding affinity towards all the three proteins. In the case of protein FP-2, Friedelin showed binding energy of -10.2kcal/mol which is better when compared with standard artemisinin (-9.71kcal/mol) and chloroquine (-6.2kcal/mol). In case of FP-3, Friedelin displayed binding energy of -8.54kcal/mol which is better than chloroquine (-6.06kcal/mol).

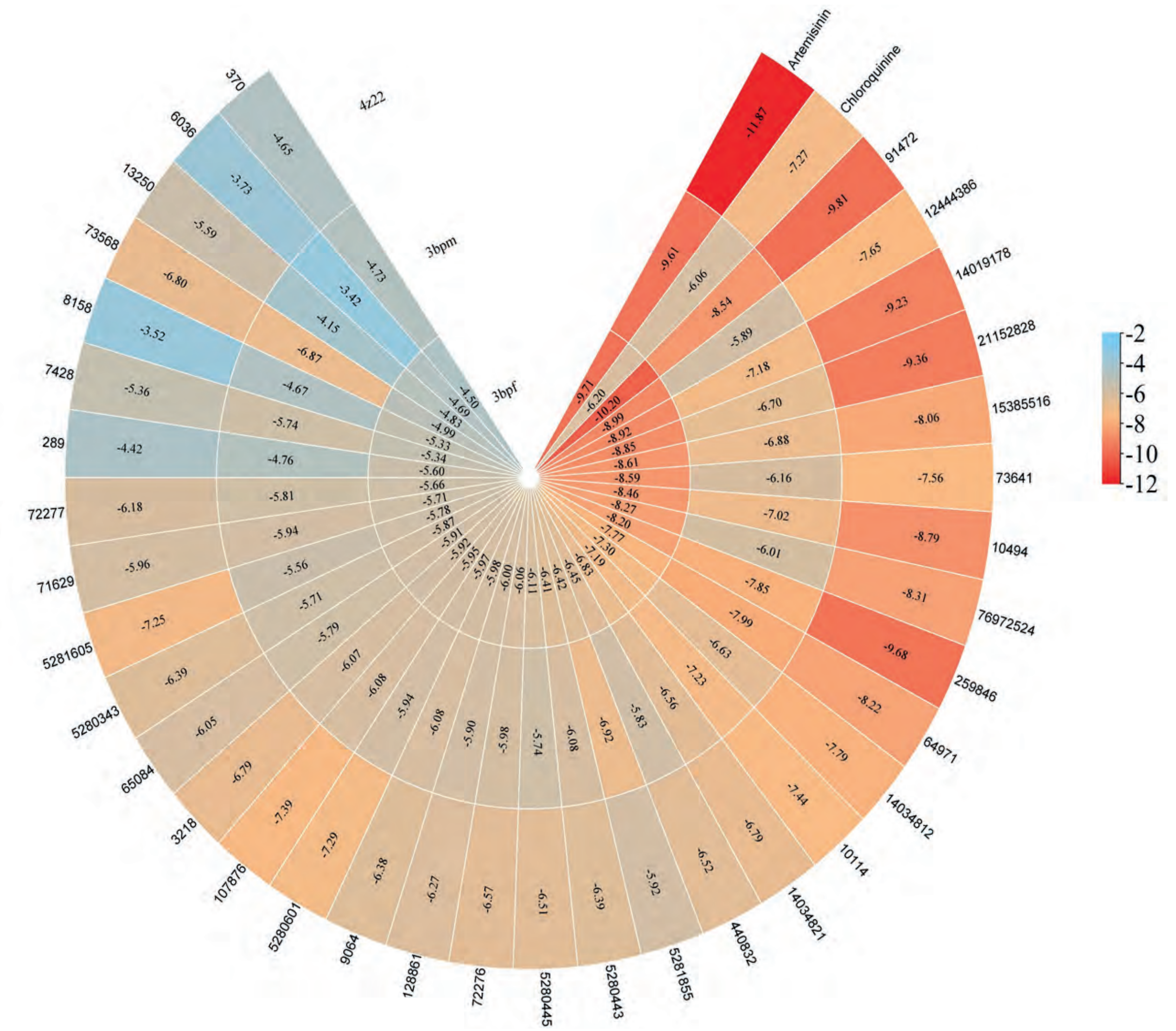

Figure 2. Heatmap showing lowest binding energy of the compounds of T. arjuna with the three proteins along with standard artemisinin and chloroquine.

Furthermore, binding energy of -9.81kcal/mol was reported for Plm-2, which is better when compared to that of chloroquine (-7.27 kcal/mol). Second best result was showed by Arjungenin for FP-2, Betulinic acid for FP-3 and Lupeol for Plm-2 with the binding energies of -8.99, -7.99 and -9.68 kcal/mol respectively. 3-D view of docking pose, interacting profile and 2D interactions of proteins-ligand complex of top two compounds are shown in figure 3, 4 and 5. Friedelin and lupeol was earlier isolated from *Senegalia ataxacantha* which displayed antiplasmodial activity against 3D7 and Dd2 strain (Baah et al., 2024).

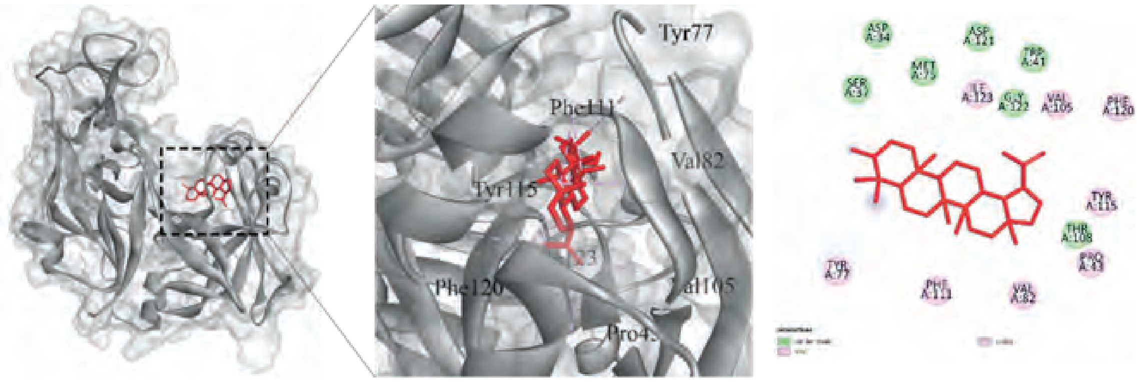

(3A)

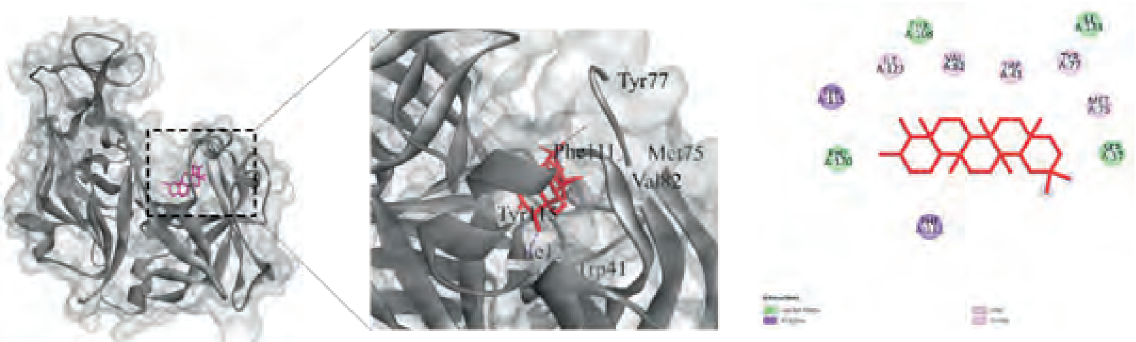

(3B)

Figure 3. 3D view of docking pose, interacting profile of top two compounds (lowest binding energy) with Plasmepsin-2 (4z22) (3A) Lupeol (3B) Friedelin.

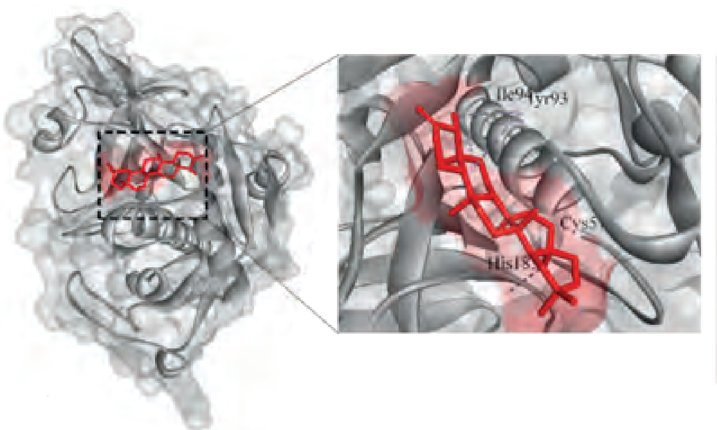

(4A)

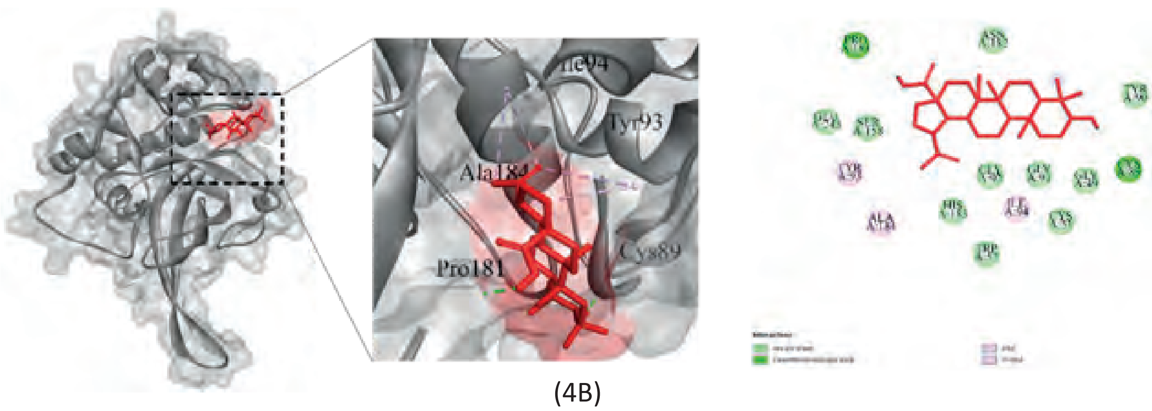

(4B)

Figure 4. 3D view of docking pose and interacting profile of top two compounds (lowest binding energy) with Falcipain-3 (PDB-3bpm) (4A) Friedelin (4B) Betulinic acid.

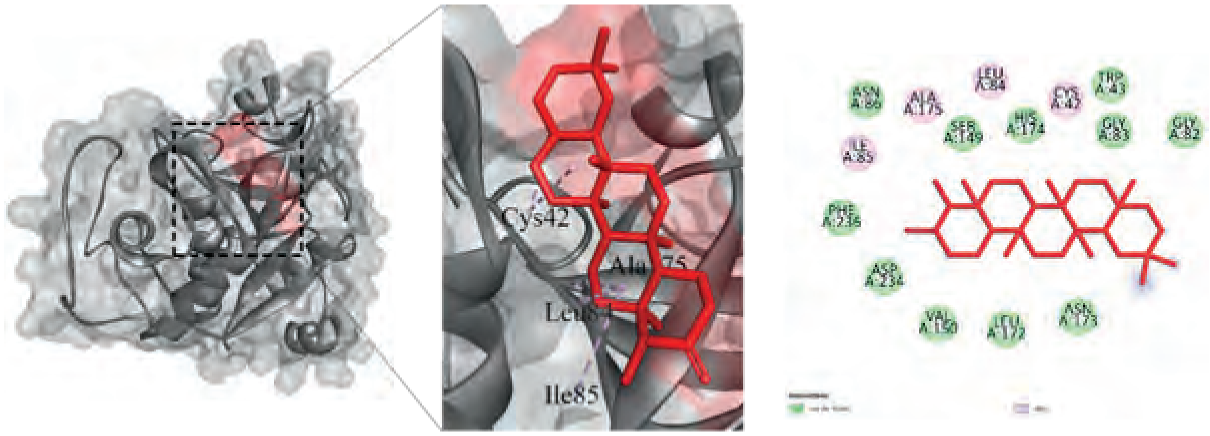

(5A)

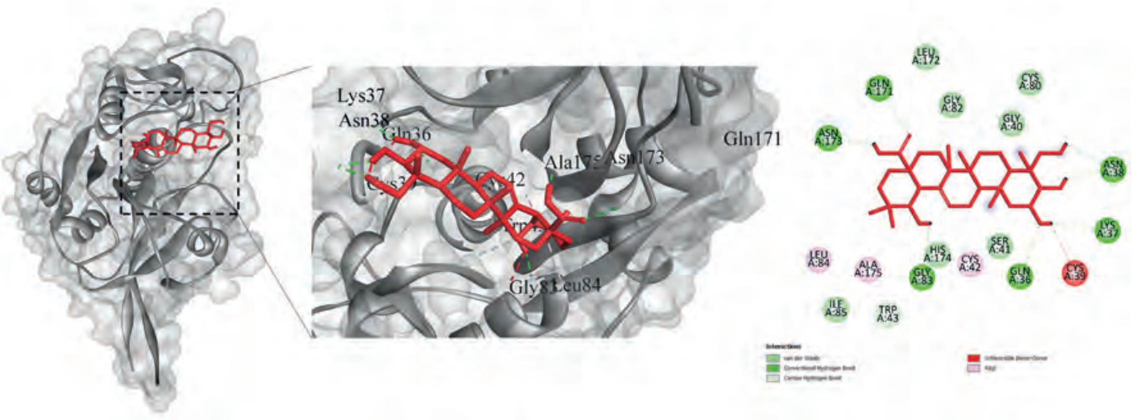

(5B)

Figure 5. 3D view of docking pose, interacting profile of top two compounds (lowest binding energy) with Falcipain-2 (3bpf) (5A) Friedelin (5B) Arjungenin.

CONCLUSION

The ongoing challenge of drug resistance in malaria highlights the need for novel treatment options. Plant based compounds have diverse therapeutic applications. The present study is highlighting the importance of bioactive compounds of *T. arjuna*. The result from this study displayed that compound Friedelin demonstrated the highest binding affinity towards all three proteins. In conclusion these results suggested that bioactive compounds may be helpful for the development of newer and more effective pharmaceutical components which may have lesser adverse effects.

Conflict of interest

The authors declare that they have no conflicts of interest in relation to this work.

Funding

No financial support was required for this work.

ACKNOWLEDGEMENTS

A. Sharma acknowledges the receipt of Junior Research Fellowship and Senior Research Fellowship (UGC Ref. No. 562/(CSIR-UGC NET JUNE 2019) to University Grants Commission (UGC), Govt. of India. Research work in R. Gill and S.S. Gill laboratory was partially supported by UGC, Department of Science and Technology (DST), Council of Scientific & Industrial Research (CSIR), Govt. of India. S.S. Gill, R. Gill also acknowledges partial support from DBT-BUILDER grant (No. BT/INF/22/SP43043/2021). We sincerely apologise to our contemporaries whose work could not be discussed in this article due to space restrictions.

References

Abebe, W., Ashagre, A., Misganaw, T., Dejazmach, Z., Kumie, G., Nigatie, M., ... & Reta, M. A. (2025). Prevalence of antimalaria drug resistance-conferring mutations associated with sulphadoxine-pyrimethamine-resistant *Plasmodium falciparum* in East Africa: A systematic review and meta-analysis. *Annals of Clinical Microbiology and Antimicrobials, 24*(1), 25. https://doi.org/10.1186/s12941-025-00795-7

Amalraj, A., & Gopi, S. (2017). Medicinal properties of *Terminalia arjuna* (Roxb.) Wight & Arn.: A review. *Journal of Traditional and Complementary Medicine, 7*(1), 65–78. https://doi.org/10.1016/j.jtcme.2016.02.003

Baah, K. A., Acheampong, A., Amponsah, I. K., Adjei, S., Jibira, Y., Nketia, R. I., ... & Kontoh, E. Q. (2024). Hydroethanol extract and triterpenoids of *Senegalia ataxacantha* show antiplasmodial activity and the compounds are predicted to inhibit parasite lactate dehydrogenase (pfLDH) as indicated by molecular docking studies. *Scientific African, 26*, e02455. https://doi.org/10.1016/j.sciaf.2024.e02455

Basu, L., Bhowmik, B., Pal, A., Roy, P., Dey, B., Mondal, R., ... & Halder, L. (2025). Drug resistance and new strategies of prevention against malaria: An ongoing battle. *Journal of Vector Borne Diseases, 62*(1), 9–15. https://doi.org/10.4103/JVBD.JVBD_72_24

Dakorah, M. P., Aninagyei, E., Attoh, J., Adzakpah, G., Tukwarlba, I., & Acheampong, D. O. (2025). Profiling antimalarial drug-resistant haplotypes in *Pfcrt, Pfmdr1, Pfdhps* and *Pfdhfr* genes in *Plasmodium falciparum* causing malaria in the Central Region of Ghana: A multicentre cross-sectional study. *Therapeutic Advances in Infectious Disease, 12*, 20499361251319665. https://doi.org/10.1177/20499361251319665

Flage, B., Dent, M. R., Tejero, J., Amoah, L. E., & Ofori-Acquah, S. F. (2023). Heme promotes sexual conversion of *Plasmodium falciparum* in human erythrocytes. *Frontiers in Malaria, 1*, 1161750. https://doi.org/10.3389/fmala.2023.1161750

Garnie, L. F., Egan, T. J., & Wicht, K. J. (2025). Heme detoxification in the malaria parasite *Plasmodium falciparum*: A time-dependent basal-level analysis. *bioRxiv*. https://doi.org/10.1101/2025.03.06.641703

Gogoi, B., Chowdhury, P., Goswami, N., Gogoi, N., Naiya, T., Chetia, P., ... & Handique, P. J. (2021). Identification of potential plant-based inhibitor against viral proteases of SARS-CoV-2 through molecular docking, MM-PBSA binding energy calculations and molecular dynamics simulation. *Molecular Diversity, 25*(3), 1963–1977. https://doi.org/10.1007/s11030-021-10211-9

Kumar, V., Sharma, N., Saini, R., Mall, S., Zengin, G., Sourirajan, A., ... & El-Shazly, M. (2023). Therapeutic potential and industrial applications of *Terminalia arjuna* bark. *Journal of Ethnopharmacology, 310*, 116352. https://doi.org/10.1016/j.jep.2023.116352

Lai, Y., Chu, X., Di, L., Gao, W., Guo, Y., Liu, X., ... & Ding, X. (2022). Recent advances in the translation of drug metabolism and pharmacokinetics science for drug discovery and development. *Acta Pharmaceutica Sinica B, 12*(6), 2751–2777. https://doi.org/10.1016/j.apsb.2022.03.009

Mishra, M., Singh, V., & Singh, S. (2019). Structural insights into key *Plasmodium* proteases as therapeutic drug targets. *Frontiers in Microbiology, 10*, 394. https://doi.org/10.3389/fmicb.2019.00394

Mishra, V., Deshmukh, A., Rathore, I., Chakraborty, S., Patankar, S., Gustchina, A., ... & Bhaumik, P. (2024). Inhibition of *Plasmodium falciparum* plasmepsins by drugs targeting HIV-1 protease: A way forward for antimalarial drug discovery. *Current Research in Structural Biology, 7*, 100128. https://doi.org/10.1016/j.crstbi.2024.100128

Moura, P. A., Dame, J. B., & Fidock, D. A. (2009). Role of *Plasmodium falciparum* digestive vacuole plasmepsins in the specificity and antimalarial mode of action of cysteine and aspartic protease inhibitors. *Antimicrobial Agents and Chemotherapy, 53*(12), 4968–4978. https://doi.org/10.1128/aac.00882-09

Nasamu, A. S., Polino, A. J., Istvan, E. S., & Goldberg, D. E. (2020). Malaria parasite plasmepsins: More than just plain old degradative pepsins. *Journal of Biological Chemistry, 295*(25), 8425–8441. https://doi.org/10.1074/jbc.REV120.009309

Nkungli, N. K., Fouegue, A. D. T., Tasheh, S. N., Bine, F. K., Hassan, A. U., & Ghogomu, J. N. (2024). In silico investigation of falcipain-2 inhibition by hybrid benzimidazole-thiosemicarbazone antiplasmodial agents: A molecular docking, molecular dynamics simulation, and kinetics study. *Molecular Diversity, 28*(2), 475–496. https://doi.org/10.1007/s11030-022-10594-3

Padmavathy, B., Ebinezer, B. S., Amalraj, S., Kadaikunnan, S., Arumugam, M., Karthick, V., ... & Thiruvengadam, R. (2024). Cytotoxicity effects of *Terminalia arjuna* bark-derived nano-ZnO on MCF-7 cells and enhanced anti-breast cancer potency of its phytochemicals upon Zn-capping. *Materials Chemistry and Physics, 328*, 130030. https://doi.org/10.1016/j.matchemphys.2024.130030

Pandey, V., Kennedy, J. F., & Raghav, N. (2025). Falcipain-2: A review on structurally diverse non-peptide inhibitors. *International Journal of Biological Macromolecules*, Article 142817. https://doi.org/10.1016/j.ijbiomac.2025.142817

Patra, J., Rana, D., Arora, S., Pal, M., & Mahindroo, N. (2023). Falcipains: Biochemistry, target validation and structure–activity relationship studies of inhibitors as antimalarials. *European Journal of Medicinal Chemistry, 252*, 115299. https://doi.org/10.1016/j.ejmech.2023.115299

Rajguru, T., Bora, D., & Modi, M. K. (2022). Identification of promising inhibitors for *Plasmodium* haemoglobinase Falcipain-2, using virtual screening, molecular docking, and MD simulation. *Journal of Molecular Structure, 1248*, 131427. https://doi.org/10.1016/j.molstruc.2021.131427

Ramesh, P., & Palaniappan, A. (2023). *Terminalia arjuna*, a cardioprotective herbal medicine – Relevancy in the modern era of pharmaceuticals and green nanomedicine: A review. *Pharmaceuticals, 16*(1), 126. https://doi.org/10.3390/ph16010126

Tehlan, A., Saha, A., & Dhar, S. K. (2023). Targeting proteases and proteolytic processing of unusual N-terminal extensions of *Plasmodium* proteins: Parasite peculiarity. *Frontiers in Drug Discovery, 3*, 1223140. https://doi.org/10.3389/fddsv.2023.1223140

World Health Organization. (2024). *World malaria report 2024*. https://www.who.int/teams/global-malaria-programme/reports/world-malaria-report-2024

Table and Figure Legends

Table 1. Compounds of *T. arjuna* with CID, structures and molecular weight.

Table 2. ADMET properties of phytochemicals of *T. arjuna*

Figure 1. Crystal structure of chain A of *P. falciparum* proteins (A) Falcipain-2 (PDB-3bpf) (B) Falcipain-3 (PDB-3bpm) C) Plasmepsin-2 (PDB-4z22)

Figure 2. Heatmap showing lowest binding energy of the compounds of *T. arjuna* with the three proteins along with standard artemisinin and chloroquine

Figure 3 3D view of docking pose, interacting profile of top two compounds (lowest binding energy) with Plasmepsin-2 (4z22) (3A) Lupeol (3B) Friedelin.

Figure 4. 3D view of docking pose and interacting profile of top two compounds (lowest binding energy) with Falcipain-3 (PDB-3bpm) (4A) Friedelin (4B) Betulinic acid.

Figure 5. 3D view of docking pose, interacting profile of top two compounds (lowest binding energy) with Falcipain-2 (3bpf) (5A) Friedelin (5B) Arjungenin.

PASTINACA DENTATA (APIACEAE): A NEW SPECIES RECORD FOR THE FLORA OF AZERBAIJAN

Husniya Mammadova[1]*|https://orcid.org/0000-0002-8936-9562
Tatiana Ostroumova[2]|https://orcid.org/0000-0002-7734-5133
Ivan Tatanov[3]|https://orcid.org/0000-0002-7914-8248
Zemfira Aliyeva[4]|https://orcid.org/0009-0004-3243-9111

[1] Sumgait State University, Sumgait, Azerbaijan
[2] Lomonosov Moscow State University, Moscow, Russia
[3] Komarov Botanical Institute of RAS, St. Petersburg, Russia
[4] Institute of Botany, Ministry of Science and Education of the Republic of Azerbaijan, Baku, Azerbaijan

Correspondence: husniya.mammadova@mail.ru

Article Info
DOI: https://doi.org/10.30546/abc.2025.0038
Pages: 77-84
Received: May 12, 2025 | Revise: September 06, 2025 | Accepted: October 01, 2025

Abstract

The article discusses the discovery of a new and rare plant subspecies in the flora of Azerbaijan. The new subspecies, Pastinaca armena subsp. dentata (Freyn & Sint.) Chamberlain, belongs to the genus Pastinaca L. and was first discovered in 1892 in the Kastamonu province (Paphlagonia) of Turkey. The genus Pastinaca L., to which Pastinaca dentata belongs, is one of the polymorphic genera of the Apiaceae Lindl. family. The newly identified subspecies was found in the middle mountain belt of the Lesser Caucasus, specifically on the northern slope of the mountain pass between the villages of Kichik Garamurad and Emir in the Gadabay region. The plant was collected from a protected area designated for mowing purposes. The new subspecies is distributed at an altitude of 1400–1600 meters above sea level. Pastinaca dentata Freyn & Sint. is recorded for the first time as a new subspecies for the flora of the Caucasus. The entire distribution area of this subspecies features mountainous terrain, and in these regions, it forms associations with four other species of the same genus within a narrow habitat in the phytocoenosis. The new subspecies differs from other species in the genus by its morphological characteristics.

Keywords: *Pastinaca dentata, Apiaceae, Caucasus flora, plant taxonomy, floristic novelty, morphological differentiation, endemic species, biogeography, Gadabay district, high-altitude vegetation*

INTRODUCTION

The species of the genus Pastinaca L. are widely distributed in Turkey, Russia, Azerbaijan, Germany, the United Kingdom, Greece, Hungary, Kazakhstan, the North Caucasus, and other regions (POWO, 2024; Ibrahimova et al., 2019; Flora of Azerbaijan, 1955).

Field studies conducted in the western region of Azerbaijan from 2017 to 2024 are currently ongoing, and an intriguing finding for the national flora has been included in this article. The discovery of new species during these studies holds particular significance for the conservation of natural biodiversity. The plant diversity in this region, located in the Lesser Caucasus, is richer compared to other regions (Zulfugarova et al., 2015). Overall, we report the discovery of the subspecies Pastinaca dentata Freyn & Sint., which is not mentioned in the works on Caucasus flora by Grossheim (1936) or in the Flora of Azerbaijan (1955). This species, found incidentally, will expand the list of Caucasus plants. Therefore, the primary focus should be on conserving rare plant species.

Prior to our presentation, four species of the genus Pastinaca L. were reported to be distributed in the flora of Azerbaijan (P. sativa, P. armena, P. pimpinellifolia, P. glandulosa; Asgarov, 2006). With the new information presented in this article, the number of species belonging to the genus Pastinaca L. in the flora of Azerbaijan increases to five.

MATERIALS AND METODS

In 2023, during a scientific research study dedicated to investigating the species within the Apiaceae Lindl. family in Azerbaijan, we conducted fieldwork in the western region of the Lesser Caucasus (Gadabay district) to search for plants. During this research, we encountered a plant that particularly caught our attention due to its distinct morphological features. Initially, the plant stood out due to its flower color (golden yellow), the variety of leaf shapes on the stem, the presence of prominent ridges on the stem, a denser covering of hairs on the lower part of the stem, and the unique serrated form of the leaf margins.

In the upper part of the branched stem, the plant has lanceolate leaves, while in the lower part of the stem near the ground, it possesses basal leaves of various shapes with deeply serrated margins. The leaves near the base of the stem differ in size and shape from those located in the upper part of the stem. Interestingly, in the flora of Azerbaijan, the species P. sativa, P. armena, P. pimpinellifolia, and P. glandulosa are found within the same phytocoenosis. This suggests that, due to the area being a protected zone, these species have a rich reserve. Our observations have determined that the cross-pollination by insects, which is characteristic of the species within the genus Pastinaca L., is also typical for P. dentata.

Experimental studies have confirmed that new species can arise from hybrids formed through cross-pollination in flowering plants (Juan, 2019). Therefore, it can be concluded that Pastinaca dentata is an independent species that originated from a hybrid resulting from the cross-pollination of parent subspecies. As an ecological unit, species interact with other species living in the same environment.

The plant material of Pastinaca armena subsp. dentata (Freyn & Sint.) Chamberlain was first collected on July 16, 1892, in the Kastamonu province of Turkey (Paphlagonia) by Freyn and Sint, and was identified by J. Freyn (Oesterreichische Botanische Zeitschrift, 1894). Pastinaca dentata Freyn & Sint. was described as an independent species in 1894 in the Oesterr. Bot. Z. 44: 103. D.F. Chamberlain (1972) considered this taxon as a subspecies of P. armena Fisch. However, in 2014, Pimenov and Sutorý noted: "We believe that P. dentata should be considered an independent species, not only due to the general size of plant parts and fruits, but also because of its ribbed stems and more deeply serrated leaf margins." It also has a distinct distribution area in Turkey: Kastamonu and Giresun. Pimenov and Sutorý (2014) regard P. dentata as an independent species.

As stated in the article, the subspecies of Pastinaca dentata has only been compared with the species P. armena Fisch. This comparison is presented below in Figures 1 and 2.

The plant material we collected was identified as Pastinaca dentata (specimen number 4641) based on comparison with herbarium material available in online databases. The identification was carried out using various relevant floras (Pimenov et al., 2014; BHL; GBIF; WFO).

The new distribution area of Pastinaca dentata is located on the northern slope of the mountain pass between the villages of Kichik Garamurad and Emir in the Gadabay district, in the western part of the Lesser Caucasus. This area, protected for haymaking purposes, is situated at an altitude of 1400–1600 meters above sea level. Due to its status as a protected area, the natural vegetation cover has been well preserved. The entire area features a mountainous terrain and is characterized by a climate with cold, dry winters and moderately warm, dry summers. Summer temperatures range between +23–26°C, while winter temperatures vary from –5 to –8°C. In the area where Pastinaca dentata is found, other species of the genus, particularly P. sativa and P. armena, are

Figure 1. Pastinaca dentata

Figure 2. Pastinaca armena

more abundant. Pastinaca dentata has spread in a narrow range within the phytocoenosis, forming associations with other species. The presence of a species or subspecies in any area is consistently linked to time and space.

The plant material was collected on June 30, 2023, during the flowering phase, and on July 10, 2023, during the fruiting phase, from the above-mentioned region. The identification of the plant was carried out with the consultation of specialists from the Laboratory of Higher Plant Systematics and Geography at the Institute of Botany, the Komarov Botanical Institute of the Russian Academy of Sciences, and the Department of Systematics at Lomonosov Moscow State University.

Pastinaca dentata is a plant that reaches a height of 80–90 cm and is densely covered with hairs. The stem is straight, branched, and has a ribbed and rigid structure. The stem has 9 ribs that are visible to the naked eye, with inter-rib spaces that are concave. Pastinaca dentata has a taproot system with a root length of 15–20 cm (Figure 3). Most species within the genus Pastinaca have a fibrous neck at the base of the stem, close to the root, which is covered with fibrous threads. This feature is characteristic of each species, although in very rare cases, the fibrous neck is absent. Pastinaca dentata, being one of these rare species, lacks a fibrous neck.

The petiole of the basal compound leaf is 20–22 cm long and bears 14 pairs of opposite leaflets and 1 terminal leaflet (oval-round in shape), totaling 29 leaflets. The length of these leaflets is 2.3–2.5 cm, and the width is 2.5 cm. The margins are irregularly serrated. The plant has simple pinnate compound leaves. At the point where the leaf petiole joins the stem, the leaf sheath externally encircles the petiole in a cup-shaped manner, causing the leaf to stand parallel to the stem. Above the basal leaves, the second group of lanceolate leaves starting from the 3rd node is located; these are simple pinnate compound leaves with serrated margins,

Figure 3. Root system of P. dentata

Figure 4. Seed development stage of P. dentata

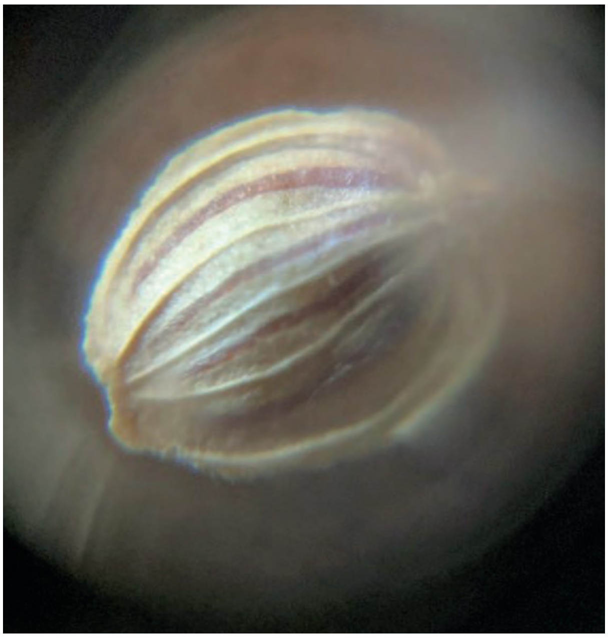

Figure 5. Dorsal view of P. dentata mericarps.

Figure 6. Dorsal view of P. armena mericarps.

measuring 8–9 cm in length. The leaflets on the petiole are 3 cm long. In the upper part of the stem, near the umbel, the third group of elongated sessile leaves is located. These leaves are 2–3 cm long.

The number of flower rays in the umbel is 8–9, and they are arranged unevenly. Of these, 5 flower rays are 5 cm long, while 4 flower rays are relatively shorter, measuring 3.5 cm. The petals are dark yellow, and the rays are uneven and covered with hairs (Figure 4).

The immature fruit of Pastinaca dentata is borne on a single stalk. The fruits are 6–7 mm long and 5 mm wide. Under a light microscope (UM-301) at 7×8 magnification, it is evident that the fruit stalk is covered with spiny projections and hairs, with two parallel channels running along the fruit stalk. As the fruit approaches maturity, bifurcation occurs, and when fully mature, the fruits split into two seeds. Under a light microscope, the mature oval-shaped fruits reveal four clearly visible dark-colored oil ducts, which adhere to the fruit wall. These ducts, in terms of shape, include two spherical and two relatively straight ones. The 5 transparent, rigid ribs are thin, long, and thread-like (Figure 5). Of these ribs, 4 are lateral ribs, and one is the central rib, differing in shape. The central rib has 2 ribs on the right and 2 ribs on the left. Thus, when observing the mericarp under microscope, 5 ribs are visible (Figure 5). For comparison, the microscopic view of the collected fruits of Pastinaca armena is presented in Figure 6.

A comparison between Pastinaca dentata and Pastinaca armena collected from the same area is presented in Table 1.

Table 1. Comparison table of *Pastinaca dentata (*Freyn et Sint*)* and *Pastinaca Armena (*Fisch. & CA Mey*)*

Pastinaca dentata (Frain və Sint.)	**Pastinaca armena Fisch. Mey.**
- Stem height (80 - 90 cm), strong, tough, ribbed; - Number of ribs on the stem - 9; - The length of basal leaves is 20 cm, pinnate, oval-round, with serrated edges; - The length of the lanceolate common leaf petiole is 8 - 9 cm, with serrated edges, and the upper lanceolate edges are entire; - Root length - 15 - 20 cm, and there is no fibrous neck; - Internode distance is 5 - 6 cm; - The fruit is 6 - 7 mm long, 5 - 6 mm wide; - The number of grooves on the fruit- 5 + 4 (9)	- The stem is weak and thin (30 - 50 cm); - Number of ribs on the stem 5 – 7 - Basal leaves are 10 - 15 cm, pinnately divided, with segments that are broadly ovate, sharp or bluntly serrated; - The length of the root system is 7 - 10 cm and has a fibrous neck; - The fruit is 5 - 6 mm long, 4-5 mm wide; - The root is 10 cm long, with a fibrous neck; - The number of grooves on the fruit- 3 + 4 (7)

We consider Pastinaca dentata subspecies as a distinct species due to differences in leaf and fruit size and shape, the number of secretion channels in the fruits, root system structure, and other morphological characteristics compared to the species it has been previously associated with. Originally discovered 132 years ago in the Kastamonu province, this plant has now been identified for the first time in Azerbaijan (Gadabay district) and is a new addition to the Caucasus flora. There is a distinct distribution area for Pastinaca dentata in Azerbaijan. It was recorded in the Gadabay region (40°33'56'' N, 45°48'58'' E), near the villages

Figure 7. Map showing the region where Pastinaca dentata was collected (in red).

of Kichik Garamurad (40°33'16'' N latitude) and Emir (40°34'59'' N latitude), in the middle mountain belt at an altitude of 1400–1600 m above sea level on June 30, 2023. A herbarium specimen was deposited in the herbarium fund of the Institute of Botany, Baku (Figure 1).

The subspecies we found enriched the composition of wild plants in Azerbaijan. The biological resource of the subspecies was estimated based on the method of Schreter (1972) and Schreter et al. (1986). The distribution area of the new subspecies is 16 hectares. The resource for this area has been calculated (Table 2).

Table 2. Biological resource estimation of *P. dentata* in Azerbaijan

Species	Biological stock (kg)	Exploitable stock (kg)	Annual potential stock (kg)
Pastinaca dentata	514.75 ± 90.06	102.95 ± 17.09	10.25 ± 1.78

The biological resource of the subspecies Pastinaca dentata has been recorded in the territory of Gadabay district. The area of distribution of the species is marked in red on the map (Figure 7).

RESULTS AND DISCUSSION

1.Results

As a result of botanical expeditions conducted in the Gadabay district of western Azerbaijan in June 2023, a new locality of Pastinaca dentata was discovered. Previously, this subspecies was known only from northern Turkey. The specimens were collected at elevations of 1750–1800 m a.s.l., on mesophytic grassy slopes interspersed with sparse shrubs (Berberis iberica, Spiraea hypericifolia).

Morphological analysis confirmed that the collected specimens belong to Pastinaca dentata and are clearly distinguishable from the closely related species P. armena, which occurs in similar habitats. The most significant diagnostic characters include the greater plant height (80–90 cm vs. 30–50 cm in P. armena), a glabrous stem with 9 longitudinal ribs, and a cylindrical root lacking fibrous remnants in contrast to the fibrous base observed in P. armena. The basal leaves are 2–3-pinnately divided with serrate leaflets reaching up to 9 cm in length. The inflorescences are umbels with 10–18 rays bearing yellow flowers. The fruits of P. dentata possess 5 prominent ribs and 4 oil ducts, whereas P. armena has only 3 ribs and 4 oil ducts. Seeds are flattened and light brown.

These morphological differences are summarized in Table 1, where a comparative analysis between P. dentata and P. armena is provided. In addition to morphological distinctions, a clear geographic separation was identified. The Azerbaijani population of P. dentata is located approximately 400 km east of its known range in Turkey, suggesting a relic or disjunct distribution pattern. All specimens were herbarium mounted and deposited at the Herbarium of the Institute of Botany (BAK). Photographs of plants in situ, along with microscopic images of the fruits, are presented in Figures 1–5.

Thus, the results indicate a significant eastward extension of the known range of P. dentata and support its taxonomic distinctiveness based on consistent morphological characters.

2.Discussion

Our morphological comparison between P. dentata and the closely related P. armena, which co-occurs in the same phytocoenosis, revealed distinct and consistent differences. P. dentata exhibits taller plant height (80–90 cm compared to 30–50 cm in P. armena), a greater number of visible stem ribs (9), the absence of a fibrous neck at the root base, and more deeply serrated and differently shaped leaf margins. Furthermore, the fruits of P. dentata have 5 ribs and 4 oil ducts. In P. armena, there are 3 ribs and 4 oil ducts. Differences were also observed in the oil ducts within the mericarps and the general structure of both basal and cauline leaves.

These findings strongly support the view expressed by Pimenov and Sutorý (2014), who argued that P. dentata should be treated as a distinct species rather than a subspecies of P. armena, as previously proposed by Chamberlain (1972). Our observations regarding fruit morphology, root structure, and stem characteristics reinforce their conclusions and justify species-level recognition.

Given the observed morphological divergence and the geographically isolated population found in the Lesser Caucasus, it is plausible that P. dentata has evolved as a separate species through processes such as ecological and geographical isolation. Considering the entomophilous pollination mode characteristic of the genus Pastinaca, which can promote hybridization and subsequent speciation, the hypothesis proposed by Juan Isaac regarding hybrid origin and independent species development is relevant in this context (Juan, 2019).

In conclusion, the data obtained in our study—including morphological, anatomical, and ecological features—support the recognition of Pastinaca dentata as a valid, independent species. Its discovery in Azerbaijan, for the first time, enriches the national and regional floristic records and highlights the importance of continued botanical surveys in the Caucasus region.

CONCLUSION

A new subspecies, Pastinaca dentata, has been recorded for the first time in the flora of Azerbaijan. This taxon is also new to the flora of the Caucasus region. The morphological characteristics of Pastinaca dentata and the observed features in the microscopic structure of its seeds support its recognition as a separate species and suggest its classification at the species level.

References

Asgarov, A. M. (2006). Higher plants of Azerbaijan: Synopsis of the flora of Azerbaijan. Baku.

Biodiversity Heritage Library. (n.d.). Retrieved from https://www.biodiversitylibrary.org/page/8735767

Biodiversity Heritage Library Item. (n.d.). Retrieved from https://www.biodiversitylibrary.org/item/91326

Flora of Azerbaijan. (1955). Institute of Botany.

GBIF Occurrence 1. (n.d.). Retrieved from https://www.gbif.org/occurrence/439078490

GBIF Occurrence 2. (n.d.). Retrieved from https://www.gbif.org/occurrence/3037033640

GBIF Species. (n.d.). Retrieved from https://www.gbif.org/species/5538988

Grossheim, A. A. (1936). Analysis of the flora of the Caucasus (Vol. 1). Baku.

Grossheim, A. A. (1940). Flora of the Caucasus (Vol. 2). Baku.

Gurbanov E., Ibrahimov Sh, Huseynova H. (2022). Plant ecological research for the bioremediation from pollution by oil and oil products in Absheron peninsula (Azerbaijan). Bulletin of Science and Practice. Vol. 8. №12. https://doi.org/10.33619/2414-2948/85

Ibrahimova, A., Alizade, V., Mehdiyeva, N., & Kerimov, V. (2019). Plants of the Greater Caucasus (Azerbaijan). Baku.

Juan, I. M.-H., & Nathan, M. (2019). Importance of pollinator-mediated interspecific pollen transfer for angiosperm evolution. Annual Review of Ecology, Evolution, and Systematics, 50, 191–217.

Mammadova, H. G., Aghayeva, E. M., & Narimanov, V. A. (2021). Antimicrobial effects of extract and essential oil derived from Pastinaca dentata. Azerbaijan Pharmaceutical and Pharmacotherapy Journal, 1, 22–26.

Pimenov, M. G., & Sutorý, K. (2014). Name typification of Umbelliferae taxa described by Joseph Franz Freyn. Plant Biosystems, 148(6), 1102–1111.

POWO. (2024). Plants of the World Online. Retrieved July 22, 2024, from https://powo.science.kew.org/taxon/urn:lsid:ipni.org:names:892142-1

Schreter, A. I., & Krylova, I. L. (1986). Methodology for determining reserves of medicinal plants. Medicina.

Schreter, G. K. (1972). Medicinal plants and plant materials included in domestic pharmacopoeias.

Medicina.
World Flora Online. (2024). Pastinaca dentata (Freyn & Sint.). Retrieved from https://wfoplantlist.org/taxon/wfo-0001365030-2024-12
World Flora Online. (n.d.). Retrieved from https://www.worldfloraonline.org
Zulfugarova, P. V., & Ibadullayeva, S. J. (2015). Population structure and reserves of Laser trilobum in the flora of Azerbaijan. Scientific Works of the Institute of Botany of ANAS, 35, 69–75.

CONTENTS

Baku State University Publishing House.
Signed for printing: 28.12.2025
Font headset: Calibri
Format: 60x84 $^{1}/_{8}$
Copies: 50

ISSN 2958-0536

www.botanic.az